Novel chloroplast compartments are sites of photosystem II biogenesis and mRNA management during stress in the chloroplast of *Chlamydomonas reinhardtii*

James Uniacke

A Thesis

in

The Department

of

Biology

Presented in Partial Fulfillment of the Requirements

For the Degree of Doctor of Philosophy at

Concordia University

Montreal, Quebec, Canada

May 2009

Your file Votre référence
ISBN: 978-0-494-63359-5
Our file Notre référence
ISBN: 978-0-494-63359-5

Abstract

Novel chloroplast compartments are sites of photosystem II biogenesis and mRNA management during stress in the chloroplast of *Chlamydomonas reinhardtii*

James Uniacke, Ph.D.

Concordia University, 2009

Eukaryotic cells are highly compartmentalized. Many processes and metabolic pathways occur within specific organelles such as the nucleus, endoplasmic reticulum, Golgi apparatus, mitochondria, and peroxisomes. These compartments themselves are highly compartmentalized. In plants and algae, chloroplasts carry out photosynthesis, the biosynthesis of lipids, pigments, cofactors, amino acids, and function in the assimilation of S, P, and N. However, chloroplast cell biology has lagged behind that of other organelles. Classic models for the spatial organization of these processes are contradictory and based on EM and subcellular fractionation with no use of modern fluorescence microscopy. Here, chloroplast processes are revealed as highly compartmentalized within the chloroplast of *Chlamydomonas reinhardtii* with the first extensive use of fluorescence in situ hybridization, immunofluorescence staining and confocal microscopy. In Chapter 2, I propose that the processes underlying the biogenesis of thylakoids are compartmentalized in the chloroplast of *C. reinhardtii*. Chapter 4 describes the discovery of chloroplast stress granules, a compartment that manages mRNAs during oxidative stress. Chapter 3 assigned known targeting

mechanisms to specific chloroplast proteins while identifying new examples of localized translation. Because the pyrenoid, a largely unexplored chloroplast compartment in most algae, plays a central role in many of my findings, and little is known about this compartment, I isolated it and characterized its proteome by mass spectrometry. The pyrenoid proteome consisted of proteins with roles in starch metabolism, CO_2 assimilation and nitrite reduction. Taken together, these findings reveal that the *Chlamydomonas* chloroplast is more highly compartmentalized and complex than has been appreciated and that it can be used as a model system to study fundamental cell biological questions. This work has advanced our understanding of the cell biology of chloroplasts and provides a new conceptual framework for research into chloroplast biogenesis.

Acknowledgments

I thank Grant Brown, Marc Champagne, Daniel Colon-Ramos, Dion Durnford, Britta Forster, Michel Goldschmidt-Clermont, Elizabeth Harris, Muriel Herrington, Paul Lasko, Rachid Mazroui, Ursula Oberholzer, Alisa Piekny, Jean-David Rochaix, Enrico Schleiff, Michael Schroda, Michal Shapira, Robert Spreitzer, Olivier Vallon, and Francis-Andre Wollman for helpful comments and technical advice.

I thank Normand Brisson, Elizabeth Harris, Michael Hippler, Stephen Mayfield, Kevin Redding, and Michael Schroda for antisera; Kevin Redding for the *psaA* deletion mutant; Robert Spreitzer for the *RbcS* deletion mutant; and Genhai Zhu and Pioneer Hi-Bred International for the *rbcL* deletion mutant MX3312.

I thank all members of Dr. Zerges' lab, past and present: Simon Arragain, Brendan Gunther, Suzanne Kames, Sebastien Pisterzi, Oussama Rifai, Madhav Soowamber, Anguel Stefanov, Yu Zhan, Ying Zhang.

I thank Dr. Elaine Newman, Dr. Vladimir Titorenko for their helpful comments during committee meetings. I would especially like to thank my supervisor Dr. William Zerges for his guidance and supervision throughout my time in his lab.

Table of Contents

List of Figures

List of Tables

List of Abbreviations

cpSGs	chloroplast stress granules
DA	dark-adapted
DCMU	3-(3,4-dichlorophenyl)-1,1-dimethylurea
ER	endoplasmic reticulum
FCCP	carbonylcyanide-*p*-trifluoromethoxyphenylhydrazone
FISH	fluorescent in situ hybridization
GFP	green fluorescent protein
HL	high light
HSM	high-salt minimal medium
IF	immunofluorescence
LHC II	light-harvesting complex II
LSU	large subunit of Rubisco
ML	moderate light
RBP	RNA binding protein
ROS	reactive oxygen species

SG	stress granule
SRP	signal recognition particle
PABP	poly(A)-binding protein
PB	processing body
TAP	Tris-acetate phosphate
VRC	vanadyl ribonucleoside complex

1 Introduction

Eukaryotic cells are highly compartmentalized. Many processes occur in specific organelles such as the nucleus, the endoplasmic reticulum (ER), the Golgi apparatus, mitochondrion, chloroplasts, peroxisomes and lysosomes. Many organelles themselves are known to be highly compartmentalized. For example, within the nucleus the nucleolus is the site of rRNA transcription and ribosome assembly, while the ER is divided into rough and smooth regions. In plants and algae, plastids are an organelle class which includes chloroplasts, amyloplasts, chromoplasts, and etioplasts. In photosynthetic tissues, chloroplasts differentiate from the proplastids, the "stem organelle" where they carry out photosynthesis, the biosynthesis of lipids, pigments, cofactors, amino acids, and function in the assimilation of S, P, and N. The chloroplast is the organelle with the greatest number of known compartments. It has six compartments including the outer and inner envelope membranes, the inter-membrane space, the stroma, the thylakoid membranes and the thylakoid lumen.

Most cellular compartments were identified by electron microscopy (EM) and then isolated with sub-cellular fractionation and analyzed by biochemical approaches. More recently, the use of fluorescence microscopy including fluorescent in situ hybridization (FISH), immunofluorescence (IF) and green fluorescent protein (GFP) fusion proteins has made significant contributions to our understanding of cellular compartmentalization. However, with respect to the use of fluorescence microscopy, the analysis of chloroplasts has lagged behind that of other organelles mainly due to the high background caused by chlorophyll autofluorescence.

GFP is a widely used tool to visualize proteins in their native environment in living cells. The GFP gene has been introduced and expressed in many systems such as bacteria, yeast, fungi, and mammals. Since GFP has been codon-optimized for expression in plants, it has been used to determine whether a protein is localized to the plastid [1, 2]. While GFP may be a good method to determine the intracellular location of a protein, it is not suitable for determining its intraorganellar location in plants. Overexpression of GFP could affect localization of a protein and chlorophyll autofluorescence masks subtle localization patterns. Therefore, the use of FISH, to visualize mRNAs, and IF to visualize proteins within chloroplasts could reveal a degree of compartmentalization not seen before without having to introduce GFP fusion proteins into the chloroplast.

My thesis work includes the first extensive in situ study of the localization of chloroplast mRNAs and proteins. I adapted FISH and IF techniques to examine the localization of specific mRNAs and proteins in the chloroplast of the green alga *Chlamydomonas reinhardtii* from a study that used these methods to localize proteins and mRNAs in the cytoplasm of this alga [3]. My findings reveal a high level of compartmentalization within the *C. reinhardtii* chloroplast that has not been seen before, such as a distinct compartment for de novo photosystem II (PS II) biogenesis (Chapter 2), chloroplast protein targeting by localized translation (Chapter 3), and RNA granules that form during oxidative stress conditions (Chapter 4). I also examined the functions of these granules (Chapter 5) and the pyrenoid, a chloroplast compartment (Chapter 6).

1.1 The compartmentalization of chloroplasts

Photosynthesis involves several pathways that are highly compartmentalized within chloroplasts. For example, in the land plants, CO_2 assimilation occurs in the stroma, which is analogous to the cytoplasm of a cell [4]. However, in green algae, this process occurs in the pyrenoid [5]. The light-dependent reactions occur within the membranes of an elaborate network of flattened vesicles, the thylakoids. These reactions are performed by three multisubunit complexes: photosystem I (PS I), PS II, and the cytochrome b6/f complex [6]. Thylakoids themselves are compartmentalized. PS II is localized in thylakoid membranes that are appressed within the stacks of thylakoid vesicles called grana, while PS I is localized in the non-appressed thylakoid membranes that are exposed to the chloroplast stroma [7].

The biogenesis of chloroplasts also involves many well-characterized pathways, but much less is known about the spatial organization of these pathways [8-10]. In situ data are sparse regarding the locations of the biosynthesis and assembly of the component lipids, pigments and proteins of the various chloroplast compartments and the steps in the expression of the chloroplast genome. Of the few reported in situ studies, two showed that proteins that function in chlorophyll synthesis and lipid transport to thylakoids are localized in punctate patterns near the periphery of the chloroplast [11, 12]. These processes would thus appear to be more compartmentalized than previously realized. The biogenesis of PS II has been studied extensively. This complex uses energy from light to carry out the first charge separation reaction of oxygenic photosynthesis [12, 13]. Many of the 25 PS II subunits are encoded by nuclear

genes, synthesized in the cytoplasm by 80S ribosomes, imported into the chloroplast, and finally targeted to thylakoid membranes [14, 15]. However, the major integral membrane subunits of PS II are encoded by chloroplast genes, whose mRNAs are translated by bacterial-like 70S ribosomes within the chloroplast [16]. These include D1, D2, CP43, and CP47, which are encoded by the chloroplast genes *psbA*, *psbD*, *psbB*, and *psbC*, respectively. While all subunits are synthesized for de novo assembly of the PS II complex, the D1 subunit is also synthesized to replace D1 subunits damaged by photochemical reactions inherent to PS II activity, oxidative stress, or both [17, 18]. This D1 repair synthesis is elevated under high light (HL) stress conditions. It is widely accepted that D1 synthesis for PS II repair occurs at stromal thylakoids because the results of subcellular fractionation support this occurrence [19]. My 2007 article provides the first in situ evidence for this model.

1.1.1 The location of de novo PS II biogenesis

There is a debate over the intra-chloroplast location where mRNAs are translated and thylakoids are generated. A widely accepted model proposes that chloroplast-encoded PS II subunits are synthesized directly into thylakoid membranes (Figure 1.1 A). This model is supported by two lines of evidence. First, chloroplast polysomes synthesizing subunits of PS II and other thylakoid membrane proteins co-fractionated with thylakoid membranes on sucrose density gradients [20-29]. These membranes were proposed to be stroma thylakoids based on results of thylakoid fractionation experiments [19, 25, 30-33].

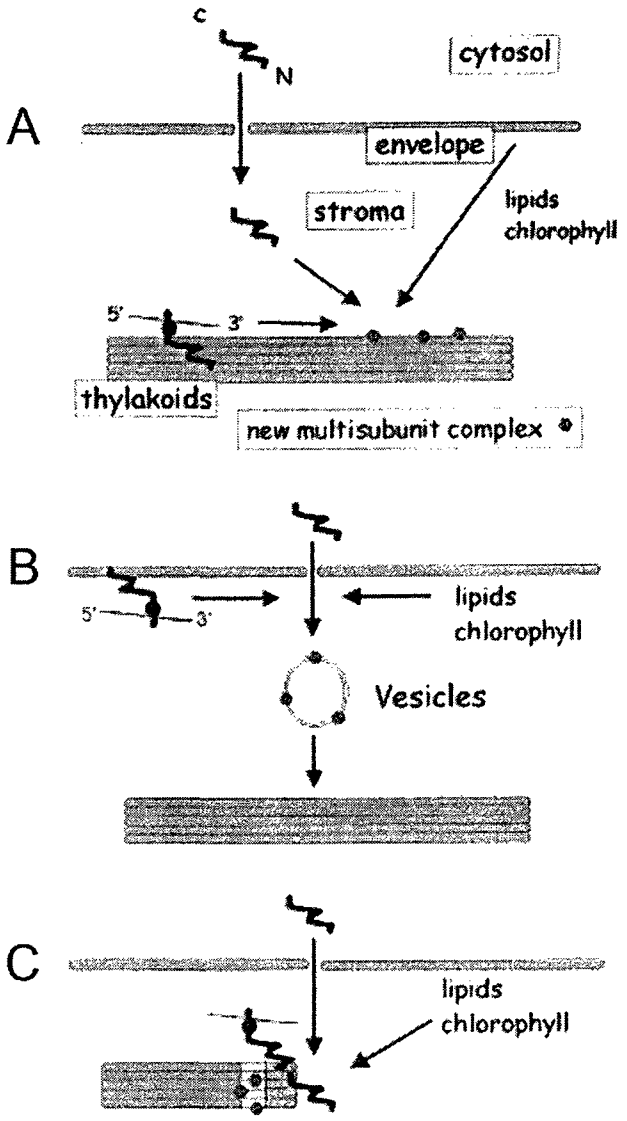

Figure 1.1. Three models describe possible locations in chloroplasts where mRNAs are translated.

A) Chloroplast mRNAs are translated in association with thylakoid membranes. Glycerol lipids and pigments are transported from their site of synthesis at the envelope to thylakoid membranes by transferase proteins. Proteins encoded by nuclear genes are imported through the chloroplast envelope. These components assemble in thylakoid membranes to form the integral membrane complexes of the photosynthetic apparatus. **B)** Chloroplast mRNAs are translated in association with the inner membrane of the chloroplast envelope, where they assemble with in-coming proteins from the cytosol and newly synthesized chlorophyll. Assembled integral membrane complexes are transported to thylakoids with membranous vesicles. **C)** Chloroplast mRNAs are translated at the ends of thylakoid grana, the stacks of disk-like thylakoid membranes. There they assemble with chlorophyll and nucleus-encoded thylakoid proteins to form the integral membrane complexes of the photosynthetic apparatus. Lipids, pigments and thylakoid proteins from the cytosol could be transported membranous vesicles and/or by transferase proteins [8].

Second, in situ evidence for this model was provided by EM images of isolated thylakoid membranes, which revealed chloroplast ribosomes or incompletely assembled PS II subcomplexes primarily at non-appressed stroma thylakoid membranes [21, 25, 34, 35]. While it has been assumed that thylakoid membrane protein synthesis and assembly occur in stromal thylakoids throughout the chloroplast, to our knowledge, the possibility that these processes could occur in specialized domains of stromal thylakoids or a compartment specialized in thylakoid biogenesis had not been explored prior to this thesis work.

In an alternative model, the inner membrane of the chloroplast envelope has been proposed to house the synthesis and assembly of the chloroplast-encoded thylakoid membrane proteins (Figure 1.1 B). Chloroplast membranes that resemble the inner envelope membrane in buoyant density and pigment composition were found to be associated with RNA binding proteins (RBPs) and a homolog of poly(A) binding protein (PABP) [42, 61]. Similar non-thylakoid membranes co-fractionated with 50% of chloroplast ribosomes [36]. The credibility of this alternative model was increased by the discovery that thylakoid biogenesis requires vesicular transport from the inner envelope membrane [37-40]. Although these data would seem to contradict the aforementioned evidence for thylakoids as the location of PS II subunit synthesis, they do not necessarily. For example, most of the EM images cited above were taken of isolated thylakoids, recognized by their stacked regions. However, other membranes with bound ribosomes in the same fractions would have been disregarded as contaminating rough ER [21]. Moreover, the thylakoid membranes that were concluded

to have bound chloroplast polysomes were in sucrose density gradient fractions that are heavily contaminated by membranes that resemble the membranes of the chloroplast envelope [41, 42]. The latter membranes have been hypothesized to be undifferentiated thylakoid membranes of an unknown location in the chloroplast of *C. reinhardtii* [42].

The location of the de novo assembly of the photosynthesis complexes has also been addressed in *Synechocystis*, the closest known bacterial relative of the chloroplasts of the green plants (which include *Chlamydomonas*) [43]. Results of cellular subfractionation experiments provided strong evidence for the assembly of PS I and PS II occurring in the plasma membrane [44, 177], which is considered to be homologous with the inner membrane of the chloroplast envelope [45]. Yet, the three-dimensional structure of this bacterium obtained by electron tomography revealed that most ribosomes are within 6 nm of a membrane (i.e., sufficiently close to be inserting a nascent protein) and were on or near thylakoid membranes [46]. The possibility that an unknown membrane type gives rise to thylakoid membranes was suggested by the description of unit membrane–like sheets that had dense clusters of ribosomes and were connected to thylakoid membranes (Figure 1.1 C) [47]. Similarly, in *Chlamydomonas* and pea (*Pisum sativum*), many of the chloroplast ribosomes seen by EM were in clusters located near isolated thylakoid membranes but not directly on them [21, 25]. Therefore, many lines of evidence support different models for the location(s) of de novo PS II biogenesis, and an in situ approach might shed some new light on this longstanding question.

1.2 Chloroplast protein targeting

Each organelle in a eukaryotic cell requires a distinct protein complement to carry out its specialized functions. Therefore, newly synthesized proteins are targeted to specific organelles and compartments within them. This is known to involve three general mechanisms. In a post-translational mechanism, the import machinery of the organelle selects the correct proteins by virtue of their having a transit peptide or nuclear localization signal (Figure 1.2 A). In a co-translational mechanism, the signal sequence in the nascent polypeptide binds signal recognition particle (SRP), which represses further translation, docks the mRNA-ribosome-nascent polypeptide complex at the ER, whereupon translation resumes for the insertion of the elongating polypeptide into the ER lumen or membrane (Figure 1.2 B). Lastly, in an mRNA-based mechanism, the untranslated mRNA is localized by an RBP associated with a molecular motor or the target membrane and translation is initiated only upon mRNA localization [47, 48] (Figure 1.2 C). The two latter mechanisms appear to operate together in protein targeting to the mammalian ER [49].

The chloroplasts of plants and green algae import a few thousand proteins to function in photosynthesis and other processes [50]. These proteins are believed to be synthesized at random cytoplasmic locations and undergo post-translational import because isolated chloroplasts can import proteins synthesized in vitro and EM studies have observed only outer chloroplast envelope membranes without bound ribosomes [51]. However, at least a few proteins are trafficked to chloroplasts via the secretory system, implying they are first targeted to the ER by the co-translational SRP pathway

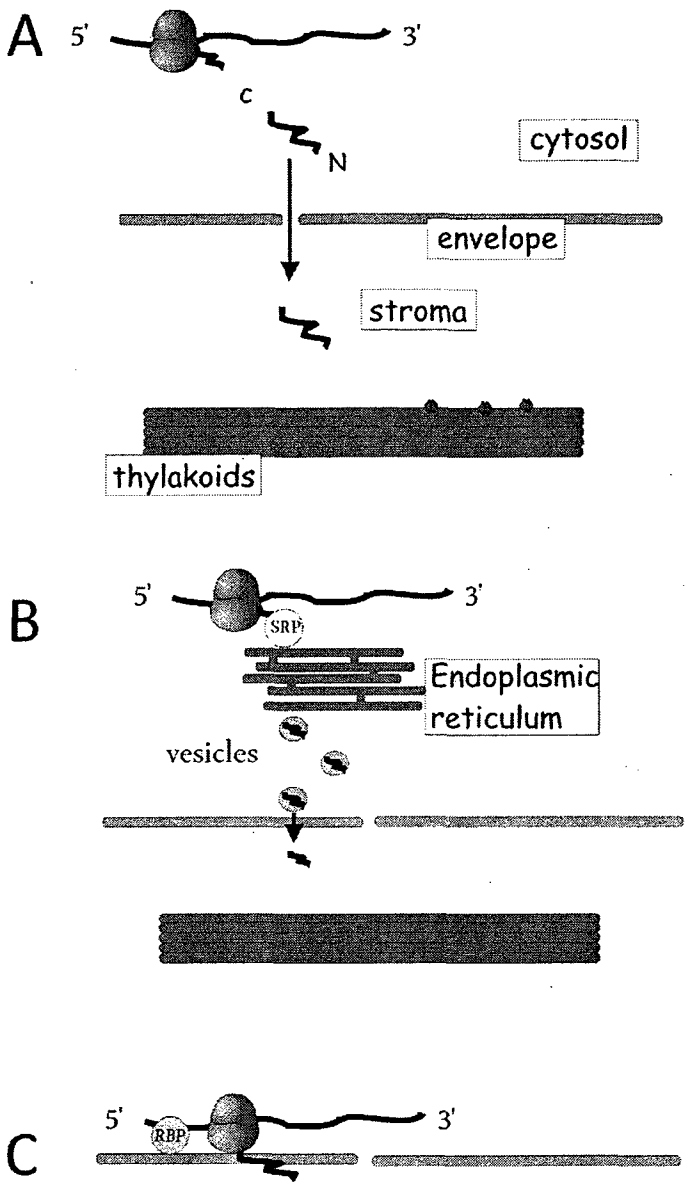

Figure 1.2. The three general mechanisms of protein targeting.

A) In a post-translational mechanism, the protein is synthesized in the cytoplasm and the import machinery of the organelle selects the correct proteins by virtue of their having a transit peptide or nuclear localization signal. **B)** In a co-translational mechanism, the signal sequence in the nascent polypeptide binds SRP, which represses further translation, docks the mRNA-ribosome-nascent polypeptide complex at the ER, whereupon translation resumes for the insertion of the elongating polypeptide into the ER lumen or membrane. Proteins are transported via vesicles and fuse to the correct target membrane. **C)** In an mRNA-based mechanism, the untranslated mRNA is localized by an RBP associated with the target membrane and translation is initiated only upon mRNA localization.

[52-54]. Despite several decades of research on chloroplast protein import, nothing is known about the location(s) of chloroplast protein synthesis in the cytoplasm.

A minor protein contingent is expressed from the chloroplast genome and targeted to specific compartments within this organelle [8]. Some of these "chloroplast-encoded" proteins are targeted to thylakoid membranes where they function as subunits in the photosynthesis complexes. Others are targeted to the stroma. In green algae, the large subunit of Rubisco (LSU) is targeted to the pyrenoid [55]. However, little is known about the targeting mechanisms involved. We do know that thylakoid membrane proteins are synthesized by membrane-bound chloroplast polysomes [21, 26]. A chloroplast homologue of the SRP subunit that binds the signal sequence, cpSRP54, was shown to bind the nascent chain of the D1 subunit of PS II in a reconstituted chloroplast translation system and to be required for thylakoid membrane biogenesis [56-59]. In addition, mRNA-based mechanisms probably target chloroplast-encoded proteins. First, only one protein is known to have a transit peptide, indicating that post-translational mechanisms are not predominant [57]. Second, cpSRP54 is not absolutely required for thylakoid biogenesis in *Arabidopsis,* indicating the existence of another pathway [60]. Finally, several membrane-associated RBPs have been identified in the chloroplast of the eukaryotic green alga *C. reinhardtii* [61, 62]. Therefore, much work remains to be done to identify and characterize the mechanisms and machinery involved in the targeting of chloroplast-encoded proteins.

1.3 Translationally silent mRNAs localize to RNA granules during stress

Research on translation has focused primarily on general mechanisms by which ribosomes synthesize polypeptides and how the translation of specific mRNAs is regulated or localized to specific cytological locations [48]. More recently, the nature of translationally silenced mRNAs has come into attention, first with regards to their metabolism and degradation and, of late, the intracellular localization of these processes. During conditions of translational repression in a variety of eukaryotes, specific mRNAs have been seen to localize in discrete cytoplasmic foci called stress granules (SGs) and processing bodies (PBs) (reviewed by [63, 64]). These classes of RNA granules are being revealed as complex, functionally related compartments involved in the control of mRNA fates and RNA silencing.

SGs form within 15-30 minutes of exposure to various stress conditions, including high temperature, oxidative stress due to the production of reactive oxygen species (ROS), damage induced by UV irradiation, and osmotic shock [64]. They have been described in mammalian and plant cells, and possible orthologs exist in the fission yeast Schizo*saccharomyces pombe* and trypanosomes [65-68], but no stress-induced RNA granule has been observed in any prokaryote or organelle. Recruitment into SGs is thought to regulate mRNA stability by storing them for translation upon the restoration of homoeostasis [69]. SGs are believed to harbor stalled translation pre-initiation complexes because they lack the large ribosomal subunits, contain small ribosomal subunits, certain translation initiation factors, the PABP and several other RBPs [65, 69-72]. PBs are more mobile and ever-present than SGs, but do increase in size and number

during certain stress conditions [65, 73, 74]. PBs are believed to be specialized cytological locations for mRNA decay because they contain mRNA decapping proteins DCPI and DCP2, exonuclease Xrn1, and the deadenylase CCR4 [75-77]. PBs are also distinct from SGs in that they lack both ribosomal subunits and translation initiation factors [78]. Although SGs and PBs are distinct by these criteria, real-time fluorescence imaging experiments revealed that they share and exchange common components [79]. PBs move to and from stationary SGs after docking for a few minutes. Together, these observations are the basis for the current model that SGs are a triage compartment during stress where translationally silent mRNAs are directed either back to the pool of translating mRNAs or to PBs for degradation [69]. However, other models have not been excluded.

1.3.1 The proposed functions of stress granules

The fundamental function of SGs is not clear. There is evidence in mammalian cells that SGs have a role in stress tolerance. Lethality is associated with deficiency for two proteins in two separate mutant cell lines that did not form SGs when stressed [80, 81]. These cell lines had mutations in heme-regulated inhibitor kinase or the deacetylase HDAC6, which both act upstream of SG assembly. Heme-regulated inhibitor kinase is activated upon stress and phosphorylates eIF2α, which initiates the signaling cascade toward SG assembly. Deacetylase HDAC6 acts on tubulin and HSP90 and has many other functions. Therefore, assigning a stress tolerance function to SGs may be premature because of the pleiotropic effects caused by the above mentioned mutations. It has proven difficult to abolish SG formation at the assembly level in mammalian cells

because of the lethality of the mutations or the redundant pathways involved [82]. SGs have also not yet been isolated and their complete composition has not been characterized. It would be of great interest to find a system where SGs could be isolated and their assembly more directly abolished without being lethal.

1.4 The function of the pyrenoid

Aquatic photosynthetic organisms have evolved strategies to more effectively utilize CO_2. The challenge these organisms face in assimilating CO_2 is two-fold. First, the rate of diffusion of CO_2 in aqueous solution is 10,000 times slower than in air. Second, the enzyme that catalyzes the first step of the Calvin cycle by fixing CO_2 into an organic molecule, ribulose bisphosphate carboxylase/oxygenase (Rubisco), has an unusually slow catalytic activity. Rubisco can function at only 25% of its catalytic capacity at atmospheric levels of CO_2, and the high abundance of O_2 being produced in these organisms competes with CO_2 for Rubisco's active site [83, 84]. Thus, aquatic microorganisms concentrate carbon away from O_2 in the pyrenoids of many algae and in the carboxysome, the homologous compartment in cyanobacteria.

The pyrenoid is a chloroplast compartment in many eukaryotic algae and one member of the hornworts. It is not membrane-bound, but is typically surrounded by thick starch sheaths and penetrated by several pyrenoid tubules, as seen by EM [85]. These tubules are membranous and contain thylakoid vesicles that extend from outside the pyrenoid. Thylakoid membranes connect to electron dense structures in the walls of the tubules. The pyrenoid has a dense proteinaceous matrix containing up to 90% of the cellular Rubisco pool [55].

Surprisingly little is known about the function(s) of the pyrenoid. Immunolocalization studies in the eukaryotic green alga *C. reinhardtii* have provided some evidence for a role in the assimilation of CO_2. Immuno-gold EM and subcellular fractionation studies revealed that Rubisco is concentrated in the pyrenoid [5, 55]. This Rubisco is thought to be active because in vivo rates of CO_2 fixation are similar to the total amount of Rubisco activity [55]. Suss *et al* [5] identified two Rubisco forms based on differences in their spatial organization. What they called Form I localized to thylakoid membranes and stroma for CO_2 fixation. Rubisco form II localized throughout the pyrenoid matrix and was proposed to be involved in a CO_2 concentrating mechanism. Rubisco activase and nitrite reductase have also been detected within the pyrenoid by immunogold EM [5, 86]. Because the pyrenoid is surrounded by starch, it has been proposed that starch synthesis occurs within this compartment, but this hypothesis has never been tested. Results of my thesis work strongly suggest additional and novel pyrenoid functions. Chapter 2 shows that sites lateral to the pyrenoid, called T zones, are involved in the synthesis of de novo PS II assembly [87]. Chapter 4 shows that the pyrenoid harbours chloroplast stress granules (cpSGs) suggesting that it could be involved in protecting chloroplast mRNAs from ROS during oxidative stress, consistent with its proposed role of having low oxygen levels to enhance Rubisco efficiency [88]. Therefore, the pyrenoid is being revealed as a more complex compartment than previously realized. Proteomic analysis of this chloroplast compartment could reveal new functions and confirm its role in carbon assimilation and starch synthesis.

1.5 *Chlamydomonas reinhardtii* as a model system

C. reinhardtii is a widely used model organism in studies of chloroplast biology and photosynthesis. It is a unicellular eukaryotic green alga with many cell and molecular biological tools developed for it. Its chloroplast and nuclear genomes have been fully sequenced and annotated [89]. This alga is amenable to work with because it can be grown on solid media in Petri plates and has a doubling time on the order of 5 h. A major advantage of using *C. reinhardtii* instead of land plants is that photosynthesis-deficient mutants are fully viable when provided with a reduced carbon source such as acetate. Furthermore, a wealth of mutants is available from the research community and a stock center. A major contribution of my thesis is the demonstration that *Chlamydomonas* is ideally suited for characterizations of the distributions of specific mRNAs and proteins in the chloroplast by FISH and IF techniques because its single large chloroplast has a definite anatomy which is easily recognizable in every cell examined.

1.6 Thesis outline and contributions of colleagues

Chapter 2 describes my discovery of a chloroplast compartment for de novo PS II biogenesis which we call "T zones" for translation zones. These locations were defined as having colocalized chloroplast mRNAs encoding PS II subunits and proteins of the chloroplast translation machinery specifically under conditions of PS II subunit synthesis. In contrast, my results support the current belief that PS II repair occurs on thylakoid membranes throughout the chloroplast. Chapter 3 describes my use of in situ techniques to characterize the nature of the targeting mechanisms used by four chloroplast proteins, two encoded by nuclear genes and two encoded by chloroplast

genes. The three known general protein targeting mechanisms were distinguished by first observing whether the mRNA encoding a specific protein was localized (to discriminate post-translational targeting from co-translational and mRNA-based targeting). If an mRNA localization pattern was detected, co-translational and mRNA-based targeting mechanisms were distinguished by whether this localization was dependent on translation. The results reveal two novel examples of targeting by localized translation, in light-harvesting complex (LHC II) subunit import and the targeting of LSU to the pyrenoid of the chloroplast. They also reveal examples of each of the three known targeting mechanisms: post-translational, co-translational, and mRNA-based, in the targeting of specific chloroplast proteins. Chapter 4 describes my discovery of cpSGs, the first such discovery in a bacterial/organellar genetic system. These stress-induced RNA granules are analogous to mammalian SGs in that they contain mRNAs from recently disassembled polysomes, the small ribosomal subunit and PABP. Moreover, also like mammalian SGs, mRNAs are in continuous flux between these chloroplast granules and polysomes during stress. This chapter also describes a novel function of the pyrenoid in a stress response as well as the possibility that LSU plays a role in the assembly of cpSGs. Chapter 5 provides evidence that cpSGs have a role in short-term oxidative stress tolerance, a function thought to be associated with mammalian SGs. Two mutants that do not form SGs were exposed to increasing concentrations of hydrogen peroxide but did not have lower levels of tolerance to this stress than a wild-type strain. This study also showed that these mutants do not have a pyrenoid suggesting that this chloroplast compartment has a role in cpSG formation.

Chapter 6 describes the isolation of the pyrenoid and a partial characterization of its proteome by mass spectrometry. A simple protocol was established to purify pyrenoids and they were found to have very few proteins when separated by SDS-PAGE. The proteome revealed functions in starch synthesis, CO_2 assimilation and nitrate metabolism.

Chapters 2, 3 and 4 were published in The Plant Cell [87], PNAS [90], and The Journal of Cell Biology [88], respectively. Chapter 5 is a manuscript in preparation. I carried out all of the experimental work described in these chapters and participated in experiment design, data analysis, and writing of the manuscripts.

Chapter 6 describes an ongoing project which has involved two undergraduates, Brendan Gunther and Simon Arragain, and currently involves M.Sc. student Oussama Rifai, research associate Heng Jiang and Dr. Vincent Martin. Together, we developed a pyrenoid purification protocol and determined the first pyrenoid proteome, although it is incomplete because one band from the gel was missing from the mass spectrometer results. Therefore, I have contributed approximately half of the experimental work, data analysis and experimental design for this manuscript as well as co-supervising two undergraduate and one graduate student.

2 Photosystem II assembly and repair are differentially localized in *Chlamydomonas*

Photosystem II assembly and repair are differentially localized in Chlamydomonas.
Uniacke J, Zerges W. *Plant Cell.* 2007 Nov;19(11):3640-54. www.plantcell.org

2.1 Introduction

Considering the uncertainty regarding the location of thylakoid membrane biogenesis and the lack of in situ evidence relating to this question, I addressed this problem by characterizing the locations of PS II subunit synthesis in the chloroplast of *C. reinhardtii* with FISH, IF staining, and confocal microscopy. Because FISH and IF staining had not been used in chloroplasts, I adapted these techniques which were used to detect mRNAs and proteins in the *Chlamydomonas* cytoplasm and nucleus [3]. The rationale for identifying the location(s) of PS II biogenesis was to define them as having colocalized chloroplast mRNAs encoding PS II subunits and proteins of the chloroplast translation machinery specifically under conditions of PS II subunit synthesis. While exploring the aforementioned problems, I found that *Chlamydomonas* is ideally suited for characterizing the distribution of specific chloroplast mRNAs and proteins by these techniques because its single large chloroplast has a definite anatomy that is easily recognizable in every cell examined. The findings on chloroplast morphology presented in this chapter were also published in Volume I of the *Chlamydomonas* Sourcebook [178].

2.2 Materials and Methods

C. reinhardtii culture conditions

For the dark-adapted (DA), moderate light (ML), HL, and ML5' conditions, cells were cultured photoautotrophically in high-salt minimal medium (HSM) [91] until mid-log phase (3 X 10^6 cells/mL) at 24°C and under a light intensity of 100 to 150 $\mu E \cdot m^{-2} \cdot s^{-1}$. Dark-adaptation was accomplished by a 2 h incubation in flasks wrapped with two layers of aluminum foil on an orbital shaker at 24°C. HL (2000 $\mu E \cdot m^{-2} \cdot s^{-1}$) was generated by a slide projector (Kodak) to which small (2 to 30 mL) cultures were exposed at a distance of 10 cm with manual shaking. The alb3.1 mutant (ac29; CC-245), FUD34 (CC-2518), and the control wild-type cells used in experiments with these mutants (Figure 2.7) were cultured on Tris-acetate-phosphate (TAP) medium in the dark [92]. When lincomycin was used, it was added to a final concentration of 200 µg/mL at 10 min prior to cell fixation. The chloroplast transcription inhibitor, rifampicin, was added to a final concentration of 350 µg/mL at 60 min prior to the end of the 2 h dark adaptation period for the control experiment. The rifampicin was active because it was lethal at this concentration after 24 h (data not shown).

In vivo ^{35}S pulse-labelling

The level of ^{35}S labelling of a PS II subunit during a 5 min pulse-labelling period reflects its synthesis rate, because previous studies found that the levels of the mRNA encoding these subunits do not change dramatically in response to light exposure [93, 94] and their degradation was not detected within 30 min of their synthesis [35]. Pulse-labelling was performed for 5 min with 1.2 X 10^7 cells in 0.3 mL of HSM lacking NH_4SO_4.

Cycloheximide was added to a final concentration of 10 µg/mL 5 min prior to the addition of 80 µCi of [^{35}S]SO_4. Cells were not deprived of SO_4 for more than the 15 min required for centrifugation and resuspension and treatment with cycloheximide prior to pulse-labelling, during which time 100 µM SO_4 was available from the trace element mixture present in this medium. Pulse-labelling was performed on an orbital shaker for 5 min under the light conditions described. Cells were pelleted by centrifugation at 4000 x g for 2 min, resuspended and lysed in 100 µL of SDS-PAGE loading buffer (250 mM Tris pH 6.8, 2% SDS, 20% glycerol, 50 mM DTT, and 2% 2-mercaptoethanol), and incubated at room temperature for 60 min, and then 50 µL of each sample was loaded on a 13% denaturing SDS-polyacrylamide gel (with 8M urea) on the basis of cell number (6 X 10^6 cells/lane). Following electrophoresis, the gels were dried and ^{35}S-labelled proteins were revealed by autoradiography. Coomassie Brilliant Blue staining confirmed that comparable amounts of total protein were in the lanes (data not shown). The light stimulation of the ^{35}S labelling of these proteins does not reflect effects on the rate of [^{35}S]SO_4 uptake, because a 200-fold excess of sulphate immediately prior to light exposure did not affect the pattern of labelled proteins (data not shown). The induction of protein synthesis by light was not observed in cells cultured in TAP medium (data not shown), probably because the acetate it contains induces protein synthesis in the dark [95].

FISH

Cell fixation, permeabilization, and FISH were performed as described previously with the following modifications [3]. Four FISH probes (Alpha DNA) of 50 nt were designed to

hybridize to each of the mRNAs (Table 2.1) [96-99]. The probes against the *psbA* mRNA hybridize across exon junctions. The *psbA*, *rbcL*, and *psaA* mRNA FISH signals were highly specific because they were not detected in deletion mutants for these genes [100-102] (Figure 2.3). FISH probes were labelled with either Alexa Fluor 488 or Alexa Fluor 555 (Molecular Probes) according to the manufacturer's protocol on five modified C6-dT residues with 6-10 nucleotides between each modified C6-dT. Labelled probes were purified from a denaturing 13% polyacrylamide gel by excising the bands, manually crushing them, and overnight incubation in elution buffer (0.1% SDS, 10 mM magnesium acetate, and 0.5 M ammonium acetate) at 37°C. Approximately 1 X 10^6 cells were spotted on a microscope slide coated with 0.1% Poly-L-lysine. These slides were first boiled in 1M HCL for 15 min to reduce autofluorescence and then a 10 µL drop of 0.1% Poly-L-lysine (Sigma) was spotted at one end of the slide and smeared across with another slide. These treated slides were kept in a slide rack covered with aluminum foil and left to dry for a few days to a week. After waiting 45 sec to allow the cells to adhere to the slide, the slide was inserted into a Coplin jar with a screw cap for fixation (all washes were done in Coplin jars on an orbital shaker at low speed). After fixing the cells in 4% para-formaldehyde in 1XPBS, they were incubated in two methanol washes for 10 min each at -20 °C. Cells were washed in 1 X PBS, 5 mM $MgCl_2$ twice for 10 min. Triton X-100 at 2% (v/v) in 1XPBS was used to permeabilize the cells for 10 min. Cells were washed in 1 X PBS, 5 mM $MgCl_2$ twice for 10 min. When the cells are ready for hybridization, 10 µL spots of hybridization buffer (10 mM vanadyl ribonucleoside complex (VRC), 4XSSC, 4 mg/mL of BSA) were placed in the center of coverslips laying on

TABLE 2.1. Oligonucleotide FISH probe sequences

name	probe sequence (5' → 3')
psbA-1	CTGAAACTGGTTCACGGATACCATCGATGTCTACTGGC
psbA-2	ACGGAAAGATAATTCCCACTCACGACCCATGTAGCAGTATACACTAGA
psbA-3	GAATACGATCATGAAGTTGAAAGTACCAGAGATACCTAAAGGCATACCGT
psbA-4	GGAAGATTAGACGACCAAAGTAACCATGAGCAGCTACAATGTTGTAAGTT
psbC-1	TACCTGACCACCAAGCAAAACCTGTTGTTTCTTGGTCACGGCCACCTACT
psbC-2	ATAATTTCACCACCTGGACCTACACCGTAACCTAAAGTTGCGATGTGTGG
psbC-3	GGGTTAGTAATAACACGAACGTCACCACCACCTGGAGCCCAAGTATCGTA
psbC-4	AGTCTAAACCGTTTGGACCACGTAGAGGTTCTAACCATGGACCACGGAAG
psaA-1	TTGGAACCATTCTAGTTTTGGAGCAGCTTTGTGGTAGTGGAACCAACCAG
psaA-2	CTACGTGGTGGTGAGCAGTATCACTTAACCAAAGACCACCAGTAACAGGG
psaA-3	AAGCTGTAACCGTACCCCAAACATCAGATTGCATCTTCCAGCTGAAGTGG
psaA-4	AGTAGGAGGTGCGCCTTCCAGCGAATACATGATTTTTCCCCCTTCCAGTT
rbcL-1	CCACATTCTTCAGGTGGAACACCTAGTTGTGGAGTCATACGGAATGCAGC
rbcL-2	GCAGGTGGAATACGAAGGTCTTCAAGACGTAGAGCACGTAAAGCTTTGAA
rbcL-3	GTGCATAGCACGGTGGATGTGTAGAAGAAGACCGTTGTCACGACAGTAGA
rbcL-4	CACCTGGCATTGAACACCAGTCTTGAGTGAAGTAAATACCACGGCTACGG
RbcS-1	GGGTTGCAAGTGCTCAAATACCCCATCAAACATCATCCTGGTTTGGCTGC
RbcS-2	CGGAGGACTTGGCAATGACGGCGGCCATTTTAAGATGTTGAGTGACTTCT
RbcS-3	TAGGAGAAGGTCTCGAACATCTTGACCGGGGTCCAGACCATCATCTGGTT
Rbcs-4	TTCCACATGGTCCAGTAGCGGTTGTCGTAGTACAGCTGCAAGACACGCTG
LhcII-1	GCTGCGGACGGAGGACTTCATGATGGCGGCCATTTTGATTGGTATAGACA
LhcII-2	AAGAAGCCGAACATGGAGAACATAGCCAGGCGGCCGTTCTTGATCTCCTT
LhcII-3	TCTCCGCTCAATCACGCCAGTACATGCAGCTGCCGAGGGCCAAAAATTTA
LhcII-4	TTAATCGCACGTCCCTCGCGCTCCTAAGCCTGTGAAAAGAGGCTCACACT

Boldface Ts indicate modified C6-dT residues that were labeled with Alexa Fluor 488, Alexa Fluor 555, or Alexa Fluor 633 (Molecular Probes).

a long piece of parafilm. Probe mixture (20 ng) with 100X competitor DNA (2 mg/mL each of salmon sperm DNA and *E. coli* tRNA) were air-dried in a speedvac at 43 °C and resuspended in 10 µL formamide then heated at 85°C for 5 min. The probe mixture was then spotted onto the hybridization buffer spot on the coverslip. The slide was then blotted gently with Kimwipes and placed cell-side down onto the hybridization solution on the coverslip. The slides were incubated overnight at 37°C in a slide hybridization oven. A piece of moist paper towel was included to maintain humidity. Hybridization temperature was 30.5 °C below Tm because 50% formamide was present. Post-hybridization buffer (1 X SSC, 50% formamide) was made fresh the next day and incubated for 30 min at 37 °C. Cells were incubated twice for 20 min in post-hybridization buffer, and then for 10 min each in 0.5XSSC and 0.25XSSC. Cells were washed for 10 min in 1 X PBS, 5 mM $MgCl_2$. Slides were blotted dry with KimWipes and 20 µL of ProLong Gold Anti-fade reagent (Molecular Probes) was added to the cell side of each slide. A coverslip was placed on top of the Anti-fade reagent, incubated for 2 h at room temperature and then sealed with nail polish. Slides were stored at -20 °C. All solutions were made with diethyl pyrocarbonate-treated water.

IF staining

When cells were probed for an mRNA and a protein, FISH was carried out prior to IF staining. The slide with adhered cells was incubated in blocking solution (PBS [137 mM NaCl, 2.7 mM KCl, 10 mM Na_2HPO_4, and 2 mM KH_2PO_4], 0.1% BSA, and 2mM VRC) for 30 min at room temperature by placing a 25 µL drop of blocking solution on a coverslip and placing the blotted-dry slide cell-side down onto the drop. This was followed by a 75 min

incubation with diluted primary antiserum in blocking buffer (with 10 mM VRC) at 37°C. A dilution of 1:1000 was commonly used, but this was too high for the LHC II antisera causing artifacts such as IF signal only around the perimeter of the cell or signal in aggregates. The LHC II antisera was used at a dilution of 1:4000. After washing twice in PBS, cells were incubated in a 1:200 dilution of an anti-rabbit secondary antibody in blocking buffer (with 10 mM VRC) at room temperature for 45 min. The secondary antibody was anti-rabbit IgG–TRITC or IgG–FITC (Sigma). ProLong Gold Anti-fade (Molecular Probes) was used for mounting. The in situ IF staining patterns of D1, PsaA, and the r-proteins were highly specific because each of the antibodies detected a protein of the expected molecular weight on immunoblots of total cellular protein (data not shown). The specificities of the IF signals from PsaA and D1 were also demonstrated by their absence in deletion mutants for *psaA* [101] and *psbA* (FuD7) [100], respectively (Figure 2.3 D and E). Staining with the secondary antisera alone did not generate a signal (data not shown). The r-protein of the 60S subunit of the cytoplasmic ribosome was detected by the antiserum described previously and called, in an early nomenclature, L4; it very weakly cross-reacted against two smaller r-proteins, L47 (60S) and S26 (30S) (data not shown) [103, 104]. A chicken antiserum against D1 (AgriSera) was used in conjunction with a rabbit antiserum against LHC II (Figures 6D to 6F). It was critical to titer the primary antisera (especially those against thylakoid membrane proteins) and use them at the lowest concentration required to give a signal to avoid artifactual highly punctate IF staining patterns or high general background. The 50S subunit r-protein of the 50S subunit, L2, was detected by an antiserum described previously as L-1 [105-

107]. The antiserum against the r-protein of the 30S subunit of the *C. reinhardtii* chloroplast ribosome was called S-21. Although the molecular weight of the r-protein detected with the S-21 antiserum was similar to that of the *Chlamydomonas* ortholog of S21 in *E. coli*, they drastically differ in pI [105, 108]. The protein detected by this antiserum is most similar to the plastid specific r-protein PSRP-4 in molecular mass, pI, and nuclear location of the gene(s). Despite this uncertainty, the antisera against L-1 and S-21 detected bona fide r-proteins because they were raised against proteins from highly purified chloroplast ribosome subunits and their levels were reduced several fold in a mutant strain for *ac20 and cr1*, which accumulates 30% of the wild-type level of chloroplast ribosomes (immunoblot data not shown).

Microscopy

Fluorescence signals were visualized in serial 0.2 µm optical sections obtained with a Leica TCS SP2 confocal laser-scanning microscope and image acquisition software version 2.61 (Leica). Argon and green helium neon lasers were used to produce the 488- and 543-nm stimulation of fluorophores Alexa Fluor 488 and Alexa Fluor 555, respectively. Deconvolution was not used. Cells were observed under immersion oil with an HCX PL APO objective lens of 100X and numerical aperture of 1.4. Images were acquired in 512 X 512 format with digital zoom set at 4.8X with a pinhole size of 0.84 airy. Glow-Over (Leica) images were obtained after adjusting the maximal signal in each section to just below saturation. 4',6-Diamidino-2-phenylindole was visualized with a Zeiss Axioplan fluorescence microscope with UV-G 365 filter cube, 100X oil objective with numerical aperture of 1.3, and SPOT Insight color camera model 3.2.0.

Statistical analysis of colocalization

In order to determine the percentage of pixels with strong colocalized signals in the region of T zones, from a central optical section of each cell, two areas of 10 X 10 pixels were cropped from the regions located midway between the pyrenoid and the cell periphery (i.e., where T zones were observed in ML5' cells) from DA and ML5' cells using Corel Photo-Paint. A crop in one channel (red) was taken at the precise location of the crop in the other channel (green) using the xy coordinates given on the image manipulation program. Colocalization was compared for both signals with the ImageJ plugin Colocalization Finder. To determine the percentage of pixels with intense colocalized signals in each sampled region, only pixels with both channels above a fluorescence intensity of 175 were selected from the scatterplot generated by this plugin (an 80 X 80 square in the upper right corner of the plot). It should be noted that this method of showing colocalization of the strongest signals requires that few or no pixels have strong signal in only one channel, as revealed by sampling at these regions on the plots in Colocalization Finder. For example, if one channel shows strong signal dispersed throughout the cell and the other has highly localized strong signal, the latter pattern would appear as white even though the signals are not specially colocalized.

2.3 Results

2.3.1 The *Chlamydomonas* chloroplast as revealed by fluorescence confocal microscopy

In order to validate my identification of relevant cellular compartments by fluorescence confocal microscopy, Figure 2.1 shows an illustration of a typical cell (A) and the IF

staining patterns of four marker proteins (B to G). Each cell is shown with its apical basal axis oriented from left to right (Figure 2.1 A). The globular basal region of the chloroplast contains the pyrenoid, which was identified by its IF staining for Rubisco (Figure 2.1 B) [5, 55, 109]. In the images throughout this report, the pyrenoid is seen as a spherical region that is largely devoid of fluorescence signals from chloroplast mRNAs or marker proteins. The IF signal from a marker protein for the cytoplasm, an r-protein of the 60S subunit of the cytoplasmic ribosome, revealed the outer perimeter of the chloroplast (Figure 2.1 C). The chloroplast extends apically from the basal region to skirt the cytosol, thereby enclosing a central region with the nucleus, cytoplasm, and other organelles. Thylakoids and stroma are interspersed throughout the chloroplast, as seen from the IF staining patterns of marker proteins for these compartments: PsaA (Figures 2.1 D and F) and HSP70B (Figures 2.1 E and G), respectively [101, 110].

Although the chloroplast is widely believed to resemble a cup, with the basal region as its base and a continuous rim with its brim near the apical cell pole [85], my images revealed more complex and variable chloroplast morphologies. Similar features were described previously based on three dimensional reconstructions of a few *Chlamydomonas* cells from serial EM images. In one report, the chloroplast is described as having, instead of an apical rim, a few elongated finger-like lobes [111]. I observed many chloroplasts with such lobes, as seen outlined by the IF signal from the cytoplasmic r-protein (Figure 2.1 C). The authors of another report likened the chloroplast to the white of a boiled egg with the narrowest (apical) end cut off to form an opening and having large perforations in the resulting rim [112]. I saw these features

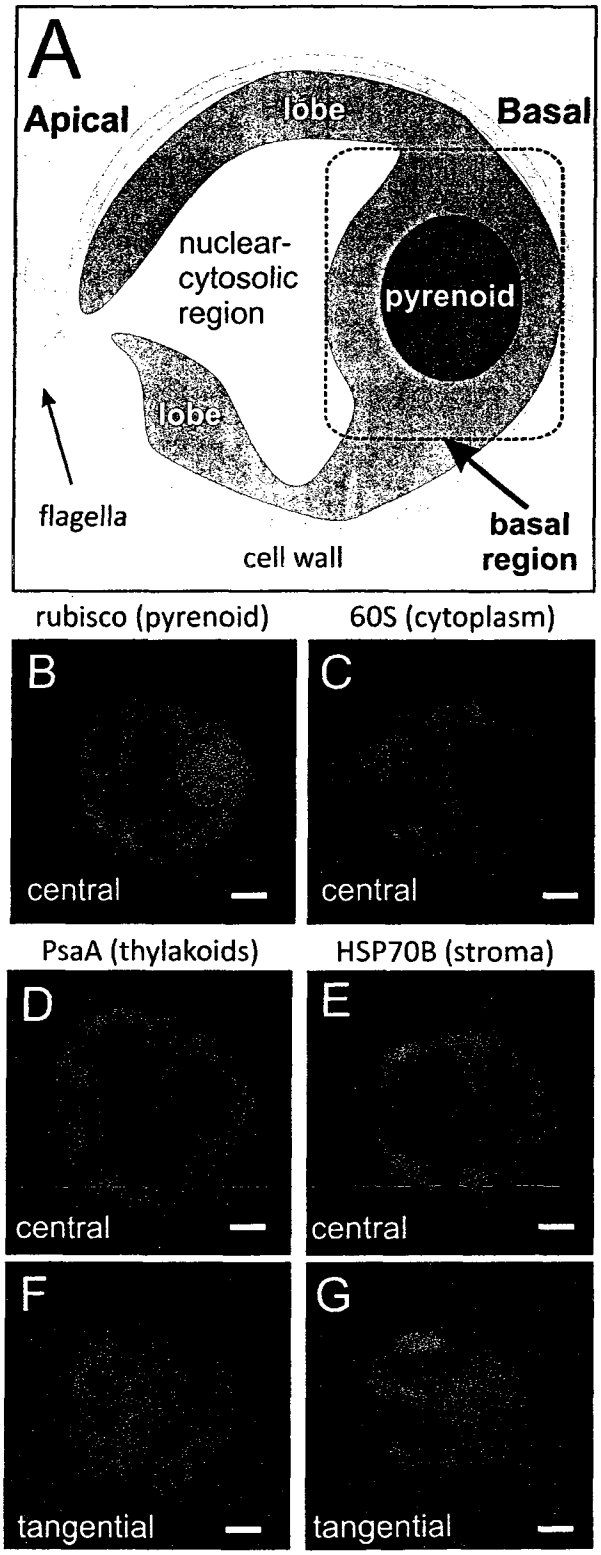

Figure 2.1. IF staining patterns of marker proteins reveal chloroplast anatomy and morphology.

A) An illustration of a typical longitudinal cell section shows the chloroplast (green) as composed of apical lobes and a basal region, which contains the pyrenoid (blue).
B) to G) Images show 0.2 µm central optical sections of cells that were IF-stained for a marker protein for the pyrenoid and thylakoids (Rubisco) **(B)**, the cytoplasm, an r-protein of the 60S subunit of the cytoplasmic ribosome **(C)**, thylakoids (PsaA) **(D)**, and stroma (HSP70B) **(E)**. In tangential optical sections taken between the center and the periphery, **(F)** and **(G)** show the organization of lobes in the same cells shown in **(D)** and **(E)**, respectively. Cells are shown with their apical–basal axis oriented from left to right. Bars, 1.0 µm.

in other cells, in which chloroplast lobes appeared to connect at their apical ends, as seen in the tangential optical sections, which were taken within the forward-most lobes to the viewer (Figures 2.1 F and G).

2.3.2 The *psbA* and *psbC* mRNAs colocalized to discrete regions in the chloroplast basal region during the induction of PS II subunit synthesis and assembly

To determine where chloroplast mRNAs and translation components colocalize specifically for de novo PS II assembly, I first needed to establish conditions that rapidly induce translation for this process but do not significantly induce *psbA* translation for PS II repair. ML (50 to 200 $\mu E \cdot m^{-2} \cdot s^{-1}$) activates the translation of multiple chloroplast mRNAs for the biogenesis of the photosynthesis complexes [21, 94, 113], while preferential *psbA* translation for D1 repair synthesis is evident only under high intensity light (HL; >700 $\mu E \cdot m^{-2} \cdot s^{-1}$) [114, 115]. These two distinct modes of translational regulation were revealed by the results of in vivo ^{35}S pulse-labelling experiments (Figure 2.2). Cells were treated with cycloheximide, which specifically inhibits translation by 80S ribosomes, so that only chloroplast-encoded proteins would be radiolabelled. Cells cultured photoautotrophically under ML (150 $\mu E \cdot m^{-2} \cdot s^{-1}$) synthesized several proteins at higher rates than did cells from the same culture at the end of a 2 h incubation in the dark (Figures 2.2 A, lanes 2 and 3, and 2.2 B, lanes 1 and 2). Hereafter, these are called ML cells and DA cells, respectively. ML cells synthesized PS II subunits primarily for de novo complex assembly, because the bands corresponding to D1 and D2 were of similar intensities, consistent with their equal stoichiometry in the PS II complex. The synthesis of CP43 and CP47 also appeared to be positively regulated by light (see Figure 2.2).

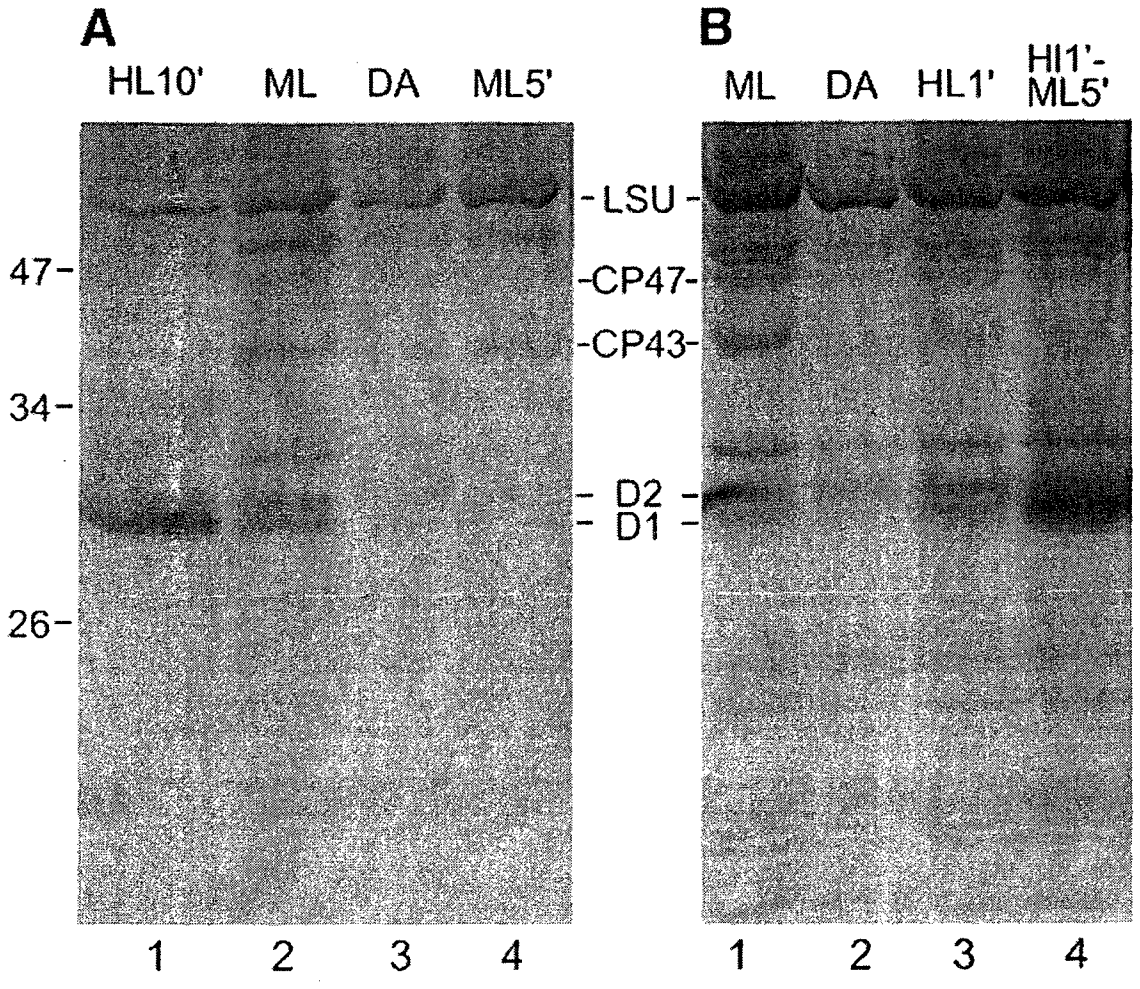

Figure 2.2. Protein synthesis for PS II assembly and repair is induced by light.

Synthesis of the PS II subunits D1, D2, CP43, and CP47 was monitored in vivo by ^{35}S pulse-labelling for 5 min. Protein synthesis by 80S cytoplasmic ribosomes were inhibited by cycloheximide. Of the proteins synthesized by chloroplast ribosomes, D1, D2, CP43, CP47, and LSU were recognized [116]. Cells exposed to high intensity light for 10 min (HL10') preferentially synthesized D1 for PS II repair (**A**, lane 1). Cells cultured under moderate light (ML) synthesized D1, D2, CP43, and CP47 for de novo PS II assembly (**A**, lane 2; **B**, lane 1). Lower levels of synthesis were detected in 2 h dark-adapted cells (DA; **A**, lane 3; **B**, lane 2). The induction of the synthesis of subunits for de novo PS II assembly was detected during a 5 min exposure to ML (ML5'; **A**, lane 4) or following exposure to HL for 1 min (HL1'; **B**, lane 3). Light-induced synthesis was more evident for D1 and D2 than for CP43 and CP47, possibly due to lower levels of these larger proteins that undergo a complete round of synthesis during the 5 min labelling period. HL1' cells exposed to ML for 5 min (HL1'ML5') underwent both PS II subunit synthesis for de novo assembly and preferential D1 synthesis for PS II repair (**B**, lane 4).

Subunit synthesis for de novo PS II assembly was rapidly induced when DA cells were exposed to ML for 5 min (ML5' cells; Figure 2.2 A, lane 4). The similar synthesis levels of D1 and D2 also demonstrated that D1 synthesis was not induced significantly for PS II repair by this 5 min ML exposure. Preferential

D1 synthesis for PS II repair was observed when DA cells were exposed to HL for 10 min, as seen by the predominant ^{35}S labelling of D1 in these HL10' cells (Figure 2.2 A, lane 1). The synthesis of most other proteins was down-regulated in HL10' cells, as reported previously for LSU under less severe light stress conditions [116]. The results in Figure 2.2 B, lanes 3 and 4, are described later in this section.

The green FISH signal seen throughout this section is specific to the *psbA* mRNA because it was not detected in a *psbA* deletion mutant (Figure 2.3 A). Although a *psbC* deletion mutant is not available for this control, the *psbC* FISH signal probably also is specific, because the FISH probes used are not complementary to any other sequence in the chloroplast or nuclear genomes (Table 2.1). The FISH signals from the chloroplast *rbcL* and *psaA* mRNAs (see below) also were absent in deletion mutants for these genes (Figure 2.3 B and C).

As a first approach to identify the location(s) of PS II assembly, FISH was used to determine where mRNAs encoding two PS II subunits colocalize specifically under conditions of their translation (i.e., in ML5' cells but not in DA cells). In DA cells, the FISH signals from the *psbA* and *psbC* mRNAs were detected throughout the chloroplast and their colocalization was seen in a few scattered regions (Figure 2.4 A). By contrast, in all ML5' cells examined, a punctate colocalization pattern was seen at 0.5 to 1.0 μm from

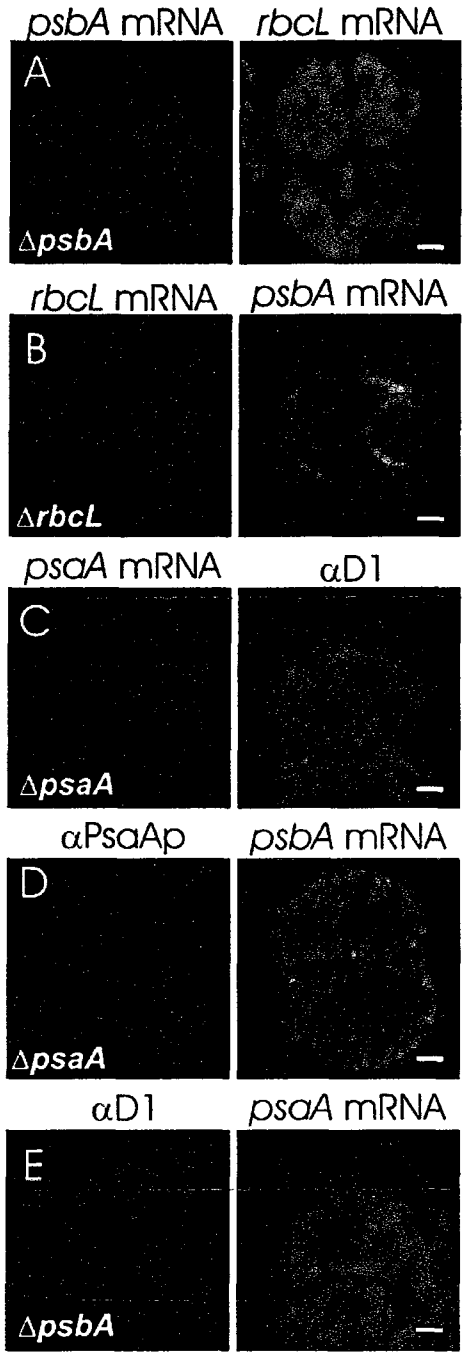

Figure 2.3. Control experiments revealed high specificities of FISH and IF signals.

Deletion mutants for the corresponding chloroplast gene lacked the fluorescence signals from the FISH probes against the mRNAs of (**A**) *psbA*, (**B**) *rbcL*, (**C**) *psaA*, and the IF signals from (**D**) PsaA and (**E**) D1. The right-hand images show the signal of other mRNAs or proteins as positive controls. Each image shows a 0.2 μm optical section. Bars, 1.0 μm.

the pyrenoid, amid weaker *psbA* and *psbC* FISH signals throughout the chloroplast (Figure 2.4 B). This punctate pattern was typically located lateral to the pyrenoid (i.e. above and below the pyrenoid in the images).

The visualization of the punctate colocalization pattern in ML5' cells was hampered by the non-localized FISH signals, which probably were from non-translated *psbA* and *psbC* mRNAs. This was expected because several *Chlamydomonas* chloroplast mRNAs accumulate in excess for their translation and for photoautotrophic growth [117, 118] and the majority of *psbA* mRNAs is not associated with polysomes [119]. To highlight this colocalization pattern, I used the Colocalization Finder plugin of ImageJ (http://www.rsb.info.nih.gov/ij; [120]) to display the pixels in which the signal was strongest in both channels in white, as seen in the fourth column of Figure 2.4 (max colocal). This analysis revealed in all ML5' cells that the strongest colocalized FISH signals were in the discrete regions lateral to the pyrenoid (Figure 2.4 B). This pattern is specific to conditions of PS II assembly (i.e., ML5' cells), because in DA cells the pixels with the strongest colocalized FISH signals were fewer and dispersed within the basal region and some were in lobes (Figure 2.4 A). This pattern is specific to the colocalized *psbA* and *psbC* mRNAs, because the pixels with only one strong FISH signal were not localized in any consistent pattern (data not shown).

These results were the initial evidence that supported our model that *psbA* and *psbC* translation for de novo PS II assembly occurs in the chloroplast basal region generally around the pyrenoid as well as in discrete regions lateral to it, hereafter called T zones (for translation zones). However, additional evidence was required to

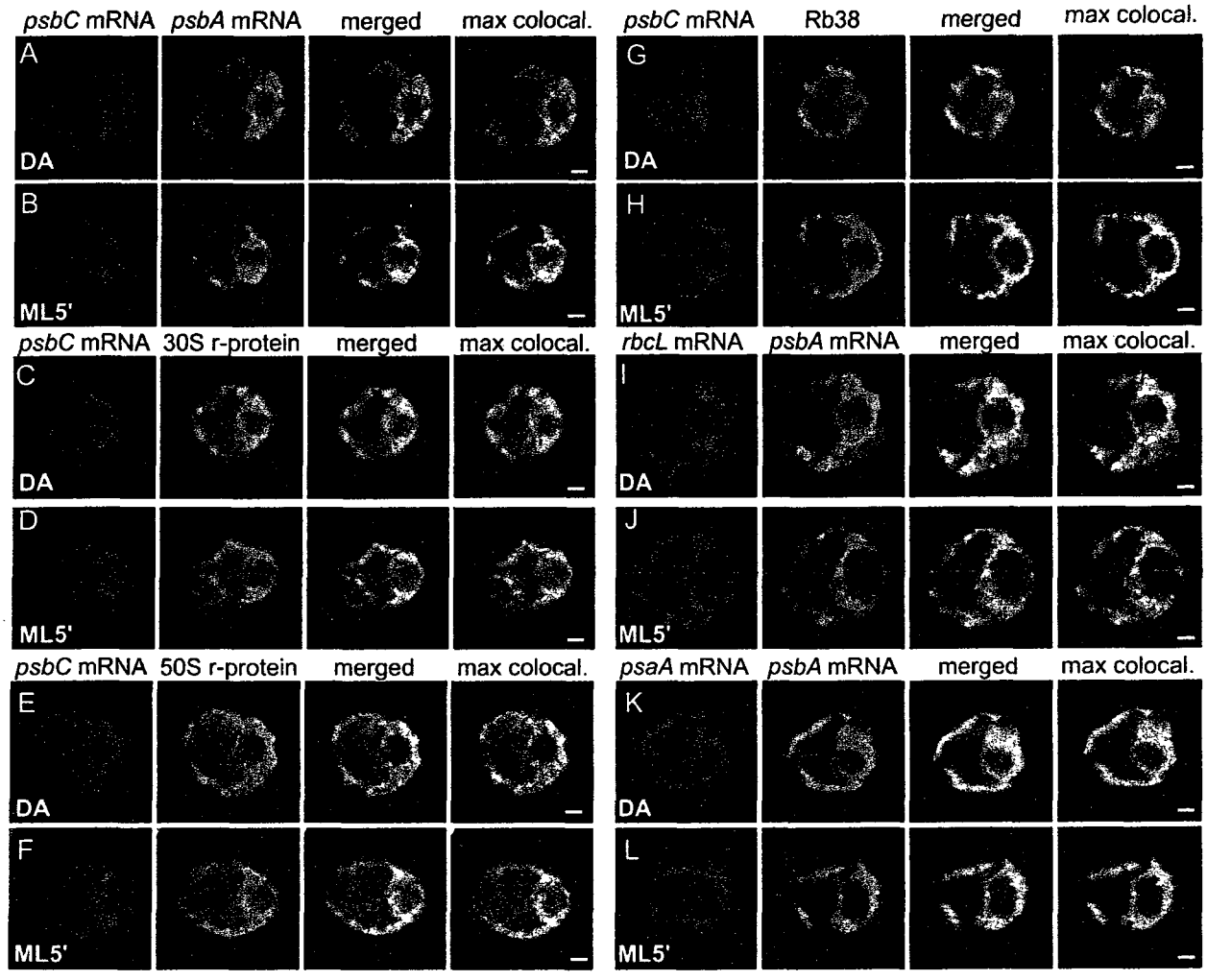

Figure 2.4. Chloroplast mRNAs encoding PS II subunits and chloroplast translation proteins colocalize in specific regions under conditions of PS II assembly.

The induction of subunit synthesis for PS II assembly that occurred while dark-adapted (DA) cells were exposed to ML for 5 min (ML5') correlated with the colocalization near the pyrenoid of the *psbC* mRNA with the *psbA* mRNA (**A** and **B**) and proteins of the chloroplast translation machinery (**C** to **H**). The percentage of cells with the localization patterns seen in each image set and the number of cells examined (n) are given for each condition. Image sets have the *psbC* mRNA FISH signal and the *psbA* mRNA FISH signal in a DA cell (90%; n = 20) and a ML5' cell (100%; n = 20) (**A** and **B**); IF from the r-protein of the 30S chloroplast ribosomal subunit in a DA cell (83%; n = 40) and a ML5' cell (100%; n = 20) (**C** and **D**); IF from the r-protein of the 50S subunit in a DA cell (83%; n = 40) and a ML5' cell (100%; n = 20) (**E** and **F**); and IF from the RNA binding protein RB38 in a DA cell (88%; n = 40) and a ML5' cell (100%; n = 20) (**G** and **H**). Non-colocalization in T zones can be seen for the *psbA* mRNA FISH signal with the *rbcL* mRNA FISH signal in a DA cell (100%; n = 8) (**I**) and a ML5' cell (100%; n = 10) (**J**) and with the *psaA* mRNA FISH signal in a DA cell (100%; n = 10) (**K**) and a ML5' cell (100%; n = 9) (**L**). The fourth column shows merged images in which the pixels with the strongest colocalized signals are highlighted in white (max colocal.). Each image shows a 0.2 μm optical section. Bars, 1.0 μm.

demonstrate that mRNAs are localized in T zones for their translation rather than for other steps of their expression or their degradation.

2.3.3 Chloroplast r-proteins colocalized with the *psbC* and *psbA* mRNAs in T Zones specifically during PS II assembly

If *psbA* and *psbC* mRNAs colocalized in T zones for their translation, chloroplast ribosomes should colocalize with them specifically under conditions of de novo PS II assembly (i.e., in ML5' cells but not in DA cells). To test this prediction, I analyzed the in situ distributions of r-proteins of both subunits of the chloroplast ribosome, each in pair-wise combinations with the *psbC* and *psbA* mRNA FISH signals and in both DA and ML5' cells. In all ML5' cells examined, T zones had the strongest colocalized r-protein IF signal and FISH signal from either mRNA (Figure 2.4 D and F). By contrast, in most DA cells examined, maximal colocalization was more dispersed (Figure 2.4 C and E). Thus, these results indicate that both subunits of the chloroplast ribosome colocalize with the *psbA* and *psbC* mRNAs in the T zones specifically when the translation of these mRNAs is induced for PS II assembly (ML5' cells), consistent with protein synthesis for PS II assembly occurring in these regions.

2.3.4 Localization of the RNA binding protein RB38

I performed a similar analysis with RB38, an RBP that has been proposed to regulate the translation of the *psbA* mRNA [121]. RB38 has recently been identified as an RBP called RB40 and it was demonstrated that this protein is specifically required for translation initiation on the chloroplast *psbD* mRNA for PS II biogenesis [122]. In both DA and ML5' cells, the RB38 IF signal was distributed throughout the chloroplast (Figure 2.4 G and H).

However, in most ML5' cells, but not in DA cells, the strongest colocalized signals from RB38 and the *psbC* mRNA were primarily in T zones. Thus, the colocalization of this RBP with the *psbC* mRNA in T zones specifically in ML5' cells further supports my hypothesis that the synthesis of PS II subunits occurs in these regions.

2.3.5 Statistical analyses confirmed the colocalization patterns

The colocalization patterns shown in Figure 2.4 were quantified and statistically tabulated across the DA and ML5' conditions. I used Colocalization Finder (ImageJ) to determine the percentage of pixels that had strong signal from both molecules under comparison specifically in sampled regions (100 pixels) where T zones were observed in ML5' cells. The mean percent of pixels with strong colocalized signals in these regions of ML5' cells, relative to that in DA cells, was higher by 3.6-fold ($P < 0.001$) for the *psbA* and *psbC* mRNAs, by 2.2-fold ($P = 0.001$) and 6.4-fold ($P < 0.001$) for the *psbC* mRNA and the r-proteins of the 30S and 50S ribosomal subunits, respectively, and by 14.3-fold ($P < 0.001$) for the *psbA* mRNA and RB38 (Figure 2.5).

2.3.6 The mRNAs of *rbcL* and *psaA* are not recruited to T zones in ML5' cells

To determine whether chloroplast mRNAs encoding subunits of other photosynthesis complexes localize to T zones for their translation, I performed the analyses described above for the colocalization of the FISH signals of the mRNAs of the chloroplast genes *rbcL* and *psaA* relative to the *psbA* mRNA. *rbcL* and *psaA* encode LSU and the PsaA subunit of PS I, respectively [99]. Neither of these mRNAs showed any particular pattern of colocalization with the *psbA* mRNA; the pixels with the strongest colocalized signals were seen at apparently random locations throughout the chloroplast in both DA cells

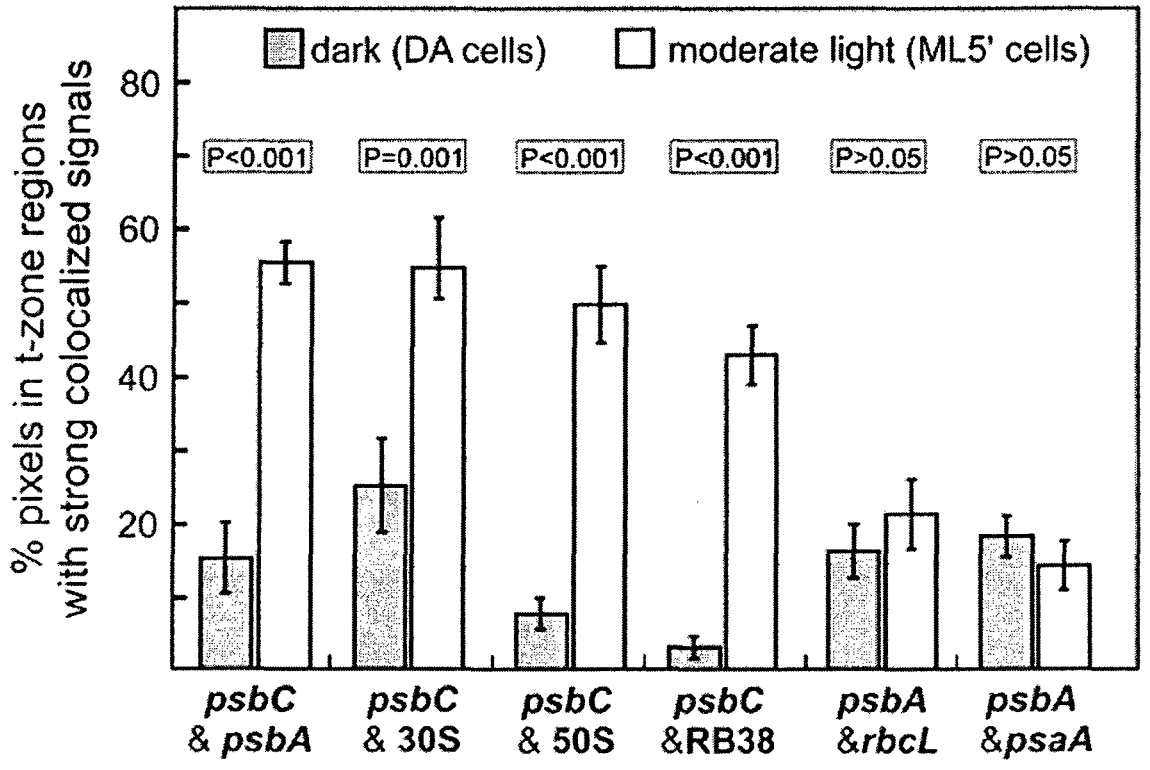

Figure 2.5. Statistical analysis of colocalization in regions where T zones are located across the DA and ML5' conditions.

Within multiple images of DA cells and ML5' cells, regions (100 pixels) located midway between the pyrenoid and the lateral cell periphery were subjected to analysis by Colocalization Finder (ImageJ) to determine the percentage of pixels with strong colocalized signals in the combinations indicated on the x-axis. Bars indicate mean values for DA cells (gray bars) and ML5' cells (white bars). Error bars indicate 2 SE. In ML5' cells relative to DA cells, statistically significantly higher levels of percentage colocalization were observed for the *psbA* and *psbC* mRNAs and the *psbC* mRNA with respect to each of the chloroplast ribosomal subunits (30S and 50S) and RB38. In ML5' cells relative to DA cells, no significant increase was observed in the mean percentage colocalization of the *psbA* mRNA with the *rbcL* mRNA or the *psaA* mRNA in the regions of T zones.

and ML5' cells (Figure 2.4 I to L). In cells cultured under constant ML, the *rbcL* mRNA localized generally around the pyrenoid, as described in Chapter 3. However, this pattern was established only 2 hr after a shift from dark to light conditions and, therefore, not observed in ML5' cells. In regions where T zones are located, the mean percentage of pixels with the strongest colocalized FISH signals was not significantly different between DA and ML5' cells (Figure 2.5) ($P > 0.05$). For the *rbcL* mRNA, this was not due to a constant level of its translation, because LSU synthesis was higher in ML5' cells than in DA cells (Figure 2.2 A, lanes 3 and 4). Moreover, positive light regulation of *rbcL* translation was demonstrated in a more comprehensive study that controlled for the level of the *rbcL* mRNA [124]. Therefore, the *rbcL* mRNA is not localized specifically to T zones during the induction of its translation in ML5' cells. However, it is not known whether *psaA* translation is activated by light. Therefore, it remains possible that localized *psaA* translation in T zones is not enhanced in ML5' cells and, therefore, is not detectable by this approach. Nevertheless, this result supports my conclusion that the *psbA* and *psbC* mRNAs colocalized in T zones for their translation for de novo PS II assembly. Additional research is required to determine whether T zones house subunit synthesis for the assembly of thylakoid membrane complexes other than PS II.

2.3.7 T zones are within stroma and overlap thylakoids

To address the location of the T zones, I localized them with respect to the marker proteins for stroma and thylakoids, HSP70B and PsaA, respectively [101, 110]. Although it was not possible to precisely determine where the *psbA* and *psbC* mRNAs localized due to the limited resolution of confocal microscopy and the interspersion of these

compartments, a few important observations were made. The FISH signals from each of these mRNAs in T zones were within regions of HSP70B or PsaA IF, which were of variable intensities and extended throughout most of the chloroplast (Figures 2.6 B and D). Clearly, T zones do not correspond to stroma and thylakoids throughout the chloroplast. Thus, my hypothesis that translation for PS II assembly occurs in T zones contradicts the current model that this process occurs generally at non-appressed thylakoid membranes. My data are consistent with the initiation steps of *psbA* and *psbC* translation occurring in the stroma around the pyrenoid and the subsequent synthesis of D1 and CP43 into the neighbouring thylakoid membranes (see Discussion section 2.5).

The similar distributions of both HSP70B (Figures 2.6 A and B) and PsaA (Figures 2.6 C and D) in DA and ML5' cells exclude the possibility that the localization patterns that formed in the T zones (Figure 2.4 B, D, F, and H) resulted from the redistribution of stroma or thylakoids. For example, the T zones clearly are not pockets of stroma with free chloroplast mRNAs, chloroplast ribosome subunits, and RB38.

2.3.8 In the FUD34 mutant, *psbA* mRNAs are localized near the pyrenoid by their translation

I took advantage of the repertoire of *Chlamydomonas* mutants that are affected in PS II assembly to address the location of translation for de novo PS II assembly. FUD34 is specifically defective for translation of the *psbC* mRNA due to a mutation in its 5' untranslated region [99, 125]. My initial rationale was to examine FUD34 cells for the absence of a *psbC* mRNA localization pattern that is formed in wild-type cells to identify the location of CP43 synthesis for PS II assembly. However, this was not possible

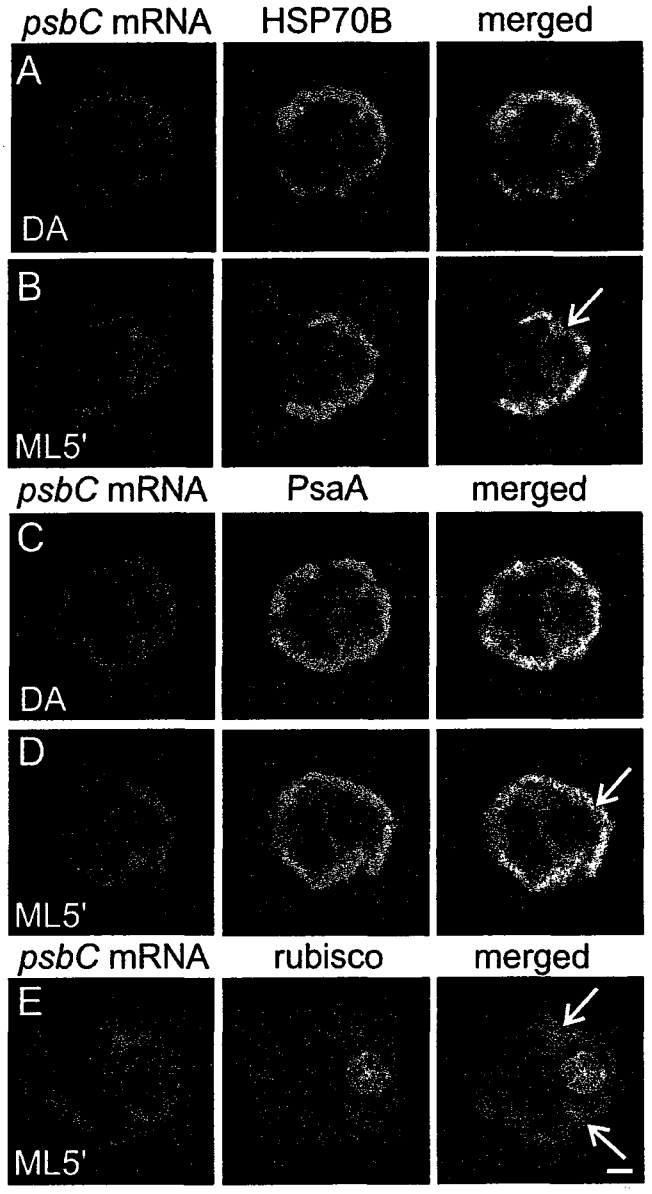

Figure 2.6. Localization of the *psbC* mRNA was compared with the distributions of chloroplast stroma and thylakoids under differential conditions for de novo PS II assembly.

The distributions of the *psbC* mRNA and marker proteins for chloroplast stroma and thylakoids are compared before and after the induction of PS II subunit synthesis in DA and ML5′ cells, respectively. Image sets show the *psbC* mRNA FISH signal and IF from the marker protein for stroma (HSP70B) in a DA cell (100%; n = 20) and a ML5′ cell (100%; n = 20) (**A** and **B**), the marker protein for thylakoids (PsaA) in a DA cell (100%; n = 20) and a ML5′ cell (100%; n = 20) (**C** and **D**), and the marker protein for the pyrenoid (Rubisco; 100%; n = 20) (**E**). Arrows indicate where the *psbC* FISH signal is localized in T zones. The percentage of cells with the localization patterns seen in each image set (and described in the text) and the number of cells examined (n) are given above. Each image shows a 0.2 μm optical section. Bar, 1.0 μm.

because detection of the relevant localization patterns in wild-type cells (Figure 2.4) required the induction of de novo PS II biogenesis with light, a process that requires functional PS II [126]. As FUD34 is deficient for PS II, this mutant and the wild-type control strain had to be cultured heterotrophically in the dark (see Methods section 2.3).

Unexpectedly, much of the *psbA* FISH signal was localized within 1 μm of the pyrenoid in >90% of the FUD34 cells analyzed (Figure 2.7 B). By contrast, 92% of wild-type cells did not show this pattern under the same conditions (Figure 2.7 A). It was not unexpected that the *psbA* mRNA could be translated in the dark under these heterotrophic growth conditions, because the acetate provided as a reduced carbon source is known to induce protein synthesis in the *Chlamydomonas* chloroplast in the dark [95]. This result seemed consistent with my hypothesis that protein synthesis for de novo PS II assembly occurs near the pyrenoid, considering that FUD34 translates the *psbA* mRNA at a wild-type level for the assembly of PS II complexes lacking CP43 [35] and the FUD34 cells did not translate the *psbA* mRNA for PS II repair (because they were cultured in the dark).

To determine whether these localized *psbA* mRNAs are translated and anchored by their nascent D1 chains to membranes around the pyrenoid, I asked whether the abolition of translation in the chloroplast delocalizes them. All FUD34 cells treated for 10 min with an inhibitor of translation initiation by chloroplast ribosomes, lincomycin [105], showed a dispersed distribution of the *psbA* FISH signal (Figure 2.7 C). This result strongly suggests that the majority of the *psbA* mRNAs localized near the pyrenoid in

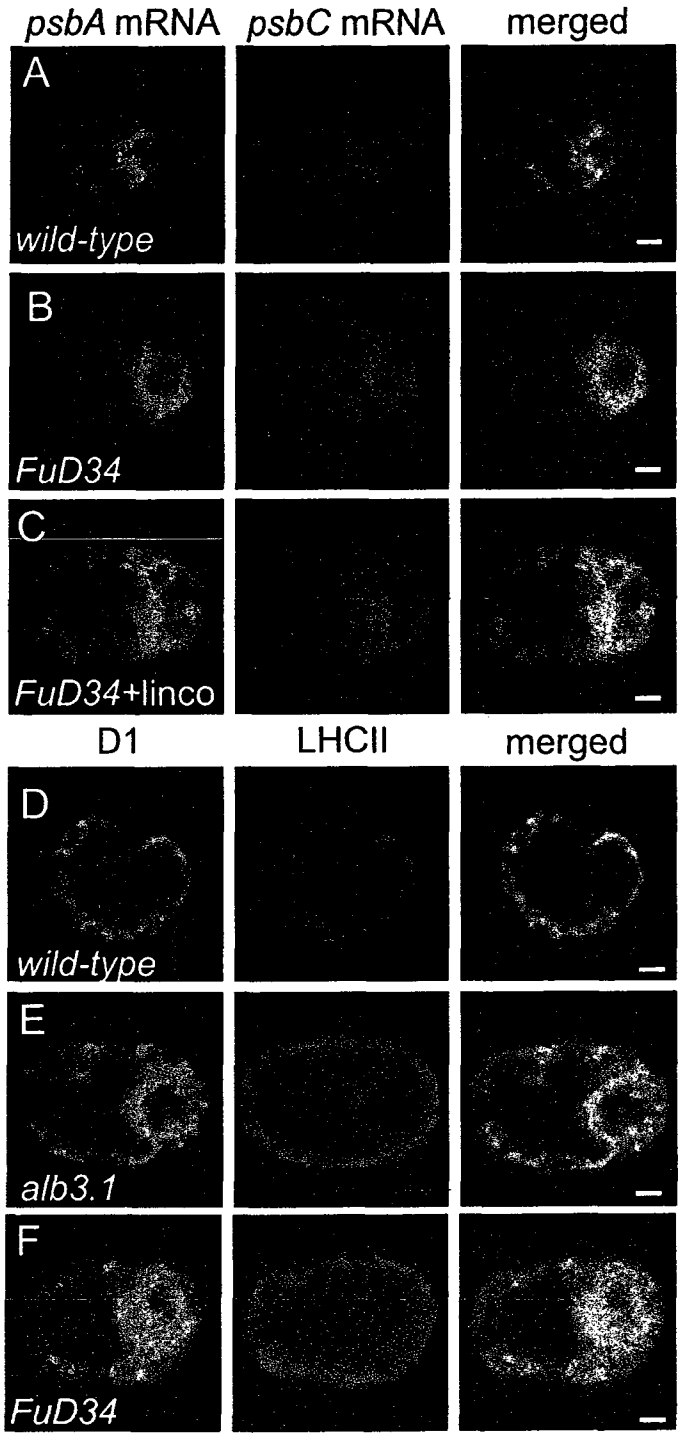

Figure 2.7. Analyses of two PS II assembly-impaired mutants: FUD34 and an alb3.1 mutant.

(A) to **(C)** Translation-dependent localization of the *psbA* mRNA near the pyrenoid was detected in the *psbC* translation mutant FUD34. The FISH signals from *psbA* and *psbC* mRNAs are shown in a wt cell (92%; n = 36) (**A**), an FUD34 mutant cell (90%; n = 20) (**B**), and an FUD34 mutant cell treated with lincomycin, an inhibitor of translation initiation by chloroplast ribosomes (100%; n = 20) (**C**). **(D)** to **(F)** Unassembled D1 and the incompletely assembled PS II subcomplex were detected around the pyrenoid in the alb3.1 mutant and FUD34, respectively, where we propose they mark the location of PS II subunit synthesis and assembly. The IF signals from D1 and LHCII are seen in a wt cell (100%; n = 20) (**D**), an alb3.1 mutant cell (81%; n = 89) (**E**), and an FUD34 mutant cell (90%; n = 20) (**F**). The percentage of cells with the localization patterns seen in each image set (and described in the text) and the number of cells examined (n) are given above. Each image shows a 0.2 µm optical section. Bars, 1.0 µm.

this mutant are translated and that this localization requires their translation. Since, in FUD34, the *psbA* mRNA is translated for (incomplete) PS II assembly, these results provide further support of my hypothesis that de novo PS II subunit synthesis occurs near the pyrenoid in the wild-type.

The *psbA* mRNA FISH signal that encircled the pyrenoid in FUD34 is distinct from the colocalization patterns in T zones, which are punctate and typically located lateral to the pyrenoid (Figure 2.4). However, in ML5' cells, I also observed a similar ring of colocalized *psbA* and *psbC* mRNAs and of the *psbC* mRNA colocalized with the r-proteins or RB38, which was not observed in most DA cells (the merged images of DA cells with ML5' cells in Figure 2.4). This region weakly IF-stained for the marker proteins for stroma and thylakoids (Figures 2.6 B and D, respectively).

2.3.9 In an ALBINO3.1 mutant and FUD34, intermediates of de novo PS II assembly localize near the pyrenoid

Additional evidence for the occurrence of PS II assembly specifically near the pyrenoid was obtained from in situ localization studies of the incompletely assembled PS II subcomplex in FUD34 and the unassembled D1 in an ALBINO3.1 mutant. I predicted that these PS II assembly intermediates might mark the location of the synthesis and assembly of chloroplast-encoded PS II subunits [31]. ALBINO3.1 functions in the incorporation of D1 during de novo PS II assembly; in the alb3.1 mutant, ac29, D1 is synthesized and integrated into the thylakoid membrane at a wild-type rate, but only 10% is assembled into functional PS II complexes [127, 128]. D1 and LHC II are components of the PS II-LHC II supercomplex in thylakoid membranes (reviewed in

[129]. In alb3.1 mutant cells, LHC II associates only with these assembled PS II complexes [128]. Therefore, to characterize the localization of the unassembled D1 in this mutant, I determined where the IF signal of D1 is in excess over that of LHC II. In all wild-type cells, the IF signals from D1 and LHC II colocalized throughout the chloroplast (except within the pyrenoid; Figure 2.7 D), consistent with previously reported results of immunogold EM [130]. By contrast, the majority of the alb3.1 cells had a dramatic localization of D1 in the chloroplast basal region, particularly within approximately 1 μm of the pyrenoid (Figure 2.7 E). This region only weakly IF-stained for LHC II, suggesting that the unassembled D1 in this mutant is localized there. This is in contrast with the lobes and the margin of the basal region, where LHC II IF was stronger than D1 IF, consistent with the proper localization of the fewer PS II-LHC II supercomplexes that assemble in this mutant. Similarly, most FUD34 cells showed localization of D1 in this pattern (Figure 2.7 F). This D1 IF signal was mostly or entirely from the incompletely assembled PS II subcomplex, because a previous study found all detectable D1 with this subcomplex in FUD34 [35]. In FUD34, LHC II probably accumulates in the absence of its association with PS II, as has been found in a mutant that is defective in the association between these complexes [131].

A general disorganization of thylakoid membranes does not localize unassembled D1 and the PS II subcomplex near the pyrenoid in the alb3.1 mutant and FUD34, respectively, because the LHC II distribution in both mutants appeared wild-type. Thus, these results further support my hypothesis that protein synthesis occurs for de novo PS II assembly in the region surrounding the pyrenoid (see Discussion).

2.3.10 *In situ evidence for D1 repair synthesis at thylakoids throughout the chloroplast*

The incorporation of newly synthesized D1 subunits into photodamaged PS II complexes during HL stress conditions is believed to occur at stromal thylakoid membranes, based on previously reported results of thylakoid subfractionation experiments [19]. However, to my knowledge, there are no reported in situ data regarding the location of this process. Therefore, I used fluorescence confocal microscopy to address this question. In HL10' cells, the specific induction of D1 synthesis for PS II repair (Figure 2.2 A, lane 1) correlated with a diffuse distribution of the *psbA* FISH signal throughout the chloroplast, where it colocalized with IF from the thylakoid marker protein PsaA, a chloroplast r-protein, and RB38 (Figure 2.8 A to C). This pattern is not common to all chloroplast mRNAs during this HL stress condition, because the *rbcL* mRNA was more concentrated around the pyrenoid in HL10' cells (Figure 2.8 D). This localization pattern will be described further in a subsequent report. These results are consistent with the current model that D1 repair synthesis occurs generally at non-appressed thylakoid membranes, because they did not reveal a specific location of *psbA* translation in cells carrying out this process.

Affirmative results in support of this conclusion were obtained when I looked for colocalization of *psbA* mRNA with the r-protein of the 30S ribosomal subunit that formed during the induction of PS II repair in cells that had localized *psbA* and *psbC* mRNAs in T zones. In this experiment, the initial localization of the *psbA* mRNA in T zones provided a reference for the identification of a repair-specific localization pattern.

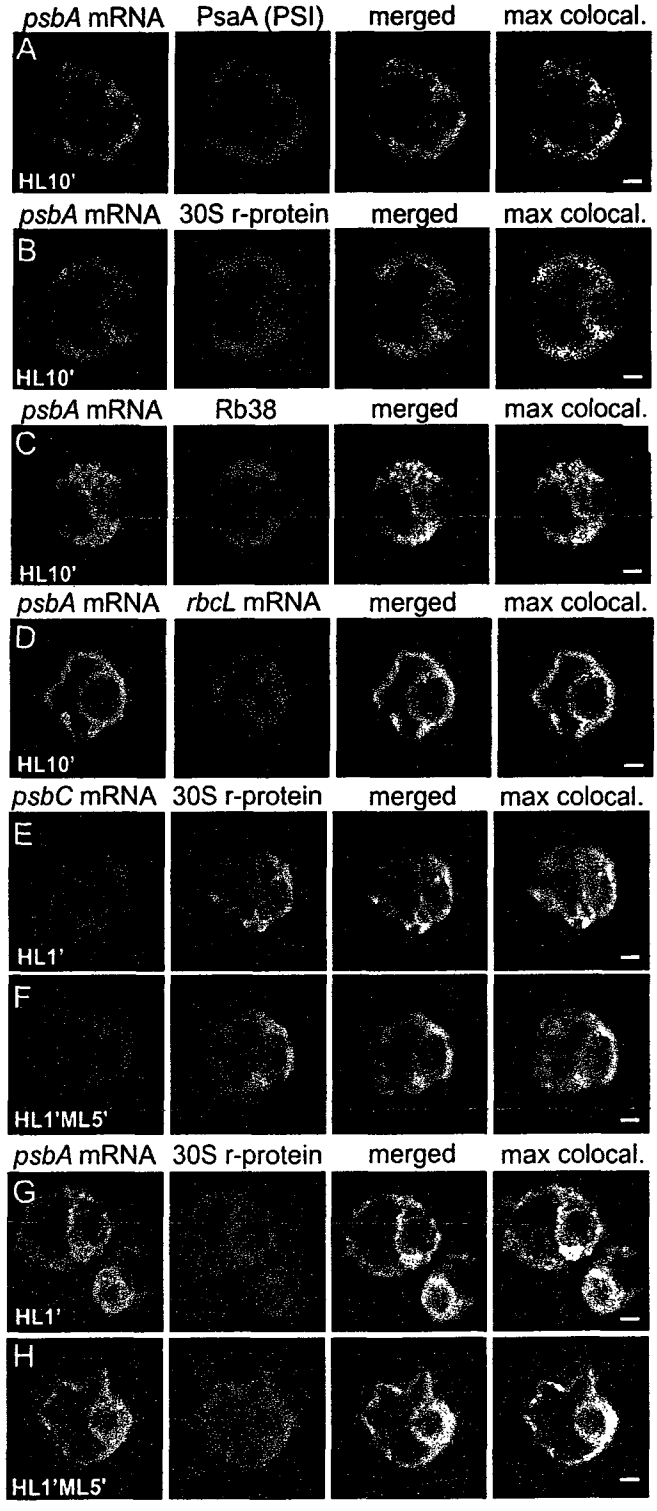

Figure 2.8. Under conditions of D1 repair synthesis, the *psbA* mRNA colocalized with thylakoids and translation-components throughout the chloroplast.

(**A**) to (**D**) DA cells were exposed to HL for 10 min (HL10' cells) to induce PS II photodamage and D1 repair synthesis and then FISH-probed for the *psbA* mRNA and concurrently IF-stained for the thylakoid marker protein PsaA (100%; n = 20) (**A**), the r-protein of the 30S subunit of the chloroplast ribosome (100%; n = 20) (**B**), the RNA binding protein RB38 (100%; n = 20) (**C**), or the *rbcL* mRNA (**D**). (**E**) to (**H**) Cells were IF-stained for the r-protein of the 30S chloroplast ribosomal subunit and co-FISH-probed for the *psbC* mRNA (**E** and **F**) or the *psbA* mRNA (**G** and **H**). The *psbA* and *psbC* mRNAs colocalized with the 30S ribosomal subunit r-protein in T zones during the induction of PS II assembly in DA cells that were exposed to HL for 1 min (**E** and **G**, respectively). Distinct localization of the *psbA* and *psbC* mRNAs during the D1 repair synthesis was induced during subsequent 5 min incubation under ML (**E** and **G**, respectively). The percentage of cells with the localization patterns seen in each image set (and described in the text) and the number of cells examined (n) are given above. The fourth column shows merged images in which the pixels with the strongest colocalized signals are highlighted in white. Each image shows a 0.2 μm optical section. Bars, 1.0 μm.

The *psbC* mRNA localized in T zones provided a negative control as an mRNA whose translation is not induced during PS II repair (Figure 2.2 A, lane 1) [132]. When DA cells were exposed to HL for only 1 min (HL1' cells), D1 and D2 synthesis were induced for de novo PS II assembly (Figure 2.2 B, lanes 2 and 3) and the strongest colocalized signals from the 30S subunit r-protein and either the *psbA* mRNA or the *psbC* mRNA were in T zones (Figure 2.8 E and G, respectively), as was observed in ML5' cells (Figure 2.4). This localization pattern was more distinct for the *psbC* mRNA than for the *psbA* mRNA, possibly because these cells were also inducing *psbA* translation for PS II repair, which became evident after a 5 min incubation under ML (HL1'ML5') (Figure 2.2 B, lane 4). This delayed induction of D1 repair synthesis occurred amid a sustained subunit synthesis for PS II assembly (Figure 2.2 B, lane 4). During this 5 min incubation under ML, the strongest colocalized signals from the *psbC* mRNA and the 30S r-protein remained localized in T zones in most HL1'ML5' cells (Figure 2.8 F).

However, in these HL1'ML5' cells, the strongest colocalized signals from the *psbA* mRNA and the 30S subunit r-protein were broadly distributed throughout the basal region and within the lobes (Figure 2.8 H). Therefore, the appearance of this dispersed distribution pattern correlated with the induction of D1 repair synthesis, and this was not seen for the *psbC* mRNA and the 30S subunit r-protein. These results further support the localization of the *psbA* translation throughout regions of the chloroplast with thylakoid membranes for the repair of photodamaged PS II complexes.

2.4 Discussion

My results provide in situ evidence for the current model that D1 synthesis for PS II repair occurs in stromal thylakoid membranes throughout the chloroplast (Figure 2.8) [19]. They also contribute to the emergent realization that the processes underlying chloroplast biogenesis are highly compartmentalized by providing three lines of evidence showing that PS II subunit synthesis and assembly occur in a specific region of the chloroplast. First, during the rapid induction of PS II assembly, I observed in punctate regions lateral to the pyrenoid, termed T zones, the colocalization of multiple components of PS II subunit synthesis: the *psbC* and *psbA* mRNAs, chloroplast r-proteins, and RB38 (Figure 2.4). Weaker colocalized signals from these mRNAs and translation proteins were localized with stroma and thylakoids around the pyrenoid, specifically in ML5' cells (Figure 2.4 B, D, F, and H). The T zones were typically within this region. Second, in the *psbC* translation-deficient mutant FUD34, ongoing *psbA* translation for attempted PS II assembly correlated with the translation-dependent localization of the *psbA* mRNA around the pyrenoid (Figure 2.7 B and C). Third, in two PS II assembly mutants, unassembled D1 and a partially assembled PS II subcomplex accumulate around the pyrenoid (Figure 2.7 E and F), where I propose that they mark a compartment of PS II subunit assembly (see below).

2.4.1 On the location of the PS II assembly compartment

Most T zones did not contact the pyrenoid (Figure 2.6 E). T zones probably are within stroma, based on comparisons of the *psbC* mRNA FISH signal and IF from HSP70B (Figure 2.6 B). Close inspection of ML5' cells that were FISH-probed for either mRNA and co-IF-

stained for the thylakoid marker protein PsaA revealed that most T zones overlapped with regions of the basal chloroplast that were densely populated by thylakoids (Figure 2.6 D).

Previous EM studies revealed that the pyrenoid is surrounded by starch plates, then by a sphere of stroma, and that stroma and thylakoids are interspersed throughout the rest of the chloroplast [85]. Chua et al. [21] proposed that translation initiation of the *Chlamydomonas* chloroplast mRNAs encoding thylakoid membrane proteins occurs in the stroma and that these ribosomes subsequently localize at thylakoid membranes for the insertion of their polypeptide products. My results are consistent with these steps occurring specifically in stroma and thylakoids within the T zones and generally around the pyrenoid.

The chloroplast envelope appears not to be a major location of PS II subunit synthesis and assembly (see Introduction section 2.2): the chloroplast periphery was not enriched in chloroplast mRNAs, chloroplast r-proteins, or RB38 under any of the conditions examined. However, my data and most of the evidence for the synthesis and assembly of photosynthetic complexes at the inner envelope membrane can be reconciled if thylakoid biogenesis occurs in an internal chloroplast membrane compartment that has properties of the chloroplast envelope (reviewed in [8]). It will be important to characterize T zones and the membranes around the pyrenoid to determine whether or not they contain known photosystem assembly factors, enzymes of chlorophyll and thylakoid membrane lipid biosynthesis, and the light-activated RBPs

that have been proposed to localize chloroplast mRNAs for thylakoid biogenesis [13, 42, 61].

In published EM images of the chloroplast basal region, I noticed discrete structures with the same approximate size and location as T zones that appeared to be distinct from thylakoids and more electron dense than stroma [85]. Thylakoids connected with these structures, and a few thylakoid vesicles extended into them. Only one report mentioned these structures, in *Chlamydomonas moewusii*, and proposed that they contain chloroplast DNA because they were seen to contain fibres [133]. Transcription could not have generated the colocalization patterns involving the mRNAs in T zones because chloroplast nucleoids (the structures that contain multiple copies of the chloroplast genome) did not consistently colocalize with the mRNAs in T zones stained with 4',6-diamidino-2-phenylindole (Figure 2.9 A). Moreover, their formation was not affected by rifampicin, an inhibitor of the chloroplast RNA polymerase in *Chlamydomonas* (Figure 2.9 B). Also, the *psbA* FISH probes hybridize across exon junctions and, therefore, do not detect the *psbA* gene or unspliced mRNAs (see Methods section 2.3). It is improbable that mature transcripts could be generated from a 6.6 kbp gene with four introns within the 2 to 3 min that the *psbA* mRNAs localized to T zones in HL1' cells (Figure 2.8 G).

2.4.2 Light regulates translation for PS II assembly and repair

The results of ^{35}S pulse-labelling experiments shown in Figure 2.2 indicate distinct modes of light regulation of protein synthesis in chloroplasts for PS II assembly and repair. While these modes of regulation have been described previously, the distinction

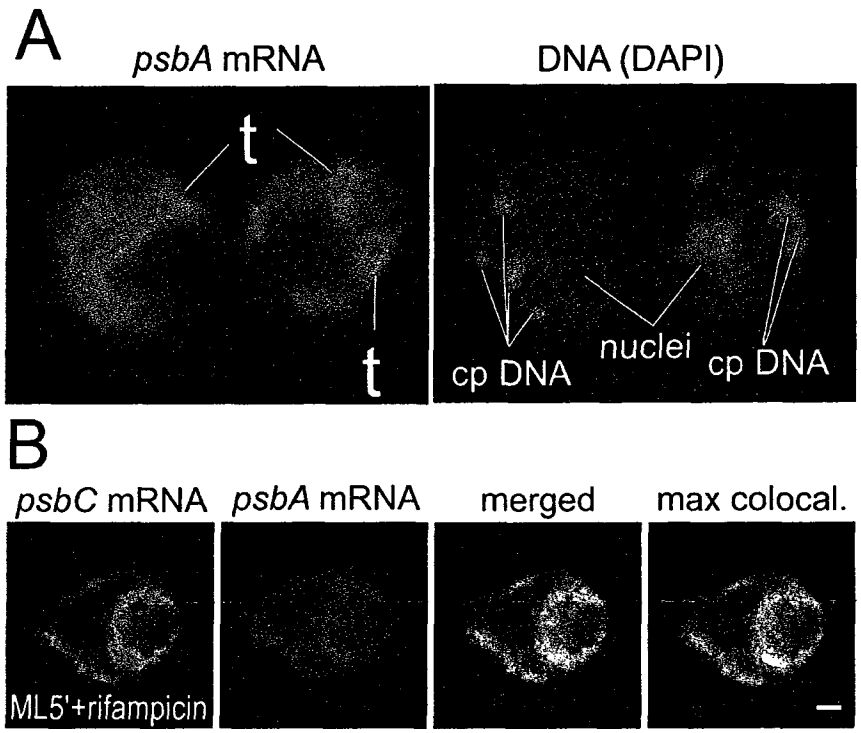

Figure 2.9 *psbA* transcription does not generate the localized *psbA* mRNAs in T zones.

(A) Epifluorescence microscopy images show ML5' cells that were FISH-probed for the *psbA* mRNA and concurrently stained with DAPI to reveal of chloroplast nucleoids (cpDNA). In the right-hand image the *psbA* FISH signal in T zones are indicated with "t". Nuclei are indicated. The upper T zone of the right-hand cell does not stain with DAPI. Other chloroplast nuclei do not have strong *psbA* FISH signal. **(B)** In the presence of rifampicin, an inhibitor of the chloroplast RNA-polymerase, the *psbC* and *psbA* mRNAs colocalized in T zones (90%, n= 20). Bar, 1 μm.

between them has not been emphasized in most publications. The mechanisms underlying these modes of light regulation, at least in *Chlamydomonas*, probably are distinct, because the *psbA* 5' untranslated region mediates the former [134, 135] but not the latter [132]. One study showed a clear distinction between the regulation of *psbA* translation by autofeedback repression for PS II assembly and by HL for D1 repair synthesis [132].

2.4.3 The morphology of the *Chlamydomonas* chloroplast is complex

Chloroplasts in my images did not have the generally accepted cup-like morphology with the apical chloroplast as a continuous rim (Figure 2.1). Rather, I observed the chloroplast morphology seen in three-dimensional reconstructions of a few cells that were made from serial EM images [111, 112]. This morphology is retained by isolated chloroplasts [136], suggesting that it is maintained by a plastoskeleton [137]. Clearly, the morphology of the *Chlamydomonas* chloroplast is complex and additional research is required to characterize it and the molecules and mechanisms underlying it.

2.4.4 PS II biogenesis may occur in a spatiotemporal pathway

My proposal that the synthesis and assembly of PS II subunits occur near the pyrenoid requires a process by which newly assembled complexes get to thylakoids throughout the chloroplast. Several of my results suggest the existence of a spatiotemporal pathway of PS II biogenesis. In this model, T zones would house the earliest stages of PS II subunit synthesis and assembly. Indeed, the colocalization patterns were detected in these regions within 1 min of light exposure (Figure 2.8 E and G). An intermediate stage in this pathway could be located around the pyrenoid, where I observed the accumulation of

unassembled D1 and the PS II subcomplex in steady state conditions in the alb3.1 mutant and FUD34, respectively (Figure 2.7 E and F). The colocalized mRNAs and translation machinery components that I observed distinctly around the pyrenoid specifically in ML5' cells, and the translation-dependent localization of the *psbA* mRNA in this region in FuD34 (Figure 2.7 B), also could reflect protein synthesis for PS II biogenesis in this proposed intermediate compartment.

Such a spatiotemporal pathway of PS II biogenesis could involve a branch of the vesicular transport system that functions within chloroplasts for thylakoid biogenesis [37, 38, 40, 85]. Alternatively, newly assembled PS II complexes might laterally migrate within pre-existing thylakoid membranes, which are largely contiguous between the basal region and the entire length of the lobes [85]. As a third possibility, thylakoids could be built upon their termini in the basal region, where they are anchored at the pyrenoid and, consequently, being pushed in an apical direction either into the lobes or even to generate the lobes during chloroplast differentiation. The pyrenoid has a system of tubules into which thylakoid vesicles extend [138]. The function(s) of these tubules, and why they contain thylakoid vesicles, are longstanding mysteries. In this third model, pyrenoid tubules could serve as the anchors.

In the context of this spatiotemporal model for PS II assembly, my observation that unassembled D1 and the PS II subcomplex localize around the pyrenoid in the alb3.1 mutant and FUD34, respectively (Figure 2.7 E and F), suggests the existence of a quality-control checkpoint that ensures that only assembled PS II complexes are transported outward. This would be analogous to the system that retains non-native

and incompletely assembled complexes in the rough ER [139]. Indeed, the half-lives of this unassembled D1 and the PS II subcomplex are >1 h [35, 128], suggesting that they should disperse by diffusion unless they are retained by some mechanism, such as a quality-control checkpoint in an active transport system.

Many problems remain to be addressed. The mechanisms that target chloroplast-encoded proteins are only beginning to be identified. It will be important to determine whether mRNAs are localized for PS II assembly and repair by RBPs, by interactions between the *Chlamydomonas* homolog of the conserved signal sequence binding protein cpSRP54 (AF238499), or by other mechanisms. These questions are addressed in Chapter 3. I expect that the cytological organization of PS II assembly and repair described here will provide a context to frame future research into thylakoid membrane biogenesis.

2.5 Conclusion

These results provide in situ evidence for the current model that D1 synthesis for PS II repair occurs in stroma thylakoid membranes throughout the chloroplast. They also provide many lines of evidence showing that PS II subunit synthesis and assembly occur in a specific region of the chloroplast that I have called translation zones or "T zones". These results do not support the proposed model of PS II biogenesis occurring at the chloroplast envelope (Figure 1.1 B) because this compartment was not enriched in chloroplast mRNAs, ribosomes or RB38 under any conditions examined. Rather, these results support PS II biogenesis occurring either at thylakoid membranes (Figure 1.1 A) or a yet undiscovered internal chloroplast compartment resembling envelope (Figure

1.1 C). The composition of T zones and the membranes surrounding them will have to be characterized in order to distinguish between these possibilities.

This contributes to the emergent realization that the processes underlying chloroplast biogenesis are highly compartmentalized.

3 Chloroplast protein targeting involves localized translation in *Chlamydomonas*

Chloroplast protein targeting involves localized translation in Chlamydomonas.
Uniacke J, Zerges W.Proc Natl Acad Sci U S A. 2009 Feb 3;106(5):1439-44.

3.1 Introduction

The high degree of compartmentalization of eukaryotic cells requires the targeting of proteins to the compartments in which they function. Of the few thousand proteins that function in chloroplasts, most are synthesized by cytoplasmic ribosomes, imported across the chloroplast envelope by well-characterized pathways, and then routed to the appropriate compartment within the organelle (reviewed by [59]). In addition, recent evidence has revealed that many proteins are routed to chloroplasts via the ER and Golgi apparatus in two vascular plants and Euglena [52-54, 140]. Although chloroplast proteins are assumed to be synthesized throughout the cytoplasm, this has not been confirmed by in situ approaches. Much less is known about the intraorganellar targeting of the small subset of proteins that are encoded by chloroplast genomes and synthesized by 70S bacterial-like ribosomes within these organelles (reviewed by [57].

To address the long-standing questions, I used in situ techniques in *Chlamydomonas* to identify the targeting mechanisms used by the following canonical chloroplast proteins: the Rubisco small subunit (SSU), LHC II subunits, and the chloroplast-encoded proteins D1 and LSU. Both mRNA-based and co-translational targeting involve the localization of the mRNA encoding the targeted protein. Therefore, to distinguish these mechanisms from post-translational targeting, I used FISH, IF

staining, and confocal microscopy to determine whether the mRNA is localized near the target compartment of the protein that it encodes. Co-translational targeting requires translation to produce a signal peptide, whereas mRNA-based targeting does not, because the localization signal is in the mRNA. Therefore, I distinguished co-translational and mRNA-based targeting based on whether or not pharmacological inhibition of translation prevents localization of the mRNA. My results reveal the use of each of these three mechanisms in chloroplast protein targeting, along with two novel examples involving localized translation.

3.2 Materials and Methods

C. reinhardtii culture conditions

Strain CC-503 was cultured in HSM [91] until the mid-log phase (ca. 3 X 10^6 cells mL^{-1}) at 24 °C. ML was 100–150 $\mu E \cdot m^{-1} \cdot s^{-2}$, and HL was 2000 $\mu E \cdot m^{-1} \cdot s^{-2}$. The deletion mutant for *RbcS1* (and *RbcS2*), T60–3, was cultured on TAP medium under indirect light [141]. The conditions used (DA, ML, ML5', HL1', HL1'ML5') and inhibitor concentrations were described previously (Chapter 2).

FISH and IF staining

The FISH and IF procedures, as well as the *psbA* and *rbcL* FISH probes, have been described previously (Chapter 2; Table 2.1; [3]). The *LhcII* and *RbcS2* FISH probes (Table 2.1) were labelled with either Alexa 488 or Alexa 633 (Molecular Probes) according to the manufacturer's protocol. The *LhcII* probes were designed to hybridize to the *LhcII-3* mRNA (Accession BAB64417), but they also were complementary to the other three *LhcII* mRNAs. The *RbcS2* probes hybridized to the *RbcS2* mRNA (Accession P08475) and

failed to produce a signal in a deletion mutant for both *RbcS* genes (Figure 3.1 A). The absence of the *LhcII* FISH signal in DA cells (Figure 3.1 B) provides negative controls for its specificity, in the absence of a deletion mutant for these genes [93]. The antisera against the ribosomal proteins were described previously [87, 103, 105-107]. The localization patterns described herein were seen in 80% of the cells examined ($n > 20$), except in the following cases. In 55% of the cells, the *rbcL* mRNA was distinctly focused at the outer perimeter of the pyrenoid (Figure 3.2 C), whereas in 40% the signal was slightly more dispersed (Figure 3.2 B), and in 5% it was not localized ($n > 20$). An atypically high percentage of cells lacked the *LhcII* mRNA signal for unknown reasons. Of the 110 ML cells examined, 62 (56%) had a very weak signal, which likely was background because it was evenly distributed throughout the cell, including within the chloroplast (data not shown). Considering just the 48 cells that had above-background *LhcII* FISH signals in the cytosolic region, 30 cells (63%) had the localization pattern shown in Figure 3.5 A, B, and G, 14 cells (29%) had a less evident semblance of this localization pattern, and 4 cells (8%) had a non-localized signal.

Microscopy

Confocal images were obtained as 0.2 µm optical sections with a confocal laser-scanning microscope (TCS SP2; Leica) and image acquisition software (version 2.61; Leica). Argon, green helium neon, and helium neon lasers were used to produce the 488 nm, 543 nm, and 633 nm stimulation of fluorophores Alexa 488/FITC, Alexa 555/TRITC, and Alexa 633, respectively. The cells were observed with immersion oil using an HCX PL APO objective lens of 100 X and NA of 1.4. Images were acquired in 512 X 512 format with

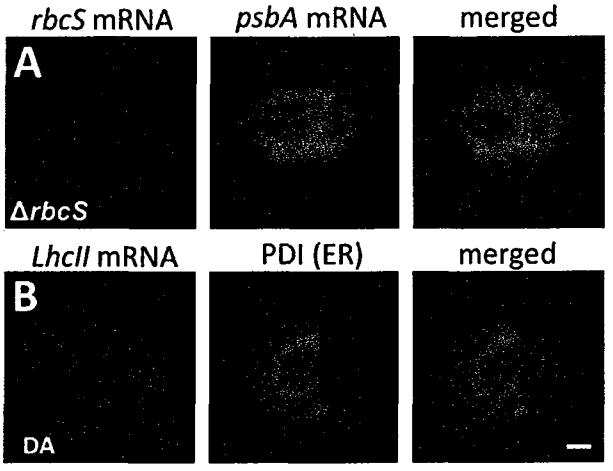

Figure 3.1. Control experiments for the specificities of the *RbcS2* and *LhcII* mRNA FISH signals.

(**A**) The *RbcS2* FISH signal was specific because it was absent in a deletion mutant for both *RbcS* genes. (**B**) The *LhcII* FISH signal could be detected only at the background level (i.e., weak and equal in the cytosolic region and the chloroplast) in dark-adapted (DA) cells, serving as a control for its specificity. The micrographs show 0.2 µm optical sections. PDI, protein disulfide isomerase. Bar, 1 µm.

digital zoom set at 4.8 X with a pinhole size of 0.84 airy. Images were acquired after adjusting the maximal signal in each section to just below saturation. Fluorescence density was measured with the Measure tool of ImageJ. Statistical analyses of colocalization were carried out as described in Chapter 2.

3.3 Results

3.3.1 LSU targeting to the pyrenoid involves a co-translational mechanism

To characterize the targeting of LSU to the pyrenoid, I used FISH to analyze the distribution of its mRNA, that of the chloroplast *rbcL* gene. The *rbcL* mRNA signal was enriched in the chloroplast basal region relative to the lobes (Figure 3.2 A–C). Co-immunostaining of these cells for Rubisco revealed that the *rbcL* mRNA was distinctly focused at the outer perimeter of the pyrenoid in most cells (see Materials and Methods section 3.3). This localization pattern was not observed in the FISH signals of three chloroplast mRNAs encoding thylakoid membrane proteins: *psbA* (Figure 3.2 C), *psbC*, and *psaA* [88]. Therefore, these results support the targeting of LSU to the pyrenoid by either a co-translational or an mRNA-based mechanism.

To determine whether these *rbcL* mRNAs are localized by targeting signals in the LSU nascent chain (in a co-translational mechanism) or in the mRNA sequence (in an mRNA-based mechanism), I explored whether this localization occurs in cells depleted of translating chloroplast ribosomes and LSU nascent chains through treatment with lincomycin [142, 143]. The *rbcL* FISH signal was not localized around the pyrenoid in cells treated with this drug (Figure 3.2 E). This localization pattern also was not seen in DA

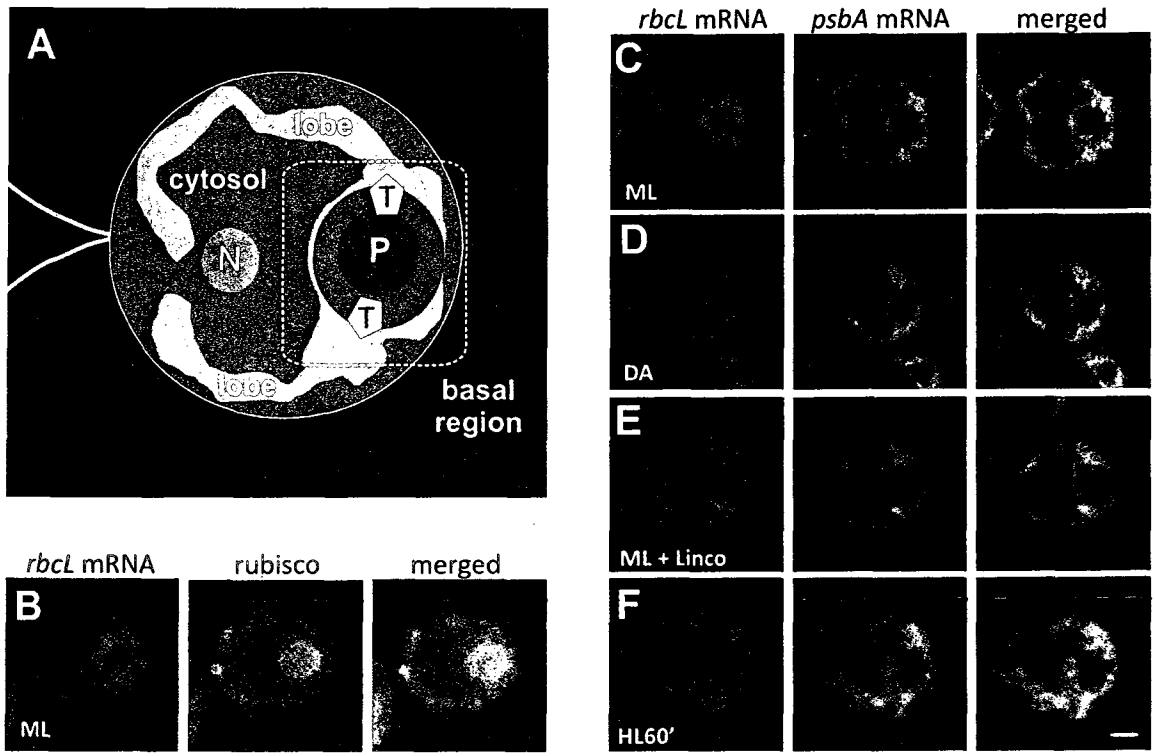

Figure 3.2. Translation-dependent localization of the chloroplast *rbcL* mRNA at the pyrenoid for LSU targeting.

(**A**) An illustration of the cell shown in (C) demonstrating the single chloroplast (green) with its lobes and globular basal region. The basal region contains the pyrenoid (P; blue). Also indicated are the cytosolic region (gray) and the approximate locations of T zones (T), the nucleus (N), and the flagella. The region in which *rbcL* mRNAs localize is shown in red. (**B**) An ML cell showing the *rbcL* mRNA signal and immunolabeled Rubisco. Signals from the *rbcL* and *psbA* mRNAs in cells from constant ML (**C**), DA (**D**), ML with lincomycin (**E**), and HL (**F**) for 60min. The punctate colocalized *psbA* and *rbcL* mRNA signals near the pyrenoid in (E) and (F) are cpSGs, which form in response to oxidative stress caused by a secondary effect of lincomycin (photosensitization to ML) or HL, respectively (21). The micrographs show 0.2 μm optical sections. For each experiment, n = 20 cells. Each pattern was observed in >80% of cells. Bar, 1 μm.

cells, a condition where *rbcL* translation is down-regulated [94, 124] or a 60 min HL exposure [116] (Figure 3.2 D and F).

The apparent higher level of the *rbcL* FISH signal in cells exposed to ML compared with DA cells and lincomycin-treated ML cells most likely reflects the concentration of the signal near the pyrenoid; four previous studies found a constant *rbcL* mRNA level across diverse light conditions in *Chlamydomonas* [28, 93, 94, 124]. Together, these results strongly support LSU targeting to the pyrenoid primarily through a co-translational mechanism.

In a minority of cells (25%; $n = 24$), Rubisco and the *rbcL* mRNA also colocalized in a structure with the size, shape, and general location of the eyespot (Figure 3.2 B). Because this localization pattern was not detected in most cells, I did not explore it further.

3.3.2 D1 targeting for de novo PS II assembly involves an mRNA-based mechanism

I also explored how D1 is targeted for de novo PS II assembly in T zones. T zones are punctate regions adjacent to the pyrenoid in which I previously observed the colocalization of multiple components in PS II subunit synthesis for de novo assembly when it was induced by shifting cells from darkness to ML for 5 min (Figure 3.2 A) (Chapter 2). Figure 3.3 A and B show the colocalization of the *psbA* mRNA and the chloroplast ribosomal protein L2 in T zones only in the inducing ML5' condition, not in the repressing DA condition. To highlight this colocalization pattern, the pixels with the strongest colocalized signals are displayed in white using ImageJ [121], as shown in the fourth image column in Figure 3.3 A–C (see also Figure 3.4 A–E). T zones are distinct

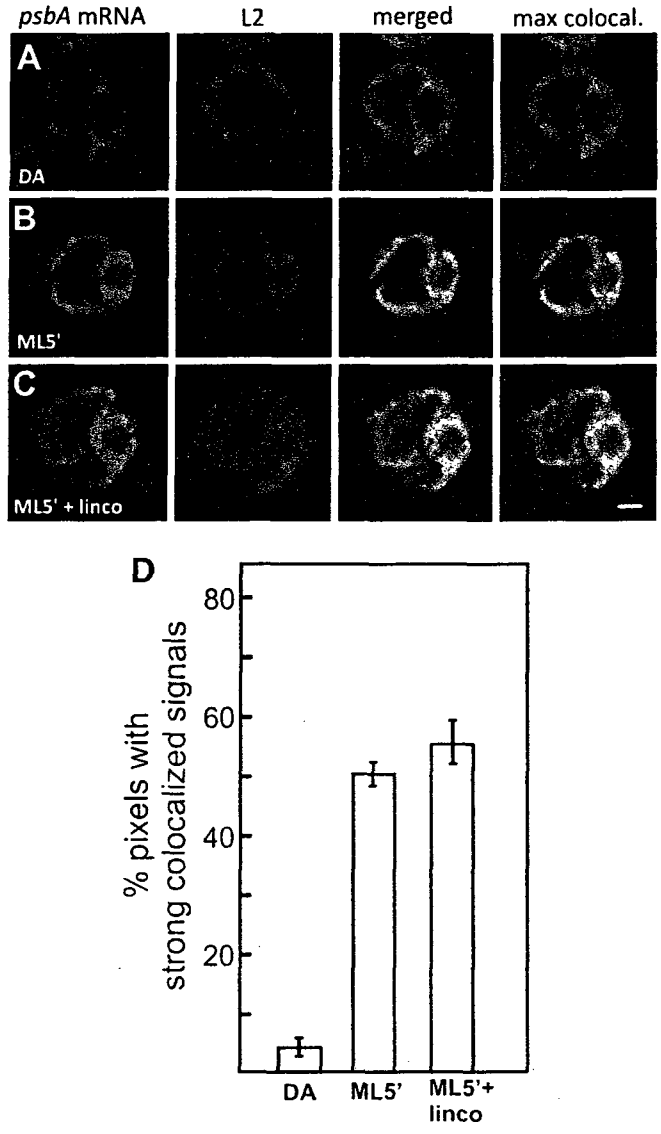

Figure 3.3. Translation-independent localization of the *psbA* mRNA in T zones for de novo PS II assembly.

Fluorescence signals from the *psbA* mRNA and the chloroplast ribosomal protein L2 in cells from the following conditions: 2 h dark-adaptation DA (**A**), after a 5 min ML exposure to initiate *psbA* translation for de novo PS II assembly (ML5') (**B**), and ML5' cells generated in the presence of lincomycin (**C**). The fourth image column shows the merged channels, with the strongest colocalized signals highlighted in white. The punctate *psbA* mRNA signal near the pyrenoid that does not colocalize with L2 is in cpSGs (21). The micrographs show 0.2 μm optical sections. Bar, 1 μm. (**D**) The percentage of pixels in sampled T zones with strong colocalized signals [white pixels in (A–C)] for each of the three conditions. The error bars indicate 2 standard errors. For each experiment, $n > 20$ cells.

from the *rbcL* mRNA localization pattern around the pyrenoid; they are punctate and located on the lateral sides of the pyrenoid, and the *rbcL* mRNA does not localize to them (Chapter 2). Because the scoring of this pattern is subjective, I analyzed each T zone for the percentage of pixels with strong colocalized signals and determined the mean value for each condition (Figure 3.3 D) (see Chapter 2 Materials and Methods). These results confirmed my previous finding that the *psbA* mRNA localizes to T zones during the induction of de novo PS II assembly. Therefore, this targeting of D1 involves either a co-translational or an mRNA-based mechanism.

To discriminate between these two mechanisms, I investigated whether or not the *psbA* mRNA localized to T zones after chloroplast mRNAs were cleared of ribosomes and nascent polypeptides by treatment with lincomycin. When ML5′ cells were generated in the presence of lincomycin, the *psbA* mRNA and L2 still colocalized in T zones (Figure 3.3 B and C). Moreover, the quantitative analyses revealed that lincomycin unexpectedly enhanced this colocalization (Figure 3.3 D). Lincomycin also enhanced colocalization of the *psbA* mRNA and a marker protein for the small chloroplast ribosomal subunit, S-21, under similar conditions that activated *psbA* translation for the de novo PS II assembly: DA cells exposed to HL for 1 min (HL1′ cells) (Figure 3.4 A–C and F). This translation-independence supports a primary mRNA-based mechanism in *psbA* mRNA localization to T zones for D1 synthesis in the de novo PS II assembly.

Comparing the distributions of L2 and S-21 revealed that chloroplast ribosomal subunits also localized to T zones through translation-independent mechanisms (Figures 3.3 and 3.4).

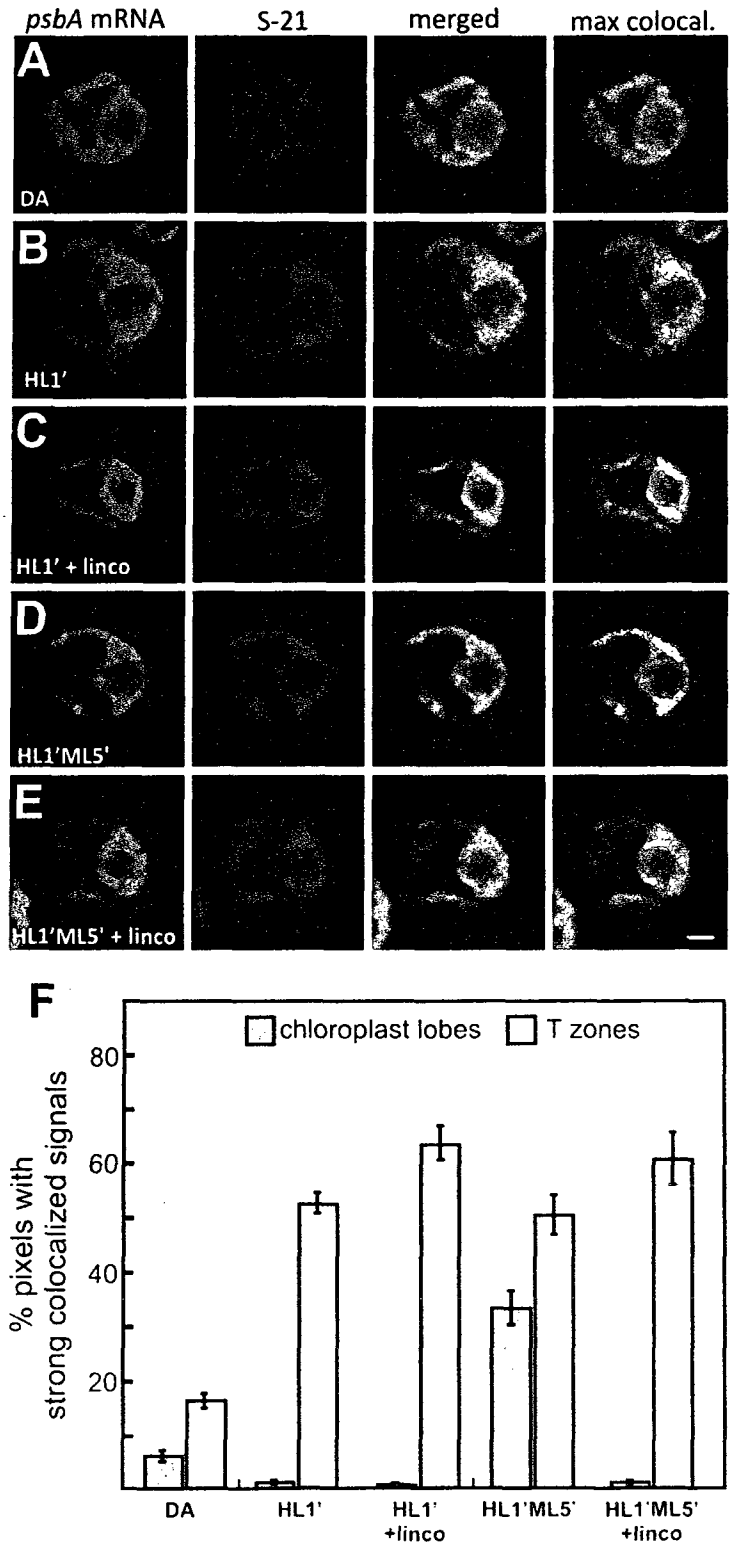

Figure 3.4. Localization of the *psbA* mRNA for the de novo assembly and repair of PS II.

Fluorescence signals from the *psbA* mRNA and the chloroplast ribosomal protein S-21 in cells from the following conditions: a 2 h dark-adaptation (DA) (**A**); DA cells exposed to HL for 1 min (HL1') to induce *psbA* translation for de novo PS II assembly (**B**); HL1' cells generated in the presence of lincomycin (**C**); HL1' cells exposed to ML for 5 min, a condition of PS II repair (HL1'ML5') (**D**); and HL1'ML5' cells generated in the presence of lincomycin (**E**). The micrographs show 0.2 μm optical sections. Bar, 1 μm.) (**F**) The percentages of pixels with strong colocalized signals in T zones (white bars) and chloroplast lobes (shaded bars) across all cells from the five conditions. The error bars indicate two standard errors. For each experiment, $n \geq 20$ cells.

3.3.3 D1 targeting to thylakoids for PS II repair involves a co-translational mechanism

During HL stress, the replacement of photodamaged D1 subunits in PS II complexes involves the localization of the *psbA* mRNA to thylakoid membranes throughout the chloroplast (Chapter 2; [19]). As a condition to induce PS II repair, I incubated HL1' cells for an additional 5 min under ML (HL1'ML5'), for reasons described in the previous report (Chapter 2). This effect can be seen as the appearance of strong colocalized signals from the *psbA* mRNA and S-21 in chloroplast lobes in HL1'ML5' cells (Figure 3.4 D) relative to HL1' cells (Figure 3.4 B; in 3.4 F, compare the second and fourth shaded bars). This localization of the *psbA* mRNA for D1 targeting in PS II repair is consistent with both co-translational and mRNA-based mechanisms. To discriminate between these possibilities, I generated HL1'ML5' cells in the presence of lincomycin. Under these conditions, I did not detect this colocalization of the *psbA* mRNA and L2 in the lobes, thus supporting a co-translational mechanism in D1 targeting for PS II repair in thylakoid membranes (Figure 3.4 C and E; in 3.4 F, compare the third and fifth shaded bars).

3.3.4 Chloroplast protein targeting from the cytoplasm

I then turned my attention to protein targeting from the cytoplasm to the chloroplast. Using FISH to characterize the distribution of *LhcII* mRNAs, which encode the subunits of LHC II [13], revealed that their FISH signal was frequently concentrated along the cytoplasmic border of the chloroplast basal region (see Materials and Methods section 3.3). This localization pattern is shown in Figure 3.5 A, in which the chloroplast was

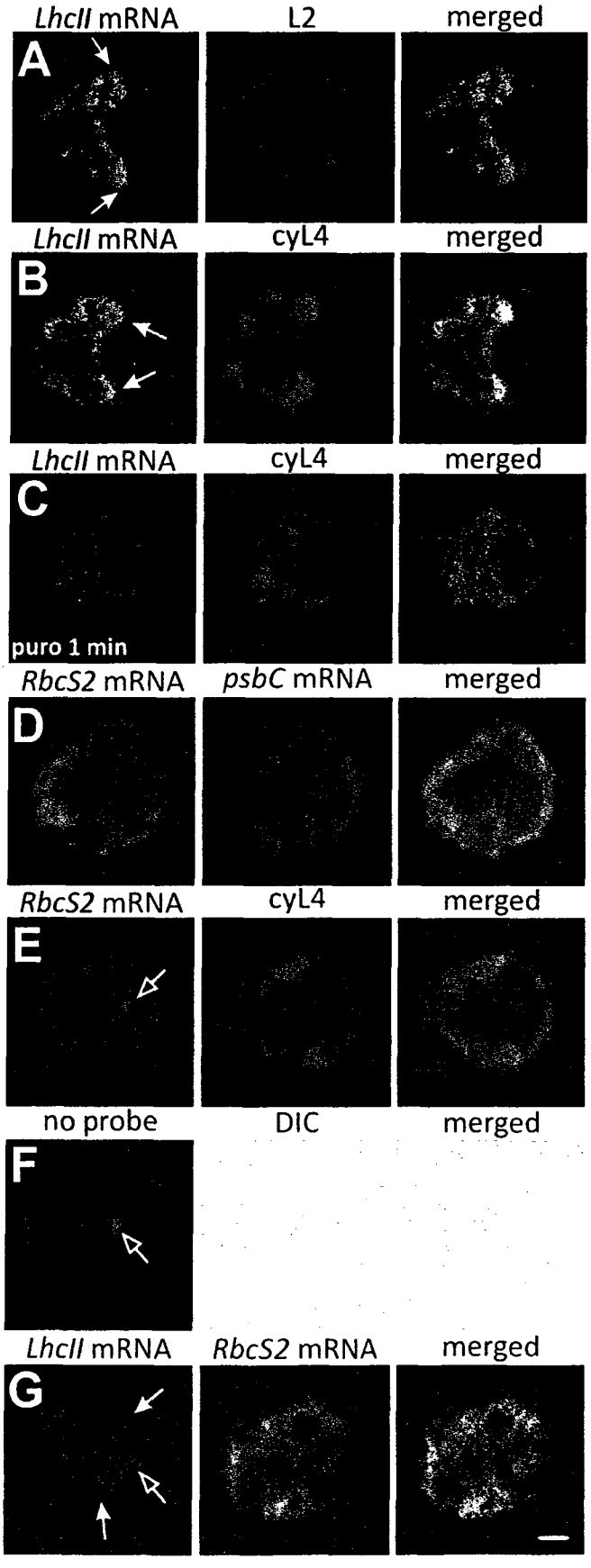

Figure 3.5. FISH analyses of two nucleocytosolic mRNAs.

(A) A moderate light (ML) cell showing the distribution of the *LhcII* mRNAs relative to the chloroplast, stained by immunolabeling L2. The closed-head arrows indicate enrichment of *LhcII* mRNAs near the chloroplast basal region. **(B)** A ML cell showing the fluorescence signals from *LhcII* mRNAs and the cytoplasmic ribosomal protein cyL4. **(C)** A ML cell exposed to puromycin for 1 min that was FISH-probed for the *LhcII* mRNAs and immunostained for cyL4. **(D)** A ML cell showing the distribution of the *RbcS2* mRNAs relative to the chloroplast, which was FISH-probed for the *psbC* mRNA. **(E)** A ML cell that was FISH-probed for the *RbcS2* mRNA and immunostained for the cytoplasmic ribosomal protein cyL4. The open-head arrow shows the autofluorescence resulting from excitation at 633 nm, seen in the nonprobed/immunostained cell in **(F)**. **(G)** A ML cell that was FISH-probed for *LhcII* and *RbcS2* mRNAs. DIC, differential interference contrast. The micrographs show 0.2 µm optical sections. Bar, 1 µm.

stained with immunolabeled L2. In other cells, the *LhcII* mRNAs that localized at the basal region were more concentrated near the bases of chloroplast lobes (Figure 3.5 B and G). These results raise the possibility that the cytoplasmic border of the chloroplast basal region is a privileged location of LHC II synthesis. This hypothesis is supported by several findings. First, different distributions were observed for the *RbcS2* mRNA (Figure 3.5 D–G; see the next paragraph) and the mRNA encoding β2-tubulin [3]. Second, the localized *LhcII* mRNAs probably were translated, because they colocalized with the concentrated marker protein for cytoplasmic ribosomes, cyL4, and this *LhcII* mRNA localization pattern was not detected after mRNAs were released from ribosomes and nascent chains by puromycin (Figure 3.5 B and C, respectively) [21, 103]. The concurrent decrease in the intensity of this signal likely reflects rapid degradation of untranslated *LhcII* mRNAs, because their translation and abundance are directly correlated in *Chlamydomonas* [93, 144]. Third, patches of strong cyL4 signals at other cytoplasmic locations were not enriched in the *LhcII* mRNA signal (Figure 3.5 B); therefore, LHC II subunits appear to be targeted to the chloroplast by the localized translation of the mRNAs encoding them. The translation-dependence of this mRNA localization pattern supports a co-translational mechanism.

Analysis of the distribution of the *RbcS2* mRNA, which encodes SSU, revealed that its FISH signal was not enriched at the chloroplast perimeter (Figure 3.5 D, E, and G). The prominent non-staining region contains the nucleus [3]. Some cells exhibited variable intensity in this signal, but this was not concentrated in any consistent location (Figure 3.5 D). This broad distribution of the *RbcS2* mRNA was quite distinct from the

LhcII mRNA localization pattern when these signals were compared in the same cells (Figure 3.5 G). Moreover, the *RbcS2* mRNA colocalized with cyL4 throughout the cytosolic region (Figure 3.5 E). Therefore, these results support the current model of SSU synthesis throughout the cytoplasm and post-translational import into the chloroplast.

3.4 Discussion

My results provide evidence of chloroplast protein targeting by the three general mechanisms described earlier and reveal a remarkably complex spatial organization of chloroplast protein synthesis. The colocalization of *RbcS2* mRNA with ribosomes throughout the cytosol provides the first in situ evidence supporting the long-standing model of SSU synthesis at random cytoplasmic locations and post-translation import into the chloroplast (Figure 3.5 E) [50, 141]. Although my findings do not exclude the possibility of a minor *RbcS2* mRNA pool localized at the chloroplast perimeter for translation and SSU targeting, this seems unlikely, because confocal microscopy is sufficiently sensitive and quantitative for detecting such a pool. Most *RbcS2* mRNAs likely are translated; their FISH signal was completely colocalized with the cyL4 signal (Figure 3.5 E). Moreover, SSU is among the most synthesized proteins in *Chlamydomonas*, and nearly all *RbcS* mRNAs are polysome-associated in barley leaf cells [141, 145].

In contrast with the non-localization of the *RbcS2* mRNA, I found evidence for localized *LhcII* translation at the cytoplasmic border of the chloroplast basal region (Figure 3.5 A, B, and G). This could localize the import of newly synthesized LHC II subunits near T zones to facilitate the assembly of the PS II–LHC II supercomplex. To

what feature of cellular architecture could *LhcII* mRNAs be localized? LHC II subunits likely are co-translationally inserted into a membrane, because they are hydrophobic integral membrane proteins. They probably are not routed to the chloroplast through the secretory system in *Chlamydomonas* as they are in other algal species because these proteins are predicted to lack a signal peptide by TargetP [146]. My working hypothesis is that polysomes with *LhcII* mRNAs are bound to specific regions of the chloroplast envelope for co-translational targeting of LHC II subunits to the chloroplast by unknown mechanisms. Although this hypothesis is seemingly contradicted by many EM images of ribosome-free outer chloroplast envelope membranes [51, 147], none of these images were obtained from cells treated with an inhibitor of translation elongation, which is required to retain chloroplast ribosomes on thylakoid membranes during cell isolation [20].

I expanded the survey of mRNA localization patterns in the *Chlamydomonas* chloroplast by demonstrating that the *rbcL* mRNA is translated at the outer perimeter of the pyrenoid, probably to target LSU for the Rubisco assembly therein (Figure 3.2 B and C) [55]. Weaker *rbcL* mRNA signals were detected throughout the chloroplast, possibly from a pool translated for the Rubisco bound to thylakoid membranes [5]. The translation-dependence of the former localization pattern supports a co-translational targeting mechanism. I also found similar evidence for co-translational targeting of D1 for the repair of photodamaged PS II complexes in thylakoid membranes throughout the chloroplast (Figure 3.4 D–F). Future research should explore whether LSU and D1 targeting involves the cpSRP54 homolog in *Chlamydomonas* (AF238499).

An mRNA-based mechanism in D1 targeting for de novo PS II assembly is supported by the translation-independence of *psbA* mRNA localization to T zones (Figures 3.3 and 3.4). The possibility exists that cpSRP54 subsequently directs nascent D1 for co-translational membrane insertion. Concerted mRNA-based and co-translational mechanisms have been speculated to operate in protein targeting to thylakoids, and there is evidence for this in protein targeting to the mammalian ER [57, 149].

I also found that chloroplast ribosomal subunits localized to T zones through translation-independent mechanisms. This finding was not unexpected because 10%–40% of chloroplast ribosomes are associated with membranes by electrostatic interactions alone in *Chlamydomonas* and Pea [20, 22, 25]. Moreover, translation-independent mechanisms localize ribosomes to the inner membrane of mitochondria in *Saccharomyces cerevisiae* and the mammalian ER [149, 150].

3.5 Conclusion

My use of in situ approaches in the analysis of mRNA localization for chloroplast protein targeting has begun to identify the targeting mechanisms used by specific proteins and for different processes in the biogenesis and repair of the photosynthesis apparatus. I have found intriguing similarities to intracellular protein targeting in many other organisms. Although the post-translational import machineries in the chloroplast envelope have been identified and are currently being dissected, much remains to be learned about the co-translational and mRNA-based pathways [50]. By revealing specific examples of chloroplast protein targeting by co-translational and mRNA-based

pathways, my results will help guide the exploration of these pathways at the biochemical level.

4 Stress induces the assembly of RNA granules in the chloroplast of *Chlamydomonas reinhardtii*

Stress induces the assembly of RNA granules in the chloroplast of *Chlamydomonas reinhardtii.* Uniacke J, Zerges W. J. Cell Biol. 2008 Aug 25;182(4):641-6.

4.1 Introduction

During my analysis of the distribution of chloroplast mRNAs, I noticed a punctate localization pattern at the internal perimeter of the pyrenoid under conditions of HL. An examination of the literature revealed that punctate cytoplasmic loci of mRNA and proteins, called RNA granules, form in the presence of stress in mammalian and plant cells [65, 67]. Therefore, I decided to examine the punctate chloroplast mRNA localization pattern further to see if it is similar to any of the RNA granules described in these other systems. In this chapter, I describe the identification and initial characterization of stress-induced RNA granules in the chloroplast of *C. reinhardtii.* As in all green plants, the chloroplast genetic system in *C. reinhardtii* is essentially bacterial, reflecting its evolution from a cyanobacterial endosymbiont [151]. Therefore, this is the first such report of an RNA granule in an organellar/bacterial lineage.

4.2 Materials and Methods

C. reinhardtii culture conditions

Strain CC-503 was cultured in HSM [91] to a cell density of 2-3 X 10^6 cells/ml at 24 ^oC under a light intensity of 100-150 $\mu E \cdot m^{-1} \cdot s^{-2}$ and with orbital shaking. HL (2000 $\mu E \cdot m^{-1} \cdot s^{-2}$) was generated by a slide projector (Kodak), to which small (2-30-ml) cultures were

exposed at a distance of 10 cm for 10 min with manual shaking. Dark adaption was a 2 h incubation of liquid cultures wrapped with two layers of aluminum foil on an orbital shaker. Lincomycin and chloramphenicol were added to final concentrations of 200 µg/ml. Puromycin was added to a final concentration of 100 µg/mL. These inhibitors were shown to be active because each abolished protein synthesis in the chloroplast after 10 min as revealed by the results of in vivo radioisotope pulse-labelling experiments. Cells were treated with rose bengal or hydrogen peroxide at concentrations of 0.5 µM and 2 mM, respectively, for 15 min. DCMU was added to a final concentration of 10 µM for 15 min. FCCP was added to a final concentration of 10 µM for 30 min. UV irradiation (20 mJ) was performed in a Stratalinker (Promega) and cells were fixed 30 min later. The conditions of heat shock, osmotic shock, and phosphate deprivation were described previously [152-154]. The colocalization of the *psbA* mRNA and the chloroplast ribosomal protein L2 to T zones was induced by exposing DA cells to ML for 5 min as described in Chapter 2. These cells were then treated with lincomycin under ML, when it does induce cpSGs by potentiating light-induced stress [155]. The effects of the inhibitors were assessed in the dark to avoid the induction of light stress. These cells were first cultured under ML (so they would have polysomes from which chloroplast mRNAs could be released) and then shifted to the dark immediately before the addition of lincomycin or puromycin.

FISH and IF staining

The procedures and probes used for FISH and IF were described previously (Chapter 2; [3]). High specificity of the *psbA* , *rbcL* , and *psaA* FISH signals were demonstrated in

Chapter 2). Indirect IF was carried out using the following primary antisera: anti-SSU, anti-LSU (N. Brisson, University of Montreal, Montreal, Canada), anti-L2, anti-S-21, anti-Rubisco (E. Harris, Duke University, Durham, NC), anti-cPABP (S. Mayfield, The Scripps Research Institute, La Jolla, CA), and anti- HSP70B (M. Schroda, University of Freiburg, Freiburg, Germany). The in situ IF staining patterns of the ribosomal proteins, PABP, and HSP70B were highly specific because each of the antibodies detected a protein of the expected molecular weight on immunoblots of total cellular protein. Secondary antisera alone did not generate a signal.

Confocal microscopy

Confocal images were obtained as 0.2 μm optical sections with a confocal laser-scanning microscope (TCS SP2; Leica) and image acquisition software (version 2.61; Leica). Argon and green helium neon lasers were used to produce the 488 and 543 nm stimulation of TRITC or the fluorophores on the FISH probes Alexa 488 and 555 (Invitrogen). Cells were observed under settings described in Chapter 3.

4.3 Results and Discussion

4.3.1 Chloroplast mRNAs localize to cpSGs in cells under HL stress

For each of the four chloroplast mRNAs examined by FISH and confocal microscopy, a fraction localized in cpSGs in most cells that were cultured under ML and then exposed to HL for 10 min (Figure 4.1 B and see Figure 4.2). This localization pattern was seen in a minority of cells maintained under ML. These chloroplast mRNAs encode subunits of PS II (*psbA* and *psbC*), PS I (*psaA*), and Rubisco (*rbcL*). This localization was quantified by determining the mean ratio of the fluorescence densities of each FISH signal in cpSGs

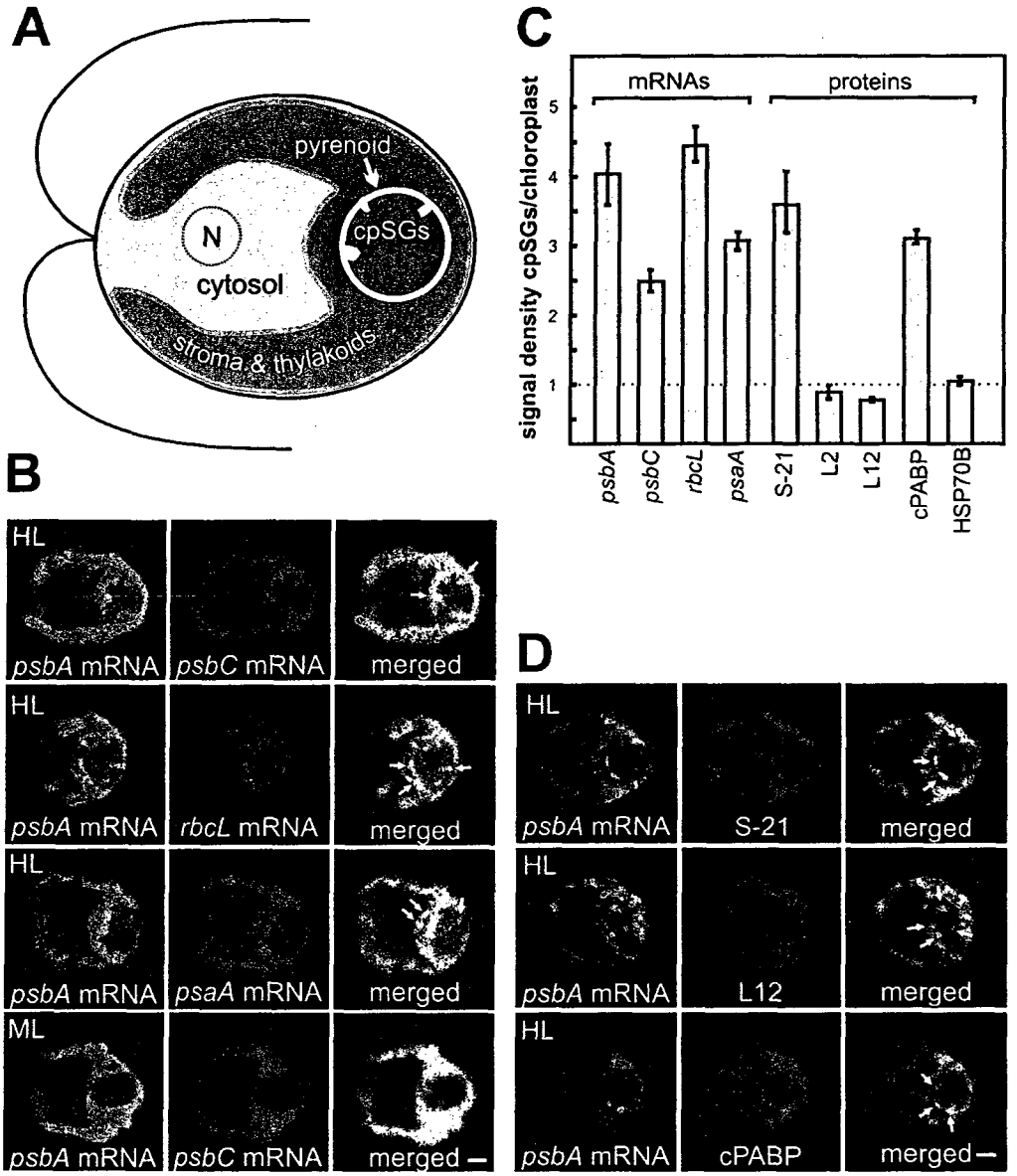

Figure 4.1. cpSGs resemble cytoplasmic SGs in their composition of translation components.

(**A**) An illustration shows the chloroplast with cpSGs (yellow), the envelope (orange), the aqueous stroma and thylakoid vesicles (green), and the pyrenoid (brown), surrounded by a starch sheath (white). Also shown are the cytosolic compartments (gray), the nucleus (N), and the flagella. (**B**) In cells under HL stress, cpSGs had strong FISH signals from the mRNAs of *psbA*, *psbC*, *rbcL*, and *psaA*. cpSGs were not seen in most cells under the nonstress condition of moderate light (ML). (**C**) Bar heights indicate a mean signal density in cpSGs standardized to the signal density of the chloroplast for the FISH signals from the mRNAs and a protein of the small ribosomal subunit (S-21), two proteins of the large ribosomal subunit (L2 and L12), and cPABP. Error bars represent two SE. A value substantially greater than one (dotted line) represents localization in cpSGs. (**D**) cpSGs revealed by the *psbA* FISH signal immunolabeled S-21, but only weakly for L12. cpSGs also showed strong IF signal of cPABP. Arrows in B and D indicate cpSGs. The micrographs show 0.2 µm optical sections. Bars, 1 µm. For each experiment, $n \geq 20$ cells.

versus in the chloroplast ($n \geq 20$ cells for each mRNA). This analysis revealed that each of these mRNAs is concentrated several fold in cpSGs (Figure 4.1 C).

4.3.2 cpSGs and SGs are similar in their composition of translation components

To determine whether cpSGs are similar to SGs or other stress-induced RNA granules, I asked whether they contain the subunits of the chloroplast ribosome and the *C. reinhardtii* PABP homologue, cPABP [120]. Hallmarks of SGs are their enrichment for PABP and the small ribosomal subunit, but not the large ribosomal subunit. In cells from the HL stress condition, cpSGs were seen to have strong IF from S-21, a protein of the small ribosomal subunit (Figure 4.1 D). Quantification revealed a 3.5 fold higher signal density in cpSGs relative to the rest of the chloroplast (Figure 4.1 C). Moreover, two proteins of the large ribosomal subunit, L12 and L2, had lower signal densities in cpSGs than in the chloroplast (Figure 4.1 C and D; and see Figure 4.3 C). Finally, the signal density of cPABP was three fold higher in cpSGs than in the chloroplast (Figure 4.1 C and D). Although stable chloroplast mRNAs are not 3' polyadenylated, genetic and biochemical evidence support a role of cPABP in chloroplast translation involving its binding to internal mRNA sequences [16, 120]. Thus, cpSGs resemble SGs in their composition of these translation components.

4.3.3 Specific stress conditions induce mRNA localization to cpSGs

To analyze factors that induce mRNA localization to cpSGs, cells were exposed to different stresses and analyzed for the *psbA* mRNA distribution. Because HL exposure induces oxidative stress and damage to PS II [156], conditions specific to each of these stresses were tested. When oxidative stress was induced by treatment with hydrogen

peroxide or rose bengal (a photosensitizer of singlet oxygen production; [157]), higher percentages of cells with cpSGs were observed relative to non-treated cells (Figure 4.2). In contrast, inhibition of PS II by 3-(3,4-dichlorophenyl)-1,1-dimethylurea (DCMU) had no significant effect.

Therefore, HL causes mRNA localization to cpSGs by inducing oxidative stress and not by damaging PS II. Other results suggest that energy deprivation also induces mRNA localization to cpSGs. First, exposure to the proton ionophore carbonylcyanide-*p*-trifluoromethoxyphenylhydrazone (FCCP), which inhibits ATP synthesis in chloroplasts and mitochondria, elevated the percentage of cells with cpSGs by more than 11 fold (Figure 4.2). Second, a three-fold increase occurred during a 2 h incubation in the dark, a condition that is unlikely to be associated with a stress condition apart from energy deprivation caused by the lack of photosynthesis. HL exposure of DA cells had little effect, possibly because they lacked polysomal *psbA* mRNAs for localization to cpSGs (see section 4.4.6; Figure 4.2; [158]). cpSGs were not described in Chapter 2, which examined DA cells under HL stress. cpSG formation was also induced by exposure to UV light or phosphate deprivation. Heat shock had no effect and osmotic shock abolished cpSGs in the minority of cells that have them under ML (Figure 4.2). Therefore, cpSGs form under specific stress conditions and the underlying inducing factors and signalling pathways remain to be determined.

4.3.4 cpSGs are located at the internal perimeter of the pyrenoid

To characterize the location of cpSGs, I used marker proteins for specific chloroplast compartments. cpSGs were detected only in the vicinity of the pyrenoid. This spherical

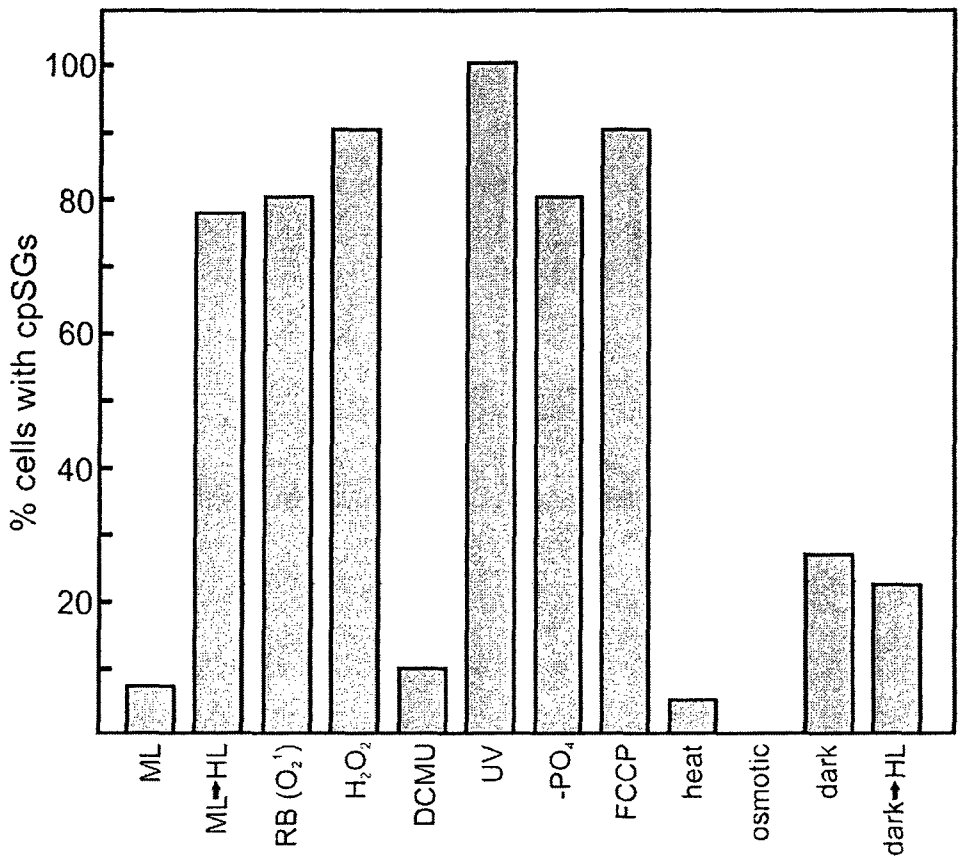

Figure 4.2. cpSGs form under specific stress conditions.

Bar heights indicate the percentages of cells with cpSGs under the following conditions: ML, constant moderate light; ML → HL, cells cultured under ML were exposed to HL; RB, oxidative stress was induced by rose bengal; H_2O_2 , oxidative stress was induced by exposure to hydrogen peroxide; DCMU, a PS II inhibitor; UV, UV light exposure; $-PO_4$, phosphate deprivation; FCCP, energy deprivation by this proton ionophore; heat, heat shock; osmotic, osmotic shock; dark, 2 h dark-adapted cells; dark → HL, 2 h dark-adapted exposed to HL. For each condition, $n \geq 20$ cells.

compartment in the chloroplasts of most algae provides a high CO_2/O_2 ratio to favour the carboxylase activity of Rubisco in the Calvin cycle [159]. In cells from the HL stress condition that were immunoprobed for the Rubisco holoenzyme to reveal the pyrenoid and FISH probed for the *psbA* mRNA, all cpSGs were located at the internal perimeter of the pyrenoid (Figure 4.3 A). However, cpSGs were within patches of IF from a marker protein for the chloroplast stroma, HSP70B, where it was not enriched relative to its mean signal density in the chloroplast (Figure 4.1 C and Figure 4.3 B; [160]). Together, these results suggest that cpSGs are in pockets of stroma within the pyrenoid. Therefore, I considered whether cpSGs are within the opening of the membranous tubules that have been seen by EM to extend into the pyrenoid [138]. Consistent with this possibility, I observed cpSGs at the termini of what appeared to be pyrenoid tubules with HSP70B in rare images that longitudinally sectioned them (Figure 4.3 B).

I proposed previously that discrete regions within the chloroplast, called T zones, house early steps of translation for de novo PS II assembly, based on the rapid colocalization therein of the *psbA* and *psbC* mRNAs and both subunits of the chloroplast ribosome specifically under conditions of de novo PS II assembly (Chapter 2). As T zones are near the pyrenoid, I compared their location with respect to cpSGs (see Materials and methods section 4.3). As seen in merged images of the fluorescence signals from the *psbA* mRNA and L2 (Figure 4.3 C), T zones (yellow) are distinct from cpSGs (green). Moreover, certain cpSGs adjoined a T zone, suggesting a functional relationship between these compartments.

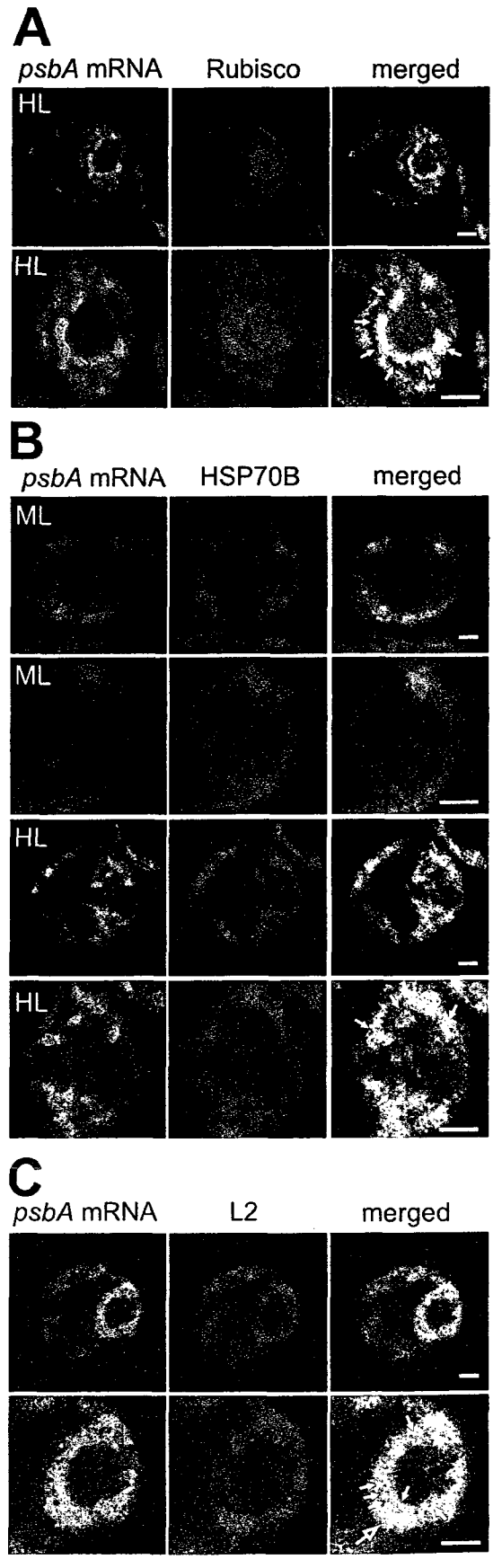

Figure 4.3. cpSGs are located at the internal perimeter of the pyrenoid.

cpSGs, with the *psbA* mRNA (green), were located relative to proteins for the pyrenoid, stroma, and T zones. For each cell, a second image set shows an enlargement of the pyrenoid region. (**A**) In HL–stressed cells, cpSGs were detected at the internal perimeter of the pyrenoid, revealed by immunolabeled Rubisco (100%, n = 20 cells). (**B**) In cells from both moderate light (ML) and HL conditions, the chloroplast stroma marker protein HSP70B was observed in lines that appear to be pyrenoid tubules. The cpSGs in HL stressed cells were detected at the peripheral termini of this HSP70B immunostaining pattern (n = 7 cells). (**C**) cpSGs are distinct from T zones (large arrow), which have colocalized *psbA* mRNA and ribosomal protein L2 (n = 20). Arrows indicate cpSGs and the larger arrow in C indicates a T zone. The micrographs show 0.2 µm optical sections. Bars, 1 µm.

4.3.5 A model for cpSG assembly involving the large subunit of Rubisco

A key difference between cpSGs and SGs are their factors for mRNA localization and assembly. SG assembly involves the self-aggregation of the RBPs TIA-1 and TIAR [161]. Homologues were not identified in Basic Local Alignment Search Tool searches of the *C. reinhardtii* genome. However, a candidate cpSG assembly factor was suggested by my review of previous reports that *C. reinhardtii* cells under oxidative stress disassemble Rubisco into its constituent LSUs and SSUs, whereupon the oxidized LSU non-specifically binds chloroplast mRNAs and forms large particles [162-164]. These authors proposed a role of LSU in the repression of the *rbcL* translation. In addition, immunogold EM revealed a particulate form of Rubisco at the internal periphery of the pyrenoid [5]. Although this was proposed to function in the Calvin cycle, it may have been LSU in cpSGs.

To determine whether cpSG assembly involves the aggregation of LSU bound to chloroplast mRNAs (Figure 4.4 A), I asked whether LSU, but not SSU, localizes to cpSGs. Indeed, when cells under HL stress were immunoprobed with antisera specific to each of these subunits, most of the LSU signal within the pyrenoid was in cpSGs, whereas the SSU signal remained dispersed (Figure 4.4 B). Quantification of the mean signal densities in cpSGs, relative to the entire pyrenoid, confirmed that LSU localizes to cpSGs, whereas SSU does not (Figure 4.4 C). Therefore, LSU could be an mRNA-binding factor in cpSG assembly, analogous to TIA-1 and TIAR in the assembly of SGs in mammalian cells [161]. Different assembly mechanisms probably would be involved because LSU lacks amino

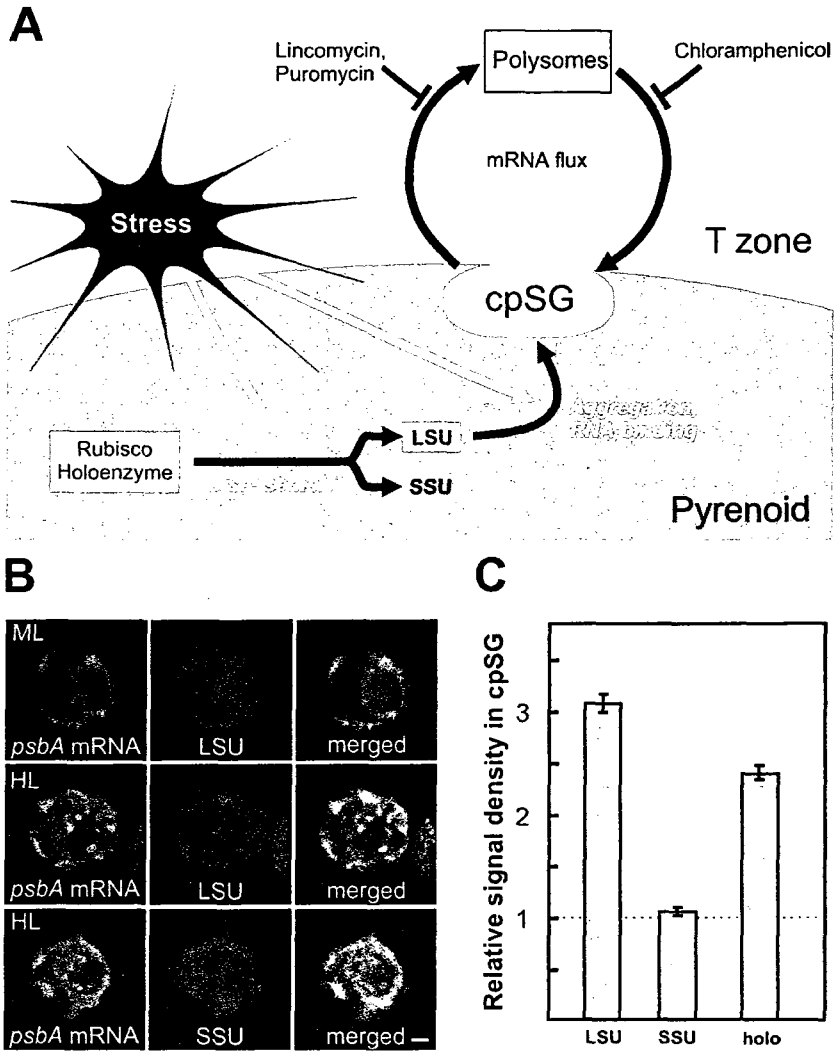

Figure 4.4. A model for cpSG assembly.

(**A**) cpSG assembly is proposed to involve the stress-induced disassembly of the Rubisco holoenzyme in the pyrenoid, the activation of the RNA-binding activity of LSU, followed by its concurrent aggregation and binding to mRNAs that are released from polysomes [163, 164]. Flux of mRNAs and small chloroplast ribosomal subunits between cpSGs and polysomes during stress was revealed by effects of the translation inhibitors. Lincomycin inhibits the initiation of protein synthesis, but allows ribosomes to complete translation, thereby liberating mRNA from polysomes. Puromycin liberates mRNAs from polysomes by inducing premature termination. Chloramphenicol prevents polysome disassembly by stalling translating ribosomes on mRNAs. (**B**) Cells from the nonstress condition of moderate light (ML) had immunolabeled LSU uniformly distributed within the pyrenoid. After the induction of stress by HL, most LSU of the pyrenoid localized in cpSGs, whereas SSU remained dispersed. (**C**) To quantify the localization of Rubisco LSU, SSU, and holoenzyme to cpSGs, the mean density of each signal therein was standardized to its density throughout the pyrenoid. A value substantially greater than one (dotted line) represents localization in cpSGs. Error bars represent two SE. The micrographs show 0.2 μm optical sections. Bar, 1 μm. For each experiment, $n \geq 20$ cells.

acid sequence similarity to the Q-rich prion-like domains in proteins that nucleate SG assembly (for review see [161]).

4.3.6 mRNAs from disassembled polysomes localize to cpSGs

I addressed the nature of the mRNAs that localize to cpSGs. Cytoplasmic SGs contain mRNAs that are liberated by the disassembly of their polysomes resulting from translational repression, but not mRNAs that are highly translated during stress [69, 165]. There is evidence for translational repression of the *rbcL* and *psbC* mRNAs during HL stress (Chapter 2; [164]). Although it is well known that HL stress activates *psbA* translation for the repair of photodamaged PS II complexes [19], a distinct *psbA* mRNA pool in T zones may become translationally repressed (Chapter 2). Although these results are consistent with the localization of mRNAs from disassembled polysomes to cpSGs, the following experiments were required to answer this question.

In mammalian cells, evidence that SGs receive mRNAs from disassembled polysomes was provided by studies involving pharmacological inhibition of translation. SG assembly was prevented by inhibitors of translation elongation, which trap mRNAs on polysomes. Similarly, treatment of *C. reinhardtii* cells with chloramphenicol, an inhibitor of translation elongation in the chloroplast, prevented cpSG assembly when oxidative stress was induced subsequently by rose bengal (Figure 4.5 A). Moreover, under these conditions, LSU was not detected in cpSGs, suggesting that the mRNAs released by polysome disassembly are required either to trigger LSU aggregation or to serve as a structural component of cpSGs (unpublished data; $n = 20$).

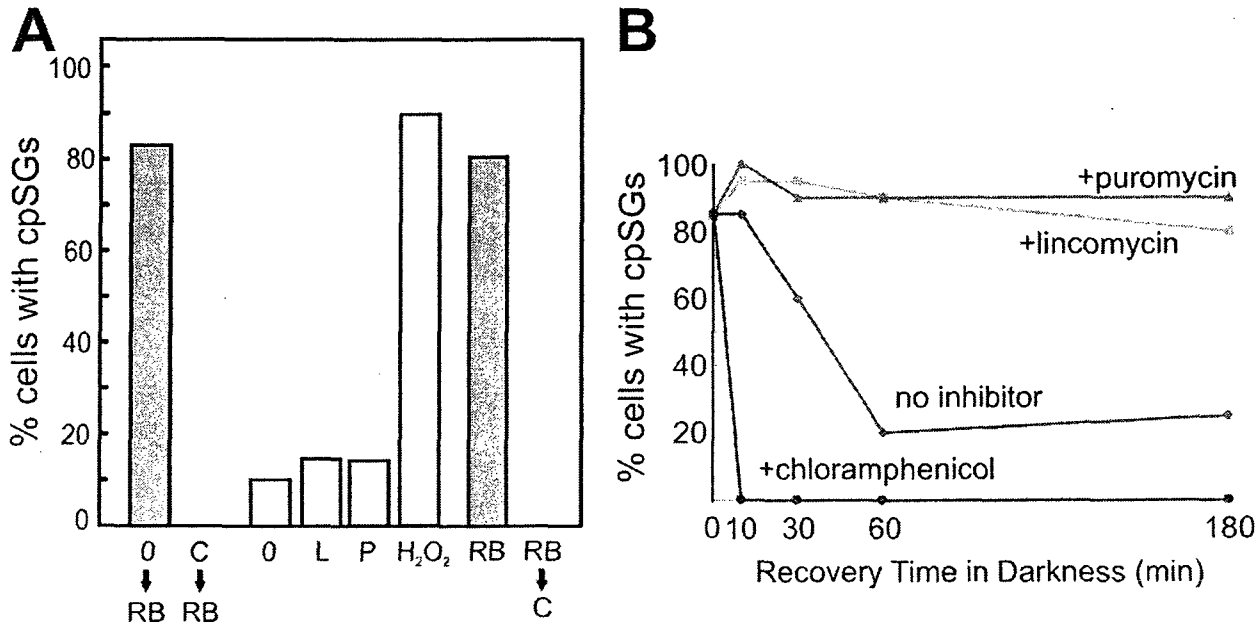

Figure 4.5. Evidence for *psbA* mRNA flux between cpSGs and polysomes during stress.

(**A**) The percentage of cells with cpSGs is graphed for moderate light cells incubated without or with chloramphenicol and then exposed to rose bengal to induce oxidative stress (shaded bars; 0 → RB and C → RB, respectively). Under non-stress conditions, mRNA release from polysomes only marginally induced cpSG formation as revealed by the percentages of cells with cpSGs that were exposed to no inhibitor (0), lincomycin (L), or puromycin (P), with treatment with hydrogen peroxide (H_2O_2) as a positive control. The cpSGs that formed in response to oxidative stress induced by exposure to rose bengal were abolished by a chloramphenicol treatment (shaded bars; RB and RB → C, respectively). (**B**) During recovery from rose bengal – induced oxidative stress in the dark, 60 min was required for the percentage of cells with cpSGs to drop to that of dark-adapted cells in the absence of inhibitor (diamonds). cpSG disassembly was accelerated by chloramphenicol (circles) and prevented by both lincomycin (squares) and puromycin (triangles). $n \geq 20$ cells for each condition.

In mammalian cells under non-stress conditions, SGs formed when mRNAs were liberated from polysomes by translation initiation inhibitors [166, 167]. However, if *cpSG formation involves stress-induced Rubisco disassembly and aggregation of LSU*, mRNAs released from polysomes in the absence of stress should not localize to cpSGs. Alternatively, if RNA-binding active LSU or any other protein that localizes mRNAs to cpSGs is always available, mRNAs released from polysomes under non-stress conditions should localize to cpSGs. Therefore, polysome disassembly in the chloroplast was induced by lincomycin or puromycin, which inhibit translation initiation and induce premature termination, respectively. In the absence of inhibitor under these conditions (see Materials and methods section 4.3), 10% of cells had cpSGs (Figure 4.5 A). In the presence of either inhibitor, 15% of the cells had cpSGs, a marginal increase compared with the effects of most stress conditions (Figure 4.2). Results of a positive control experiment revealed that most of these cells could form cpSGs upon exposure to hydrogen peroxide. Therefore, in addition to mRNAs from polysome disassembly, cpSG assembly requires a stress condition, e.g., to induce Rubisco disassembly and activate LSU for RNA binding (Figure 4.4 A).

4.3.7 mRNA flux occurs between cpSGs and polysomes

In mammalian cells, mRNA flux between SGs and polysomes was demonstrated, in part, by the rapid disappearance of SGs when mRNAs were trapped in the ribosome-bound pool by inhibitors of translation elongation during sustained oxidative stress [166]. Similar mRNA dynamics appear to occur in the *C. reinhardtii* chloroplast. First, during sustained oxidative stress induced by rose bengal, the 80% of cells that had formed

cpSGs lost them during a 10 min treatment with chloramphenicol, an inhibitor of elongation by chloroplast ribosomes (Figure 4.5 A). Second, chloramphenicol dramatically accelerated the disappearance of cpSGs during recovery from oxidative stress (Figure 4.5 B). Third, lincomycin and puromycin prevented cpSG disappearance within 180 min of recovery from stress, suggesting that mRNAs must be engaged by translating ribosomes to leave cpSGs. These inhibitors also initially enhanced the percentage of cells with cpSGs, presumably because they released mRNAs from polysomes in the minority of cells that had not done so in response to oxidative stress (Figure 4.5 B). Thus, like mammalian SGs, cpSGs do not sequester mRNAs during stress. Rather, mRNAs are in continuous flux between polysomes and cpSGs (Figure 4.4 A). Such mRNA dynamics could be facilitated by the proximity of cpSGs to T zones, where the *psbA* and *psbC* mRNAs are translated (Figure 4.3 C; Chapter 2).

4.4 Conclusion

This discovery of cpSGs reveals a novel chloroplast stress response and, to my knowledge, the first example of a stress-induced RNA granule in a bacterial lineage or organellar genetic system. The location of cpSGs suggests that the pyrenoid provides an environment depleted of ROS, which are produced during stress throughout the rest of the chloroplast and known to damage RNA [168]. My results raise the possibility of a novel function of Rubisco LSU as an mRNA-localizing and assembly factor of cpSGs. The RNA-binding activity of LSU and its activation by oxidizing conditions are conserved in higher plants, suggesting that I have identified a general chloroplast stress response [164]. It remains to be determined whether cpSGs and SGs evolved from a common

ancestral RNA granule or by convergent evolution from distinct origins in response to general requirements of mRNAs released from polysomes during stress. In either case, a comprehensive understanding of cpSGs should elucidate these requirements and the molecular mechanisms that fulfill them in chloroplasts.

5 Chloroplast stress granules are required for short term, but not long term, oxidative stress tolerance

5.1 Introduction

A major unanswered question is whether or not SGs have a direct role in tolerance to oxidative stress because of their rapid appearance during these conditions. My discovery of cpSGs led me to explore their functions. I proposed in Chapter 4 that LSU is an RBP that nucleates cpSG formation because, under oxidative stress, Rubisco disassembles into its constituent LSUs and SSUs, whereupon the oxidized LSU non-specifically binds chloroplast mRNAs and localizes to cpSGs (Chapter 4; [164]). I also proposed that the pyrenoid has a function in cpSG assembly and sequesters free mRNAs from ROS produced by thylakoid membranes throughout the rest of the chloroplast. In this Chapter, I investigated further the role of LSU and the pyrenoid in the assembly of cpSGs by using FISH to determine whether or not mutants lacking LSU and pyrenoids can form cpSGs.

Another question concerns the function(s) of SGs. In mammalian cells, SGs are thought to be involved in stress tolerance because lethality was observed in two mutant cell lines that did not form SGs when stressed [80, 81]. These cell lines had mutations in heme-regulated inhibitor kinase or the deacetylase HDAC6, which both act upstream in signal transduction pathways that activate SG assembly. Heme-regulated inhibitor kinase is activated upon stress whereupon it phosphorylates eIF2α to cause global translational repression and the release of mRNAs from polysomes. These mRNAs are also a structural component of SGs. The other protein, HDAC6, is an enzyme that

deacetylates tubulin and HSP90 and has many other targets. Since both of these proteins have essential functions which are independent of their roles in SGs, assigning a stress tolerance function to SGs may be premature because the lethality of null mutants for them could be due to effects upon other processes. Similarly, mouse mutants that are deficient for RBPs directly involved in SG assembly are either lethal because these proteins have essential functions in development or have no phenotype because there are functionally redundant proteins [65].

I was able to address these questions for cpSGs because, in C. *reinhardtii*, LSU is not essential since this alga can take up and metabolize an exogenous reduced carbon source such as acetate and thereby dispense with photosynthesis. Therefore, I was able to analyze LSU-deficient mutants that are known to lack pyrenoids and ask whether or not the LSU-deficient mutant can form cpSGs or not [173]. The question is whether the pyrenoid is required for cpSG formation or whether both LSU and the pyrenoid are not required. Analysis of the SSU-deficient mutant, which accumulates LSU (and lacks a pyrenoid), allowed me to determine whether or not LSU can form cpSGs in the absence of Rubisco holoenzyme and a pyrenoid. If the LSU-deficient mutants did not form cpSGs, I would test their tolerance to oxidative stress by monitoring their growth in such conditions.

In Chapter 4, I describe cpSGs and SGs as having translation initiation factors, the small but not the large ribosomal subunit, and that mRNA departure requires translation. This is consistent with a general, physiological role of cpSGs in the initiation of translation and concurrent protein synthesis. Upon stress, cpSGs might increase in

size and become detectable by confocal microscopy, but exist as ribonucleoprotein complexes under non-stress conditions. This hypothesis predicts that a cpSG-deficient strain would be impaired in the induction of protein synthesis in the chloroplast. In Chapter 2, I showed that the synthesis of PS II subunits is induced rapidly by a shift from dark to ML conditions. Therefore, I tested the ability of two Rubisco mutants to induce protein synthesis for de novo PS II biogenesis with in vivo ^{35}S pulse-labelling.

I found that LSU and the pyrenoid are required for the assembly of cpSGs and that cpSGs are not required for oxidative stress tolerance or the induction of protein synthesis.

5.2 Materials and Methods

C. reinhardtii culture conditions

Wild-type strain 4C+, and mutant strains MX3312 (Δ*rbcL;* Dr. Genhai Zhu (Pioneer Hi-Brid)) and T60-3 (Δ*rbcS;* [141]) were cultured on TAP medium under indirect light to a cell density of 2-3 X 10^6 cells/ml at 24°C under a light intensity of 100-150 $\mu E \cdot m^{-1} \cdot s^{-2}$ and with orbital shaking [92]. HL (2000 $\mu E \cdot m^{-1} \cdot s^{-2}$) was generated by a slide projector (Kodak), to which small (2-30-ml) cultures were exposed at a distance of 10 cm for 10 min with manual shaking. H_2O_2 was added to TAP agar medium immediately prior to pouring of the plates. Plates are stored in the dark at 24 °C to prevent H_2O_2 degradation and allowed drying of excess condensation from the solidified medium for at least 48 h before use. Strains were struck on the solidified medium. A serial dilution of a wild-type and an LSU-deficient strain was spotted on solid media containing varying H_2O_2 concentrations. Plates were incubated in the dark for 7-10 days. 500 cells of a wild-type,

an LSU-deficient strain, and an SSU-deficient strain were plated on TAP plates with increasing concentrations of H_2O_2. Plates were incubated in the dark for about a week. Growth curves of a wild-type, an LSU-deficient strain, and an SSU-deficient strain were monitored after the addition of increasing concentration of H_2O_2. Wild-type and LSU-deficient cells were exposed to 2 mM H_2O_2 and their survival was monitored over 18 h. Survival was monitored by removing some cells at the specified time points and spotting them on a microscope slide with an equal amount of 0.4% Trypan Blue (Sigma). Dead cells were distinguished from live cells by their blue staining.

FISH, IF staining, and pyrenoid staining

The procedures and probes used for FISH and IF were described previously (Chapters 2-4). To reveal the pyrenoid, the marker protein carbonic anhydrase was histochemically stained by first fixing cells in 4% para-formaldehyde (1 X PBS) and then placed in open Petri plate halves for the subsequent washing steps. A 1 mL solution of 50% acetone, 50 mM 5-Dimethylaminonaphthalene-1-sulfonamide (Fluka Cat. #39225) and a drop of 10N NaOH was placed on the slide and incubated for 5 min. The slides were then washed in a Coplin jar in 20 mM HEPES-KOH (pH 7.6) for 5 min, mounted with ProLong Gold antifade reagent (Invitrogen) and observed under UV-excitation [169].

5.3 Results

5.3.1 An LSU-deficient mutant does not form cpSGs

I first asked whether an LSU-deficient mutant lacking a pyrenoid forms cpSGs. This mutant was first exposed to HL stress and then FISH-probed for the *psbA* mRNA and co-immunostained for Rubisco to see if cpSGs could form (Figure 5.1 B). None of the LSU-

deficient cells examined had cpSGs, while most of the wild-type cells had them (Figure 5.1 A) suggesting that LSU and the pyrenoid are important factors in cpSG assembly. The red IF signal corresponds to SSU because the antiserum was raised against the Rubisco holoenzyme. It has been shown that SSU in this *rbcL* chloroplast mutant is rapidly degraded following its import into the chloroplast. It seems that there is enough SSU or SSU degradation products to detect by IF [141]. A deletion mutant for both *Rbcs* genes, T60-3, was exposed to the HL stress conditions to determine if the cpSG minus phenotype observed in the LSU-deficient strain was specific to the lack of LSU, the pyrenoid, and the Rubisco holoenzyme. No cpSGs were observed in this mutant in HL stressed cells (Figure 5.1 C). However, LSU is not stable in this mutant because it is rapidly degraded when SSU is not available [141]. Therefore, even though LSU IF signal can be observed, its localization is different in wild-type (see Chapter 4) and its rapid degradation (or the lack of a pyrenoid) could be affecting its ability to assemble cpSGs.

The LSU-deficient mutant has been shown to lack a pyrenoid [171]. I observed this strain, the SSU-deficient mutant, and the wild-type under differential interference contrast microscopy and saw differences in their chloroplast morphology (Figure 5.1 D-F). Although the mutant strains appear to have a pyrenoid, this could be a large starch granule because: 1) these mutants have an abundance of starch granule-like structures of varying sizes in their chloroplast (arrow in Figure 5.1 E) and 2) the starch sheath that is visible around the pyrenoid in wild-type strains appears to be absent in the mutants (Figure 5.1 D). The lack of a pyrenoid in the mutant strains was confirmed with a UV-

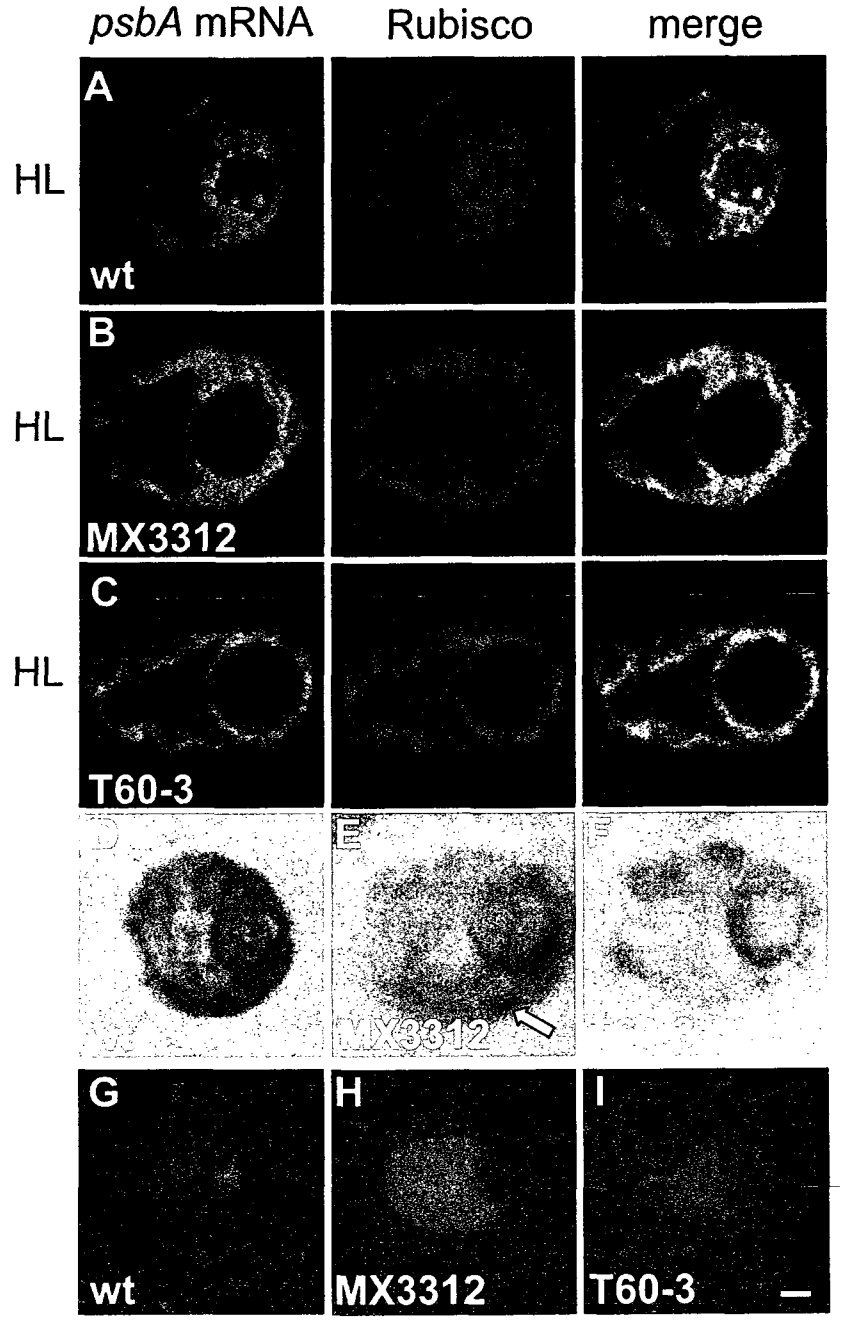

Figure 5.1. Mutants deficient for LSU or SSU do not form cpSGs and also lack a pyrenoid.

(**A**) HL stress induces the formation of cpSGs in wt cells, but not in a mutant lacking LSU (MX3312) (**B**) or a mutant lacking SSU (T60-3) (**C**). Differential interference contrast images of a wt cell (**D**), MX3312 (**E**) and T60-3 (**F**). A carbonic anhydrase stain reveals the pyrenoid in a wt strain (**G**), but not in MX3312 (**H**) or T60-3 (**I**). The micrographs show 0.2 µm optical sections. n = 20. wt, wild-type. Bar, 1 µm.

fluorescent molecule that binds to carbonic anhydrase, which is primarily localized within the pyrenoid of *C. reinhardtii* [170]. The pyrenoid can be seen in the wild-type strain as a blue sphere (Figure 5.1 G), while the two Rubisco-deficient mutants have a uniform signal distribution and unstained regions corresponding to the starch granule-like structure(s) (Figure 5.1 H-I). Therefore, the lack of carbonic anhydrase staining in these bodies provides further evidence that they are not pyrenoids. A more general link between photosynthesis and cpSG assembly was suggested because a variety of other photosynthetic mutants did not have pyrenoids and did not form cpSGs under oxidative stress conditions (data not shown). Thus, the pyrenoid appears to be required for cpSG assembly.

5.3.2 Mutants that do not form cpSGs are not detectably impaired in oxidative stress-tolerance

To test whether cpSGs function in oxidative stress tolerance, we compared the tolerance of a wild-type strain and the two Rubisco-deficient mutants to varying H_2O_2 concentrations. The first assay involved testing the wild-type and mutant strains for the ability to grow on solid medium containing varying H_2O_2 concentrations. A previous study revealed that the highest percentage of cells with cpSGs was observed in the presence of 2 mM H_2O_2 (Chapter 4). The growth of all three strains was similarly inhibited at each H_2O_2 concentration (Figure 5.2). The H_2O_2 is active because it inhibited the growth of all three strains at 5 mM (Figure 5.2 E). Because the number of cells streaked on each section of each plate is not the same in this experiment, a more precise method was employed.

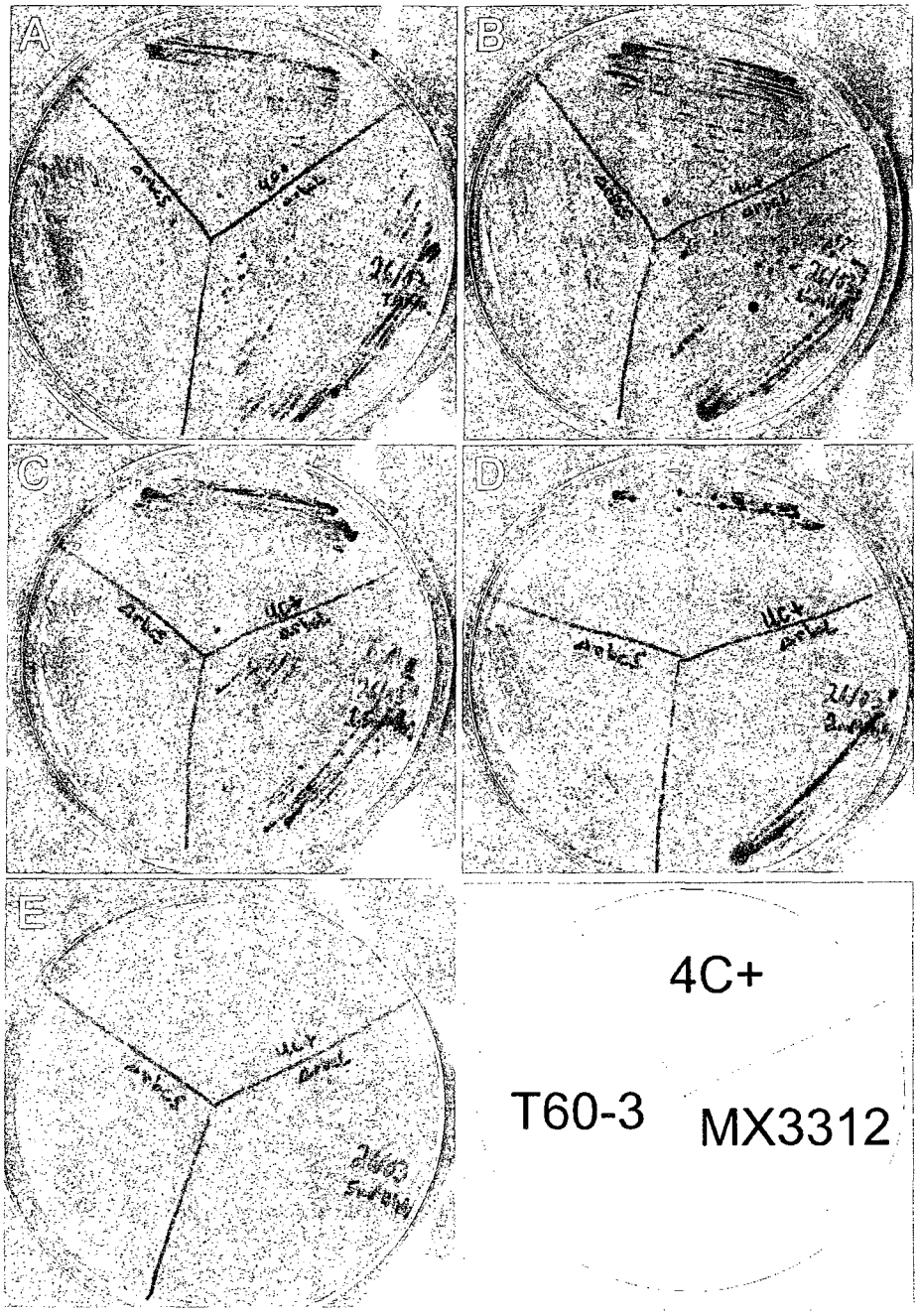

Figure 5.2. Two Rubisco-deficient strains that do not form cpSGs, MX3312 and T60-3, have wild-type levels of tolerance to oxidative stress.

The wild-type strain (4C+) and two Rubisco-deficient mutants (MX3312 and T60-3*J* were streaked on solid agar medium with increasing concentrations of H_2O_2: 0 mM (**A**), 1 mM (**B**), 1.5 mM (**C**), 2 mM (**D**), and 5 mM (**E**).

The second assay involved testing the ability of wild-type and mutant strains to form colonies by spotting cells in a serial dilution onto solid medium containing varying H_2O_2 concentrations. At the lowest dilution (40 cells), colonies could be counted so that the effect on colony size and formation could be determined. The result was the same as in Figure 5.2 except that the LSU-deficient strain grew slightly faster than the wild-type on the 1 mM, 1.5 mM and 2 mM plates (Figure 5.3). The third assay was the same except 500 cells of each strain were spread on solid media containing varying H_2O_2 concentrations to see the effect that oxidative stress had on the growth of these strains by counting the number of colonies that could form (Figure 5.4 A). Similar to the results in Figure 5.3, both Rubisco mutants developed the same number of colonies as the wild-type strain. Therefore, cpSGs appear to have no function in tolerance to H_2O_2.

Because these experiments focused on the effect of oxidative stress on solid media, I decided to test these effects in liquid media because growth rate could be measured more accurately and in a shorter time period by monitoring cell density. The fourth assay involved monitoring the effect of H_2O_2 on cell density over a period of days. H_2O_2 was added to a wild-type, an LSU-deficient, and an SSU-deficient strain at mid-log phase. Similar to the results on solidified media, the growth of these strains was similarly affected by H_2O_2. The mutant strains grew more rapidly than the wild-type strain when exposed to 2 mM H_2O_2 (data not shown). More trials are required because an increase in growth rate was observed when no H_2O_2 was added.

The fifth assay involved monitoring survival during oxidative stress over a shorter time period. When cells were shifted to 2 mM H_2O_2, about 60% of the mutant cells died

within the first 2 h when most wild-type cells remained viable. However, after 4 h, the Wild-type and *rbcL* deletion mutant strains were grown mixotrophically until mid-exponential phase and then spotted as serial dilutions on acetate-containing (TAP) agar plates of increasing H_2O_2 concentrations (0 mM, 1 mM, 1.5 mM and 2 mM). wt, wild-type.survival of the mutant cells stabilized while the survival of the wild-type cells plummeted to less than 20% between 4 h and 18 h (Figure 5.4 C). These results suggest that cpSGs could have a role in tolerance to oxidative stress only within the first few hours of stress (see Discussion). The same results were obtained for all these experiments when using other forms of oxidative stress such as HL or Rose Bengal treatment (data not shown).

5.3.3 cpSGs are not required for wild-type levels of translation initiation in the chloroplast

In Chapter 4, I show that cpSGs, like cytoplasmic SGs in other systems, contain translation initiation factors, the small but not the large ribosomal subunit, and that mRNA departure from cpSGs requires translation. While SGs and cpSGs are believed to assemble only during stress, this is consistent with a general, physiological role of cpSGs in the initiation of translation. Upon stress, in this scenario, cpSGs increase in size and become detectable by confocal microscopy. Under non-stress conditions, they exist as smaller ribonucleoprotein complexes which cannot be detected by this method. This hypothesis predicts that a cpSG-deficient strain would be impaired in the induction of protein synthesis in the chloroplast. In Chapter 2, I showed that the synthesis of PS II subunits is induced rapidly by a shift from dark to ML conditions (Figure 2.2). Therefore,

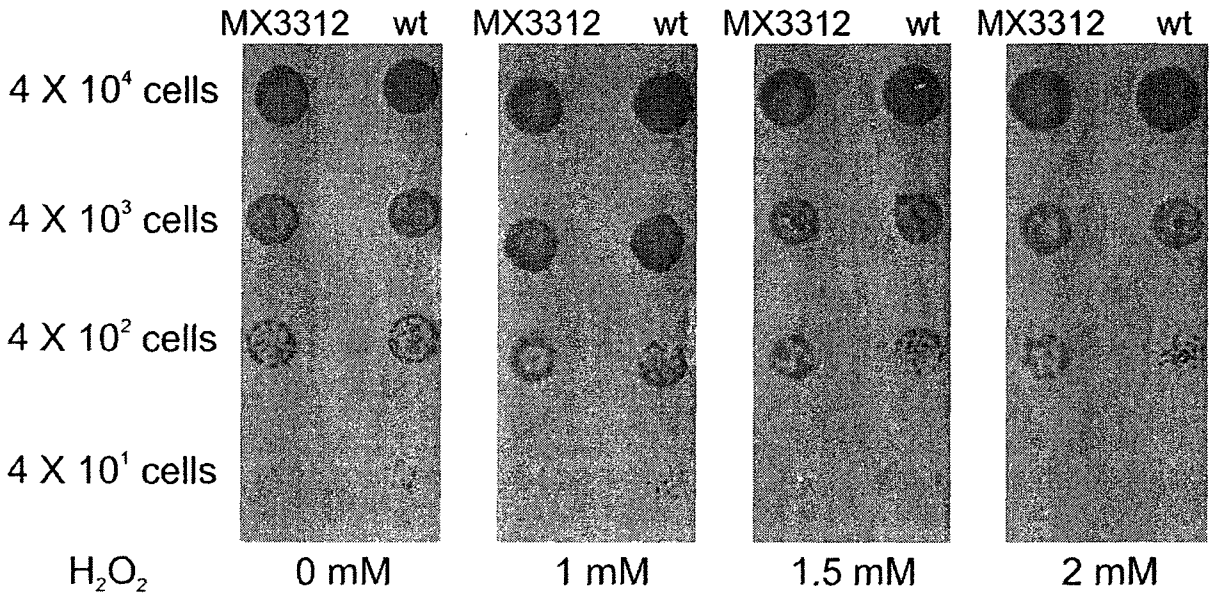

Figure 5.3. A strain that does not form cpSGs, an *rbcL* deletion mutant, has wild-type levels of tolerance to oxidative stress.

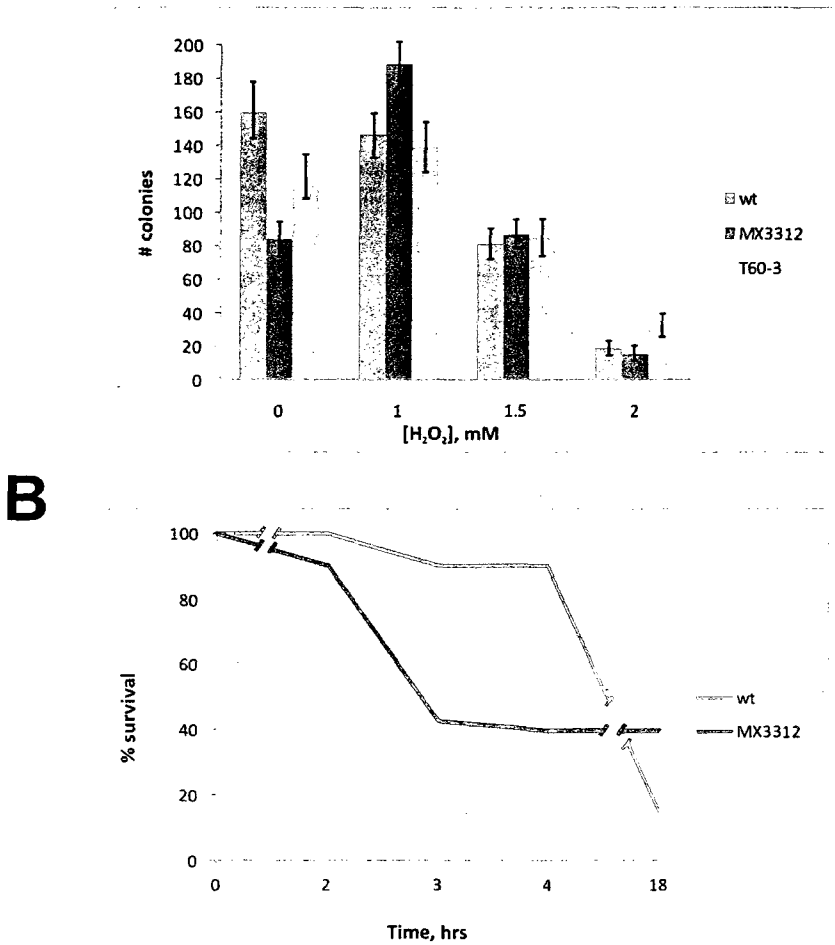

Figure 5.4. *Two Rubisco-deficient strains that do not form* chloroplast stress granules, T60-3 and MX3312, have wt levels of tolerance to oxidative stress.

(**A**) 500 cells were plated on increasing concentrations of H_2O_2 and surviving colonies were counted. The two mutants had a similar number of colonies, if not more, as the wt. Columns represent the average of 3 experiments. Error bars represent 2 SE. (**B**) A wt strain and the MX3312 mutant were exposed to 2 mM H_2O_2 and their survival was monitored in liquid culture over periods of 2, 3, 4 and 18 h. wt, wild-type.

I tested the ability of two cpSG-deficient mutants to induce protein synthesis for de novo PS II biogenesis with in vivo ^{35}S pulse-labelling. Both mutants grown in the dark for 2 h had low levels of PS II subunit synthesis (Figure 5.5 lanes 1 and 2). De novo PS II biogenesis was induced by shifting the cells to ML for 20 min. PS II subunit synthesis was induced in these mutants suggesting that their lack of cpSGs does not impair their ability to initiate PS II biogenesis (Figure 5.5 lanes 3 and 4). I also wanted to test whether these mutants could induce D1 synthesis for PS II repair because it had been previously reported that inhibiting the Calvin cycle or a missense mutation in *rbcL* abolished D1 repair synthesis [168]. My results contradict this finding. Both Rubisco deletion mutants induced D1 repair synthesis to the same extent as wild-type when exposed to HL for 20 min (as seen by the preferential D1 synthesis in Figure 5.5 lanes 5 and 6).

5.4 Discussion

My results reveal that cpSGs may be involved in short term oxidative stress tolerance, but not long term tolerance. Two Rubisco-deficient mutants, MX3312 and T60-3, did not form cpSGs (Figure 5.1 A-C), but had wild-type levels of oxidative stress tolerance (Figures 5.2, 5.3 and 5.4 A). However, when the survival of these mutants was monitored over a period of a few hours during oxidative stress, they were significantly impaired in their survival. cpSGs receive mRNAs from disassembling polysomes during the global translational arrest that occurs within minutes after stress (Chapter 4). Therefore, cpSGs may function in the early stages of oxidative stress when mRNAs are being released from polysomes.

Under long term oxidative stress (days), cultures of the Rubisco mutants grew faster than did wild-type (Figure 5.3, 5.4 A). These mutants are known to have elevated levels of H_2O_2 in their chloroplasts because interruption of the Calvin cycle and photorespiration decreases the utilization of NADPH, which leads to the reduction of O_2 to form H_2O_2 [172]. Therefore, the Rubisco mutants may constitutively express pathways that detoxify ROS or mitigate their effects, which gives them an advantage over the wild-type strain and may compensate for the lack of cpSGs during oxidative stress.

These findings contradict two reports that mammalian SGs provide long term stress tolerance [80, 81]. However, these studies analyzed mutants that are deficient for both SGs and pathways upstream of assembly that could have pleiotropic effects. The mutants are defective in cpSG assembly and deficient for Rubisco, an enzyme I proposed is involved in cpSG assembly (Chapter 4). Photosynthesis is not functional in these mutants; therefore mutations in this pathway should not have other effects.

In addition to lacking cpSGs, these Rubisco-deficient mutants also lacked pyrenoids or had empty pyrenoids lacking Rubisco and carbonic anhydrase (Figure 5.1 D-I). Therefore, the pyrenoid has a role in cpSG assembly, possibly either because Rubisco must be within the pyrenoid for its LSU to participate in assembly or the pyrenoid itself facilitates the assembly of cpSGs from components arriving from the stroma (free mRNAs, small ribosomal subunits) and the pyrenoid matrix (LSU). This is the first report of an SSU-deficient mutant without a pyrenoid, and other photosynthetic mutants having active Rubisco but no pyrenoid.

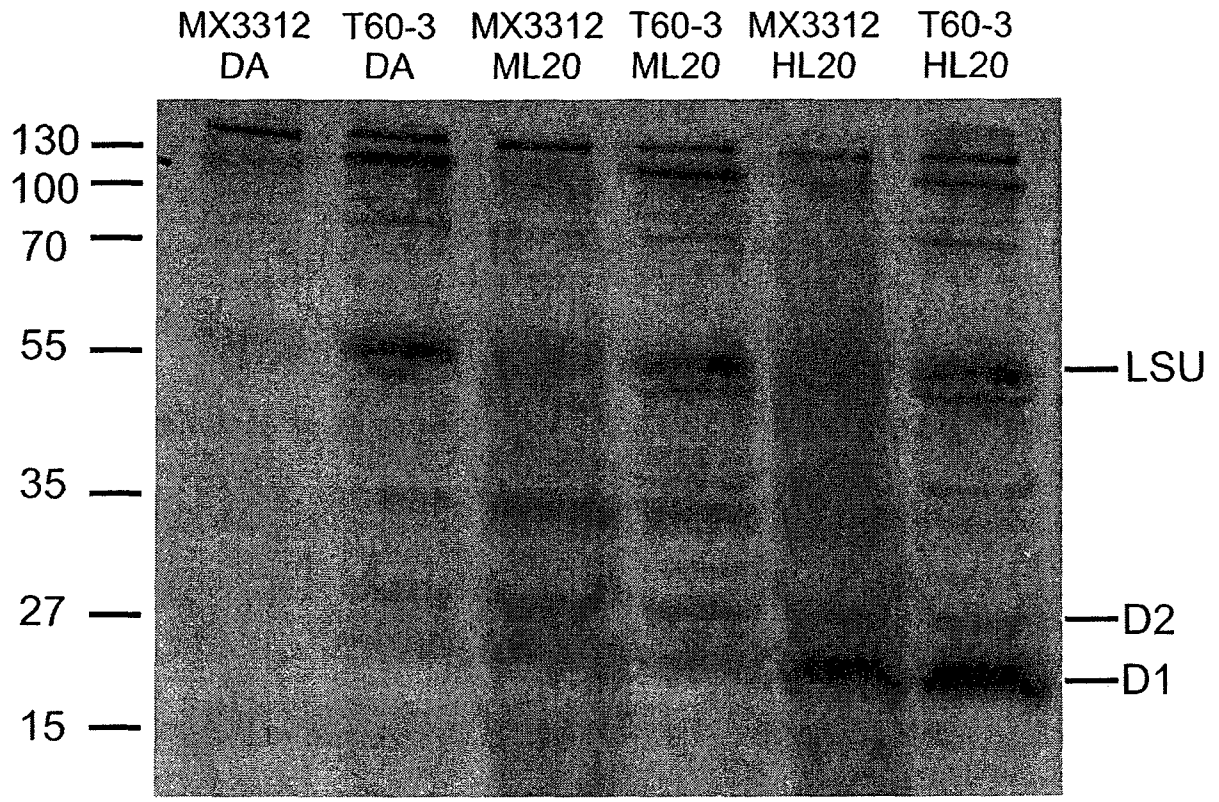

Figure 5.5. Protein synthesis for PS II biogenesis and repair is not impaired in two Rubisco-deficient mutants.

Chloroplast protein synthesis was monitored in vivo by ^{35}S pulse-labelling. Reduced protein synthesis was evident in two Rubisco-deficient mutants, MX3312 and T60-3, that were dark-adapted (DA) for 2 h (lanes 1 and 2). PS II biogenesis was induced by exposing MX3312 and T60-3 mutants to moderate light (ML) for 20 min (lanes 3 and 4). PS II repair and preferential D1 synthesis was induced by exposing MX3312 and T60-3 mutants to HL for 20 min (lanes 5 and 6). LSU, large subunit of Rubisco.

This study also ruled out a possible role of cpSGs in facilitating the initiation of de novo PS II biogenesis. Two mutants that do not form cpSGs were shown to induce protein synthesis when PS II biogenesis was induced (Figure 5.5). These findings also surprisingly contradict a previous report that the interruption of the Calvin cycle inhibits protein synthesis in the chloroplast [173].

5.5 Conclusion

These results suggest that cpSGs have a role in short term tolerance to oxidative stress, consistent with the proposed model that mRNAs from disassembled polysomes enter SGs within minutes of stress exposure. However, my results show that cpSGs do not have a critical function in tolerance to sustained long term oxidative stress. It will be interesting to test the effects of inhibiting mammalian SGs directly at the assembly level to see if they really do have a function in stress tolerance. Another roadblock in determining the function of SGs is that they have been difficult to isolate from mammalian cells. It would be interesting to try to isolate pyrenoids (see Chapter 6) in stressed *C. reinhardtii* cells and compare the proteome of these pyrenoids versus non-stressed cells to obtain a proteome of cpSGs. My findings have taken the analysis of cpSGs beyond what has been done for mammalian SGs.

6 Characterization of the pyrenoid proteome in *Chlamydomonas reinhardtii*

6.1 Introduction

The pyrenoid has been mentioned prominently throughout the preceding chapters. The pyrenoid is located close to T zones which I showed are involved in the de novo assembly of PS II (Chapter 2). The translation of the *rbcL* mRNA was found to be localized around the pyrenoid (Chapter 3). cpSGs are localized at the internal perimeter of the pyrenoid (Chapter 4) and the pyrenoid is required for cpSG assembly (Chapter 5). The complete protein composition of this chloroplast compartment is unknown. In this chapter, a fast and easy protocol for isolating a fraction enriched in pyrenoids is described. IF microscopy and mass spectrometry were performed on these fractions to characterize the proteome of the pyrenoid. From these data, we may gain a better understanding of the function of the pyrenoid.

6.2 Materials and Methods

C. reinhardtii culture conditions

The strain used in the pyrenoid isolation, KaCW15#6, is a cell wall defective mutant that was created in our lab by crossing a wild-type strain with a cell wall defective mutant carrying the CW15 mutation. KaCW15#6 was one of these progeny and was chosen based on how quickly it lysed in 2% Triton-X100. This strain was cultured either photoautotrophically or mixotrophically on HSM or TAP, respectively, until mid-log phase (3 X 10^6 cells/mL) at 24°C and under a light intensity of 100 to 150 $\mu E \cdot m^{-2} \cdot s^{-1}$.

Pyrenoid isolation

A 500 mL culture of KaCW15#6 cells was pelleted by centrifugation at 5000 x g for 10 min and resuspended at a cell density of $8X10^7$ cells/mL in 1 X Breaking Buffer (BB, 0.3 M sorbitol, 10 mM Tricine pH 7.8, 10 mM EDTA). An equal volume of 4% Triton-X100 in 1 X BB was added to the cells for a final concentration of 2% Triton-X100. This mixture was layered on 80% Percoll in 1 X BB and centrifuged at 7500 rpm for 10 min. The Triton-X100 and Percoll were removed carefully with a pipet. Excess Triton-X100 was removed by washing the pellet gently with 1 X BB. Pyrenoids can be visualized under light microscopy by spotting a few µL of the preparation on a microscope slide.

Western blot analysis

The pyrenoid pellet was resuspended in 50 µL loading buffer (2% SDS, 10% glycerol, 0.1 M DTT, 0.125 M Tric-HCl, 0.004% bromophenol blue), boiled for 1 min, and proteins were resolved by SDS-PAGE. The proteins were transferred to a nitrocellulose membrane and then blocked for 1 h in 5% milk and 1 X PBS with shaking. The membrane was probed with primary antisera diluted to 1:1000 in blocking solution for 2 h at 4 ^{o}C with shaking and then washed three times in 1 X PBS for 10 min each. The membrane was then probed with secondary antisera linked to horseradish peroxidase (Fisher Scientific SA1200) diluted to 1:20000 in blocking solution and then washed twice in 1 X PBS for 5 min each. Chemiluminescent revelation was done according to manufacturer's protocol (Millipore WBKLS0100).

Mass spectrometry

Samples of the pellet fraction, containing pyrenoids, in SDS-PAGE loading buffer were incubated at 100 ^{o}C for 1 min, and subjected to electrophoresis on a 12-18% polyacrylamide gel (overnight at 4 mA). Protein was stained with Coomassie Blue for one hour and the gel was destained until the background was clear. The gel slices (length) were excised and then cut into 1 mm^3 pieces with a razor blade, using a new blade for each cut, and starting at the low-molecular weight region of the lane. Major bands were specifically excised, while areas with few bands could be cut into larger sections. The gel pieces were incubated in 200 µL of wash solution (50% methanol and 5% acetic acid) overnight in 1.5 mL microcentrifuge tubes at room temperature. The wash solution was removed and another 200 µL was added to the gel pieces for 2 h. Next, 200 µL of acetonitrile was added for 5 min and then all the solution was removed. The gel pieces were dried completely in a speed vac for 3 min, 30 µL of 10 mM DTT was added for 30 min and then removed. Finally, 30 µL of 100 mM iodoacetamide was added for 30 min and then removed. Gel fragments were incubated in 200 µL of acetonitrile for 5 min, then in 200 µL of 100 mM ammonium bicarbonate for 10 min and then dried completely in a speed vac for 3 min. Trypsin reagent was prepared by adding 1000 µL of ice-cold 50 mM ammonium bicarbonate to 20 µg trypsin (Sigma). The gel pieces were incubated in 30 µL of the trypsin reagent on ice for 10 min with occasional gentle vortexing. The gel pieces were pelleted by centrifuging the sample for 30 sec and the excess trypsin solution was removed. Prior to vortexing, 5 µL of 50 mM ammonium bicarbonate was added to the sample, and then the samples were cenrifuged for 30 sec

at 13000 rpm. The digestion was carried out overnight at 37 ^{o}C. The next day, 30 µL of 50 mM ammonium bicarbonate was added to the digest for 10 min with occasional vortexing. The digest was pelleted by centrifuging the sample for 30 sec at 13000 rpm. The supernatant was collected and transferred to a new microcentrifuge tube. The gel pieces were incubated in 30 µL of extraction buffer (50% acetonitrile, 5% formic acid) for 10 min at room temperature. The supernatant was removed and transferred to a centrifuge tube. A second 30 µL of extraction buffer was added and incubated for 10 min. The supernatant was removed and combined in the new microcentrofige tube. The volume of the extract was reduced to 20 µL in a speed vac at ambient temperature. The samples were subjected to tandem mass spectrometry (MS/MS). Using SEQUEST from BioWorks 3.3 (Thermo Electron), the peptide sequences were searched against the *C. reinhardtii* genome version 3.0 at the Joint Genome Institute (http://genome.jgi-psf.org/Chlre3). Charge state analysis was performed during DTA file filtering, and a series of high-stringency filters was applied to the search results. The singly, doubly, and triply charged peptide ions required SEQUEST cross-correlation (XC) scores of at least 1.8, 2.5, and 3.5, respectively. We only considered peptide and protein hits identified on the basis of two or more unique peptides and with probability scores of less than 10^{-3}, as calculated by BioWorks.

6.3 Results

6.3.1 Pyrenoids can be isolated from a cell wall defective strain

It was necessary to establish a procedure for isolating pyrenoids that eliminates as many contaminants from other cellular compartments. Different techniques have been used,

but usually Triton-X100 is used to lyse the cell and solubilize membranes, and the pyrenoids are pelleted through sucrose density gradients away from most cellular debris [174]. Pyrenoids are stable in 2% (vol/vol) Triton-X100 under isotonic conditions because they are not membrane bound. Therefore, treatment of cell wall defective strains with 2% Triton-X100 solubilized most cell membranes and released the pyrenoids. We have developed a quicker and easier method by subsequently pelleting the cellular debris through an 80% percoll gradient (Figure 6.1). Kuchitsu *et al.* [174] use mercury for isolating pyrenoids from *C. reinhardtii* wild-type strains, but we found that mercury did not improve the pyrenoid yield of our fraction and decided to omit the use of this hazardous element.

To confirm that the pellet was enriched in pyrenoids, we used Western blot analysis, microscopy, IF and SDS-PAGE. First, we spread 5 µL of the pellet onto a microscope slide and observed it with a light microscope. Many spherical bodies having the approximate sizes of pyrenoids were seen, and one is seen next to an intact cell (Figure 6.2 A). Intact cells in the pellet were rare: this image was chosen to show a side by side comparison between a pyrenoid and a cell. Next, we stained these pyrenoids with a stain for the pyrenoid carbonic anhydrase (see Chapter 5) and performed IF with an α-Rubisco antibody to show that these bodies contain pyrenoid marker proteins. Strong signal could be observed from carbonic anhydrase and Rubisco within these bodies (Figure 6.2 B-D). A Western blot analysis of our pyrenoid fraction

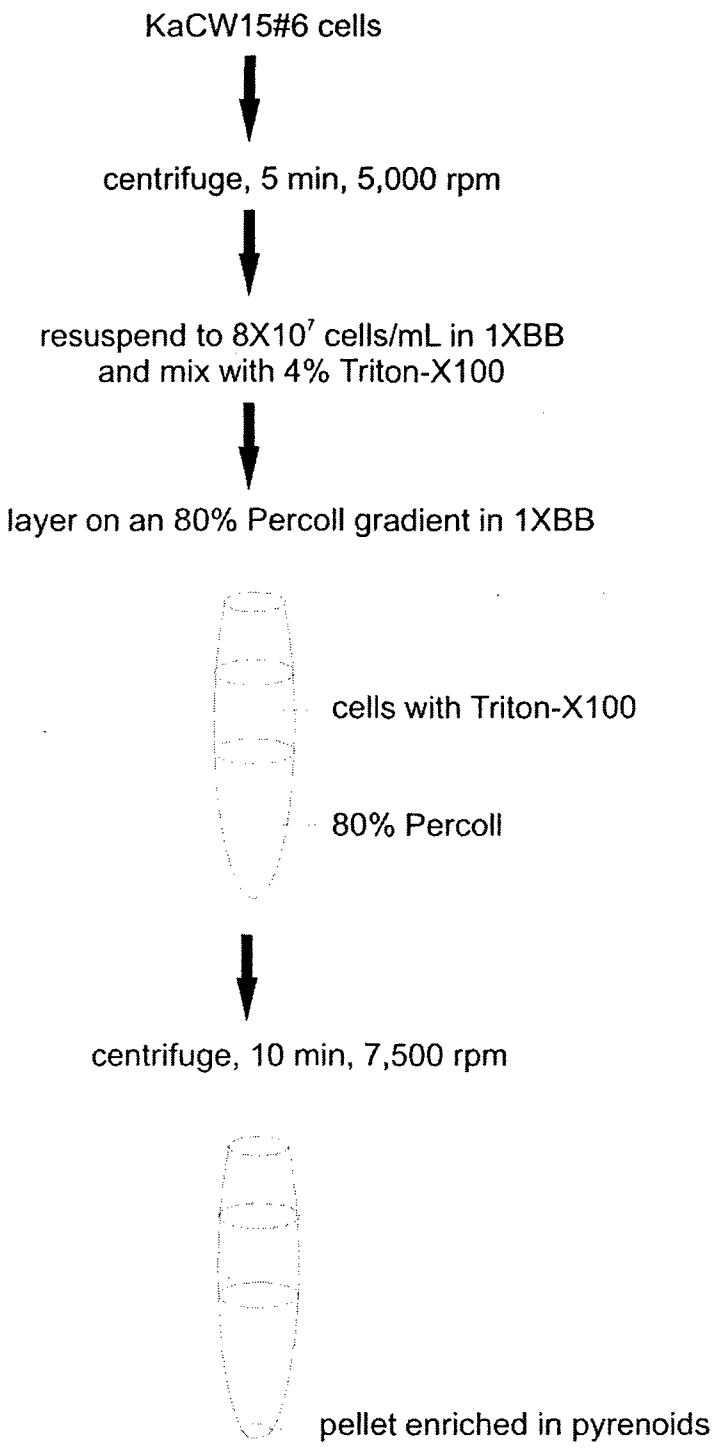

Figure 6.1. Pyrenoid isolation procedure.

KaCW15#6 cells were pelleted and resuspended to a final concentration of $8X10^7$ cells/mL in 1X Breaking Buffer (BB). An equal volume of 4% Triton-X100 in 1XBB was added to the cells. This mixture was layered on 80% Percoll in 1XBB and centrifuged at 7,500 rpm for 10 min. The pellet is enriched in pyrenoids.

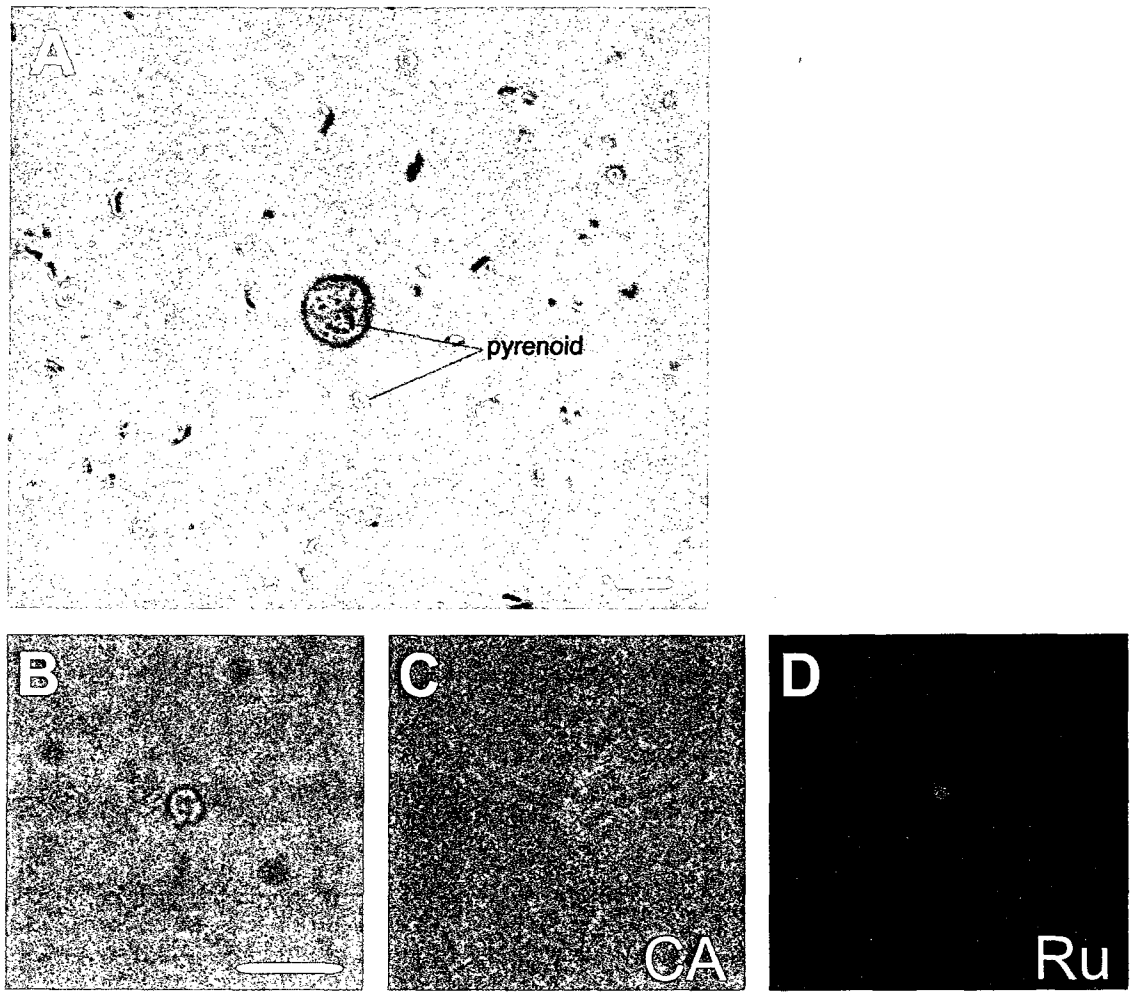

Figure 6.2. The pellet fraction is enriched in pyrenoids.

(A) Spherical bodies having the approximate size of pyrenoids can be observed next to an intact cell. **(B-D)** Signals from carbonic anhydrase (CA) and Rubisco (Ru) show that these bodies contain bona fide pyrenoid proteins. **(E)** Western blot analysis revealed that the pyrenoid fraction (lane 2) was highly enriched in the large subunit of Rubisco (LSU) compared to the supernatant (lane 1). Bars, 5 µm.

revealed that it was highly enriched in LSU compared to the supernatant (Figure 6.2 E). Finally, when the pyrenoid fraction was compared to the supernatant on an SDS-PAGE, most proteins were not detected; while known pyrenoid proteins remained (LSU and SSU) (Figure 6.3 lanes 1 and 2). These results suggest that our pellet fraction is highly enriched in pyrenoids.

6.3.2 *C. reinhardtii* pyrenoid proteome

The protein composition of pyrenoid-enriched fractions was different between cells grown mixotrophically (on TAP medium) or phototrophically (on HSM medium) (Figure 6.3 lanes 2 and 3, respectively). Pyrenoids from cells grown phototrophically were enriched in both LSU and SSU and had fewer proteins that are thought to be contaminants such as LHC II. Therefore, we prepared the pyrenoid fractions for mass spectrometry analysis from cells grown phototrophically to minimize the amount of contamination from other compartments.

The pyrenoid fraction was separated on a 12-18% gradient non-denaturing SDS-PAGE and the gel lane was cut into 14 sections (Figure 6.3 lane 3). Each section was analyzed separately by tandem mass spectrometry. Twelve proteins had P scores below the cutoff of 10^{-3} (Table 6.1). P scores reflect the probability that a peptide for a given protein has the same sequence elsewhere in the genome. Out of these twelve proteins, seven were chloroplast proteins determined by their characterization at the Joint Genome Institute. Four of the seven chloroplast proteins had functions in starch metabolism, two were Calvin cycle enzymes and one was a nitrite reductase. One protein, a putative glucoamylase I, was included in Table 6.1 as a possible pyrenoid

protein because it had a high P score and had the appropriate molecular weight for the gel section it was excised from while being involved in starch metabolism like many other proteins in the proteome. These results provide the first proteome of the pyrenoid which included eight proteins functioning in starch metabolism, CO_2 metabolism and nitrite metabolism.

6.4 Discussion

6.4.1 A simple method for isolating pyrenoids

This simple procedure for pyrenoid isolation is much faster and safer than previously described protocols (Figure 6.1) [174]. The optimal growth conditions were defined to obtain pyrenoids with the least amount of contaminating proteins. I had found previously that cells grown mixotrophically have a higher rate of protein synthesis and a higher total amount of protein than cells grown phototrophically (data not shown). Therefore, it was not surprising that pyrenoid fractions isolated from cells grown mixotrophically had a higher level of protein contamination (Figure 6.3 lane 2). Furthermore, an initial mass spectrometry analysis with mixotrophic cells produced a larger number of proteins from other compartments including flagella, the nucleus and cytoplasm (data not shown). Pyrenoids from cells grown phototrophically have fewer proteins and a higher ratio of LSU and SSU compared to the other proteins present (Figure 6.3 lane 3). This higher ratio is probably due to a requirement for many more proteins for metabolism of exogenous acetate than for photosynthesis. Therefore, pyrenoids from cells grown phototrophically were used for mass spectrometry analysis.

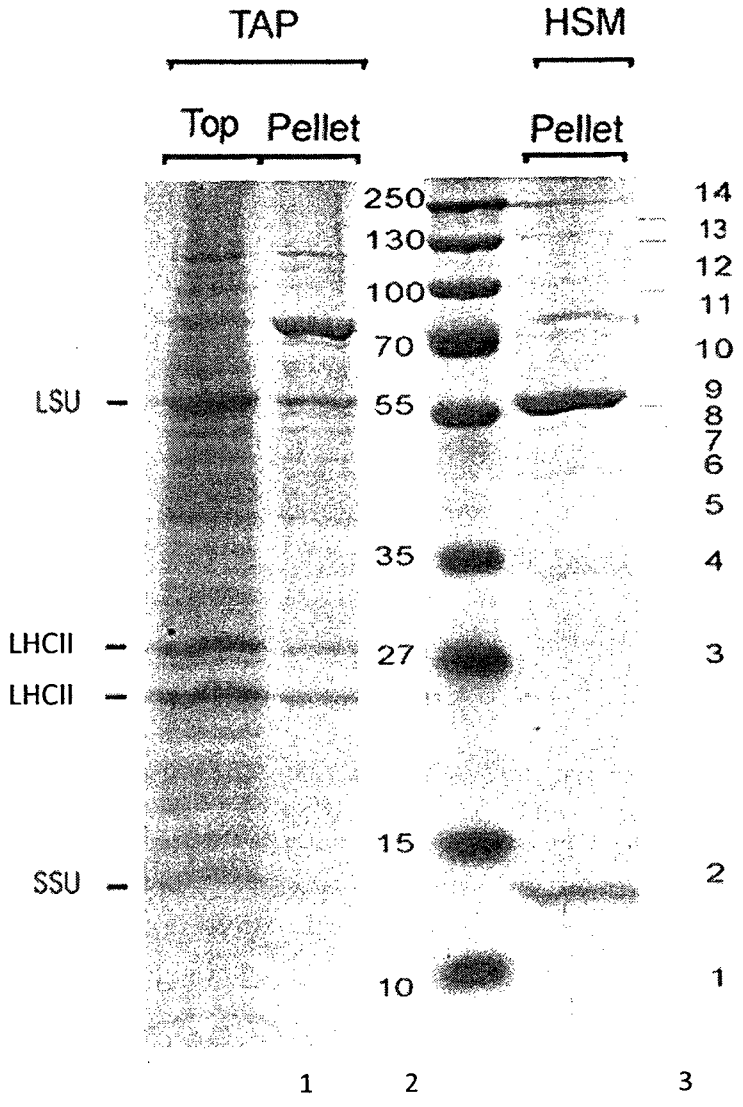

Figure 6.3. A fraction enriched in pyrenoids has few proteins.

Many proteins are absent when the pyrenoid pellet fraction was compared to the supernatant on SDS-PAGE, while known pyrenoid proteins remained (LSU and SSU) (lanes 1 and 2). The protein composition of pyrenoids was different between cells grown mixotrophically on TAP or phototrophically on HSM (lanes 2 and 3). Pyrenoids from cells grown phototrophically were enriched in both LSU and SSU and had contaminating proteins such as LHC II.

Protein	Local.	Function	P	MW (KDa)	Peptides hits
Putative granule-bound starch synthase I	cp	Starch metabolism	1.90×10^{-9}	74.6	26
6-phosphogluconolactonase	cp	Starch metabolism	9.68×10^{-8}	27.1	7
Rubisco small subunit	cp	Calvin cycle enzyme	2.30×10^{-7}	20.6	4
Nucleoside diphosphate sugar epimerase	cp	Starch metabolism	4.99×10^{-6}	44.7	8
Glycine cleavage T protein	cy	Aminomethyl transferase	4.75 C 10^{-6}	43.6	3
Glyceraldehyde-3-phosphate dehydrogenase	cp	Calvin cycle enzyme	2.51×10^{-6}	40.3	3
Beta subunit of mitochondrial ATP synthase	mt	ATP synthase	1.68×10^{-6}	61.8	14
Alpha-glucan water dikinase	cp	Starch metabolism	8.52×10^{-5}	149.8	2
Nitrite reductase	cp	Nitrite reductase	8.05×10^{-5}	52.2	5
Calmodulin-dependent protein kinase	cy	Kinase	7.67×10^{-5}	48.8	2
Lactate/malate dehydrogenase	cy	Dehydrogenase	1.17×10^{-4}	36.6	2
Pherophorin-C3	ex	Cell wall protein	1.08×10^{-4}	41.9	3
† *Putative glucoamylase I*	*cp*	*Starch metabolism*	*1*	*173.8*	*3*

TABLE 6.1. Mass spectrometry analysis of pyrenoid fraction

Mass spectrometry analysis of the pyrenoid fraction revealed 12 proteins with P values below 10^{-3} and 7 of these are chloroplast proteins (JGI, Target P). All proteins are ranked according to their P score, which is a probability that a peptide has the same sequence elsewhere in the genome. cp, chloroplast; cy, cytoplasm; ex, extracellular matrix; mt, mitochondria.

† This protein had a high P score but was included in the table because it had the appropriate molecular weight for the section of the gel it was in and it was involved in starch metabolism in the chloroplast

The proteome of the pyrenoid in mixotrophic cells could be unique and interesting but because of the large amount of contaminating proteins we did not study it further.

6.4.2 The *C. reinhardtii* pyrenoid proteome

This is the first study to describe the proteome of the *C. reinhardtii* pyrenoid. Of the eight proteins identified by mass spectrometry, 2 had been identified previously by immunogold EM: nitrite reductase and SSU [55, 86] and 5 of the other 6 are involved in starch metabolism, which is not surprising considering the large starch plates that surround the pyrenoid (see Chapter 1 Figure 1.3). Calvin cycle enzyme glyceraldehyde-3-phosphate dehydrogenase is the only other Calvin cycle enzyme to have been identified in the *C. reinhardtii* pyrenoid besides Rubisco. Kuchitsu *et al.* [174] had an enriched pyrenoid fraction but could only visually identify LSU and SSU. They mentioned proteins of 70, 66, 51, 49, and 44 kDa as possible minor pyrenoid proteins. The 70 kDa protein is most likely granule-bound starch synthase, the 51 kDa protein is nitrite reductase, and the 44 kDa protein is nucleoside diphosphate sugar epimerase. This study provides the first evidence that starch metabolism enzymes and glyceraldehyde-3-phosphate dehydrogenase are localized to the pyrenoid.

The other two minor proteins mentioned by Kuchitsu *et al.* [174] could be contaminants. We did not have a contaminant of 66 kDa in our fraction, but we did have calmodulin-dependent protein kinase as a 49 kDa contaminant. Our pyrenoid fraction had 5 out of 12 proteins that were not chloroplast proteins. This level of contamination is consistent with the proteomic analysis of other chloroplast subcompartments like the eyespot, which had approximately 20% contaminants [175]. Our pyrenoid fraction had

double this amount of contamination, but the eyespot isolation procedure is very labour intensive and most likely eliminates more contaminants than our rapid method. This level of contamination from outside the chloroplast brings into question the amount of contamination from within the chloroplast.

It must be noted that the mass spectrometer did not detect LSU in the pyrenoid fraction even though it is clearly a major band in the gel (Figure 6.3 lane 3). A possible reason for this is that the amount of trypsin was not increased when the gel band containing LSU was digested. This may have resulted in little digestion of this abundant protein and therefore too few peptides produced for the mass spectrometer to analyze. One must wonder whether other proteins are missing from our pyrenoid proteome due to this problem. Repeating these experiments by adding more trypsin to gel pieces containing high amounts of proteins could yield a more complete proteome.

6.5 Conclusion

The pyrenoid proteome has confirmed that this chloroplast subcompartment has roles in CO_2 assimilation and nitrite reduction, which have been mentioned previously based on immune-gold EM localization studies. However, this proteome also reveals a novel function of the pyrenoid in starch metabolism. There are, however, significant contaminants from other compartments and this proteome may be incomplete due to the absence of LSU which is clearly a pyrenoid protein.

This simple method for pyrenoid isolation could be used in future studies such as cpSG isolation because these granules have been shown to be at the inner perimeter of the pyrenoid (Chapter 4).

7 Conclusions and suggestions for future work

My findings have improved our level of understanding of the chloroplast. I am the first to use FISH and IF extensively within this organelle. The use of these techniques has shown that processes within this organelle are much more compartmentalized than previously thought. I have identified two novel chloroplast compartments: T zones, which house the early steps of de novo PS II biogenesis, and cpSGs, which form during oxidative stress and harbor mRNAs and protein. I am the first to show that some chloroplast proteins are targeted via their mRNA and have begun to describe the precise targeting mechanisms used. I have characterized the first proteome of the pyrenoid, which suggests that this chloroplast compartment is involved in starch metabolism, CO_2 assimilation and nitrite reduction.

7.1 PS II subunit synthesis for PSII biogenesis occurs in T zones

I have provided in situ evidence for the current model that D1 synthesis for PS II repair occurs in stroma thylakoid membranes throughout the chloroplast. I have also provided many lines of evidence showing that PS II subunit synthesis and assembly occur in a specific region of the chloroplast that I have called T zones (Chapter 2).

The next step would be to characterize, biochemically, the composition of T zones and the membranes surrounding them. We expect T zones to be heavier than thylakoid membranes based on my in situ data showing ribosomes concentrating there. Therefore, sucrose gradient centrifugation of chloroplasts could reveal membranes that are heavier than thylakoid membranes. If there are such heavy membranes, these could be analyzed by Western blot to see if they have T zone components. If they do, we could

analyze these samples by mass spectrometry to obtain a T zone proteome. This would tell us what proteins are involved in de novo PS II synthesis and assembly.

7.2 Chloroplast protein targeting involves localized translation

My use of in situ approaches in the analysis of mRNA localization for chloroplast protein targeting has begun to identify the targeting mechanisms used by specific proteins for different processes (Chapter 3). I showed that chloroplast proteins are targeted via the three known general mechanisms: post-translational, co-translational, and mRNA-based targeting. These findings reveal that chloroplasts are complex and compartmentalized systems that use protein targeting mechanisms like the well-characterized mechanisms in yeast and Drosophila.

Future studies should focus on exploring these pathways at the biochemical level. What proteins are involved in localizing the mRNA-ribosome-nascent chain complexes in co-translational targeting? Which RBPs localize the mRNAs in mRNA-based targeting? One could also use these approaches to determine the targeting mechanisms used for other chloroplast proteins.

7.3 Stress induces the assembly of RNA granules in the chloroplast of *C. reinhardtii*

The discovery of cpSGs reveals a novel chloroplast stress response and the first example of a stress-induced RNA granule in a bacterial lineage or organellar genetic system. My findings also provide novel functions for the pyrenoid in harbouring cpSGs and LSU as the cpSG assembly factor (Chapter 4).

In Chapter 5, I present evidence that cpSGs do not provide oxidative stress tolerance, therefore what is their function? To better understand the role of cpSGs, we

would like to determine their complete composition. Because cpSGs are within the pyrenoid, we have begun work to isolate cpSGs by using our pyrenoid isolation protocol described in Chapter 6. Initial trials have shown that cpSGs come apart during pyrenoid isolation. Therefore, we would like to try the addition of cross-linking agents that might hold cpSGs within pyrenoids during the isolation. Isolating cpSGs would allow us to analyze them by mass spectrometry and obtain the first proteome of any SG.

Other projects that could stem from these findings are to determine whether land plants or even mitochondria or bacteria have cpSGs.

7.4 Characterization of the pyrenoid proteome in *C. reinhardtii*

The pyrenoid proteome has revealed that this chloroplast compartment has roles in starch metabolism, CO_2 assimilation and nitrite reduction. Because this pyrenoid isolation procedure yields significant contaminants from other compartments and because this proteome is incomplete due to the absence of LSU, it will be necessary to repeat this experiment.

In Chapter 5, I describe two mutants with deletions in *rbcL* and *rbcS* that do not have pyrenoids. If these mutants were put through the pyrenoid isolation procedure, the material that was found in the pellet fraction could be considered contamination. These contaminants could be analyzed by mass spectrometry and subtracted from the pyrenoid proteome of a wild-type strain that is run in parallel. A way to do this would be to grow the mutant strain on ^{15}N and the wild-type strain on ^{14}N, mix an equal number of cells from each strain and isolate pyrenoids from this mixture [176]. The resulting pyrenoid fraction would have proteins labeled with ^{14}N and contaminating proteins

labeled with ^{15}N. The mass spectrometer is able distinguish between nitrogen isotopes and it could subtract all proteins from the proteome that have ^{15}N. This could yield a more accurate proteome because many contaminating proteins should be removed.

8 References

1. Reichel, C., Mathur, J., Eckes, P., Langenkemper, K., Koncz, C., Schell, J., Reiss, B. and Maas, C. (1996). Enhanced green fluorescence by the expression of an Aequorea victoria green fluorescent protein mutant in mono- and dicotyledonous plant cells. *Proc Natl Acad Sci U S A* 93:5888-93.
2. Hanson, M. R. and Kohler, R. H. (2001). GFP imaging: methodology and application to investigate cellular compartmentation in plants. *J Exp Bot* 52:529-39.
3. Colon-Ramos, D. A., Salisbury, J. L., Sanders, M. A., Shenoy, S. M., Singer, R. H. and Garcia-Blanco, M. A. (2003). Asymmetric distribution of nuclear pore complexes and the cytoplasmic localization of beta2-tubulin mRNA in *Chlamydomonas reinhardtii*. *Dev Cell* 4:941-52.
4. Suss, K. H., Arkona, C., Manteuffel, R. and Adler, K. (1993). Calvin cycle multienzyme complexes are bound to chloroplast thylakoid membranes of higher plants in situ. *Proc Natl Acad Sci U S A* 90:5514-8.
5. Suss, K. H., Prokhorenko, I. and Adler, K. (1995). In Situ Association of Calvin Cycle Enzymes, Ribulose-1,5-Bisphosphate Carboxylase/Oxygenase Activase, Ferredoxin-NADP+ Reductase, and Nitrite Reductase with Thylakoid and

Pyrenoid Membranes of *Chlamydomonas reinhardtii* Chloroplasts as Revealed by Immunoelectron Microscopy. *Plant Physiol* 107:1387-1397.

6. Staehelin, L. A. (2003). Chloroplast structure: from chlorophyll granules to supra-molecular architecture of thylakoid membranes. *Photosynth Res* 76:185-96.

7. Andersson, B. and Anderson, J. M. (1980). Lateral heterogeneity in the distribution of chlorophyll-protein complexes of the thylakoid membranes of spinach chloroplasts. *Biochim Biophys Acta* 593:427-40.

8. Zerges, W. (2000). Translation in chloroplasts. *Biochimie* 82:583-601.

9. Eckhardt, U., Grimm, B. and Hortensteiner, S. (2004). Recent advances in chlorophyll biosynthesis and breakdown in higher plants. *Plant Mol Biol* 56:1-14.

10. Awai, K., Xu, C., Lu, B. and Benning, C. (2006). Lipid trafficking between the endoplasmic reticulum and the chloroplast. *Biochem Soc Trans* 34:395-8.

11. Watanabe, N., Che, F. S., Iwano, M., Takayama, S., Yoshida, S. and Isogai, A. (2001). Dual targeting of spinach protoporphyrinogen oxidase II to mitochondria and chloroplasts by alternative use of two in-frame initiation codons. *J Biol Chem* 276:20474-81.

12. Xu, C., Fan, J., Froehlich, J. E., Awai, K. and Benning, C. (2005). Mutation of the TGD1 chloroplast envelope protein affects phosphatidate metabolism in Arabidopsis. *Plant Cell* 17:3094-110.

13. Minagawa, J. and Takahashi, Y. (2004). Structure, function and assembly of Photosystem II and its light-harvesting proteins. *Photosynth Res* 82:241-63.

14. Keegstra, K. and Cline, K. (1999). Protein import and routing systems of chloroplasts. *Plant Cell* 11:557-70.

15. Kessler, F. and Schnell, D. J. (2006). The function and diversity of plastid protein import pathways: a multilane GTPase highway into plastids. *Traffic* 7:248-57.

16. Beligni, M. V., Yamaguchi, K. and Mayfield, S. P. (2004). The translational apparatus of *Chlamydomonas reinhardtii* chloroplast. *Photosynth Res* 82:315-25.

17. Takahashi, S. and Murata, N. (2008). How do environmental stresses accelerate photoinhibition? *Trends Plant Sci* 13:178-82.

18. Aro, E. M., Virgin, I. and Andersson, B. (1993). Photoinhibition of Photosystem II. Inactivation, protein damage and turnover. *Biochim Biophys Acta* 1143:113-34.

19. Adir, N., Shochat, S. and Ohad, I. (1990). Light-dependent D1 protein synthesis and translocation is regulated by reaction center II. Reaction center II serves as an acceptor for the D1 precursor. *J Biol Chem* 265:12563-8.

20. Chua, N. H., Blobel, G., Siekevitz, P. and Palade, G. E. (1973). Attachment of chloroplast polysomes to thylakoid membranes in *Chlamydomonas reinhardtii*. *Proc Natl Acad Sci U S A* 70:1554-8.

21. Chua, N. H., Blobel, G., Siekevitz, P. and Palade, G. E. (1976). Periodic variations in the ratio of free to thylakoid-bound chloroplast ribosomes during the cell cycle of *Chlamydomonas reinhardtii*. *J Cell Biol* 71:497-514.

22. Margulies, M. M. and Michaels, A. (1974). Ribosomes bound to chloroplast membranes in *Chlamydomonas reinhardtii*. *J Cell Biol* 60:65-77.

23. Margulies, M. M. and Michaels, A. (1975). Free and membrane-bound chloroplast polyribosomes *Chlamydomonas reinhardtii. Biochim Biophys Acta* 402:297-308.

24. Margulies, M. M., Tiffany, H. L. and Hattori, T. (1987). Photosystem I reaction center polypeptides of spinach are synthesized on thylakoid-bound ribosomes. *Arch Biochem Biophys* 254:454-61.

25. Yamamoto, T., Burke, J., Autz, G. and Jagendorf, A. T. (1981). Bound Ribosomes of Pea Chloroplast Thylakoid Membranes: Location and Release in Vitro by High Salt, Puromycin, and RNase. *Plant Physiol* 67:940-949.

26. Margulies, M. M. (1983). Synthesis of photosynthetic membrane proteins directed by RNA from rough thylakoids of *Chlamydomonas reinhardtii. Eur J Biochem* 137:241-8.

27. Herrin, D. and Michaels, A. (1985). In vitro synthesis and assembly of the peripheral subunits of coupling factor CF1 (alpha and beta) by thylakoid-bound ribosomes. *Arch Biochem Biophys* 237:224-36.

28. Breidenbach, E., Jenni, E. and Boschetti, A. (1988). Synthesis of two proteins in chloroplasts and mRNA distribution between thylakoids and stroma during the cell cycle of *Chlamydomonas reinhardii. Eur J Biochem* 177:225-32.

29. Klein, R. R., Mason, H. S. and Mullet, J. E. (1988). Light-regulated translation of chloroplast proteins. I. Transcripts of psaA-psaB, psbA, and rbcL are associated with polysomes in dark-grown and illuminated barley seedlings. *J Cell Biol* 106:289-301.

30. Zhang, L., Paakkarinen, V., van Wijk, K. J. and Aro, E. M. (1999). Co-translational assembly of the D1 protein into photosystem II. *J Biol Chem* 274:16062-7.

31. Leto, K. J., Bell, E. and McIntosh, L. (1985). Nuclear mutation leads to an accelerated turnover of chloroplast-encoded 48 kd and 34.5 kd polypeptides in thylakoids lacking photosystem II. *Embo J* 4:1645-1653.

32. Mattoo, A. K. and Edelman, M. (1987). Intramembrane translocation and posttranslational palmitoylation of the chloroplast 32-kDa herbicide-binding protein. *Proc Natl Acad Sci U S A* 84:1497-501.

33. van Wijk, K. J., Roobol-Boza, M., Kettunen, R., Andersson, B. and Aro, E. M. (1997). Synthesis and assembly of the D1 protein into photosystem II: processing of the C-terminus and identification of the initial assembly partners and complexes during photosystem II repair. *Biochemistry* 36:6178-86.

34. Bourque, D. P., Boynton, J. E. and Gillham, N. W. (1971). Studies on the structure and cellular location of various ribosome and ribosomal RNA species in the green alga *Chlamydomonas reinhardi. J Cell Sci* 8:153-83.

35. de Vitry, C., Olive, J., Drapier, D., Recouvreur, M. and Wollman, F. A. (1989). Posttranslational events leading to the assembly of photosystem II protein complex: a study using photosynthesis mutants from *Chlamydomonas reinhardtii. J Cell Biol* 109:991-1006.

36. Margulies, M. M. and Weistrop, J. S. (1980). Sub-thylakoid fractions containing ribosomes. *Biochim Biophys Acta* 606:20-33.

37. Hoober, J. K., Boyd, C. O. and Paavola, L. G. (1991). Origin of Thylakoid Membranes in *Chlamydomonas reinhardtii* y-1 at 38 degrees C. *Plant Physiol* 96:1321-1328.

38. White, R. A. and Hoober, J. K. (1994). Biogenesis of Thylakoid Membranes in *Chlamydomonas reinhardtii* y1 (A Kinetic Study of Initial Greening). *Plant Physiol* 106:583-590.

39. Kroll, D., Meierhoff, K., Bechtold, N., Kinoshita, M., Westphal, S., Vothknecht, U. C., Soll, J. and Westhoff, P. (2001). VIPP1, a nuclear gene of *Arabidopsis thaliana* essential for thylakoid membrane formation. *Proc Natl Acad Sci U S A* 98:4238-42.

40. Vothknecht, U. C. and Soll, J. (2005). Chloroplast membrane transport: interplay of prokaryotic and eukaryotic traits. *Gene* 354:99-109.

41. Siebertz, H. P., Heinz, E., Joyard, J. and Douce, R. (1980). Labelling in vivo and in vitro of molecular species of lipids from chloroplast envelopes and thylakoids. *Eur J Biochem* 108:177-85.

42. Zerges, W. and Rochaix, J. D. (1998). Low density membranes are associated with RNA-binding proteins and thylakoids in the chloroplast of *Chlamydomonas reinhardtii*. *J Cell Biol* 140:101-10.

43. Devereux, R., Loeblich, A. R., 3rd and Fox, G. E. (1990). Higher plant origins and the phylogeny of green algae. *J Mol Evol* 31:18-24.

44. Zak, E., Norling, B., Maitra, R., Huang, F., Andersson, B. and Pakrasi, H. B. (2001). The initial steps of biogenesis of cyanobacterial photosystems occur in plasma membranes. *Proc Natl Acad Sci U S A* 98:13443-8.

45. Joyard, J., Block, M. A. and Douce, R. (1991). Molecular aspects of plastid envelope biochemistry. *Eur J Biochem* 199:489-509.

46. van de Meene, A. M., Hohmann-Marriott, M. F., Vermaas, W. F. and Roberson, R. W. (2006). The three-dimensional structure of the cyanobacterium Synechocystis sp. PCC 6803. *Arch Microbiol* 184:259-70.

47. Sanchirico, M. E., Fox, T. D. and Mason, T. L. (1998). Accumulation of mitochondrially synthesized Saccharomyces cerevisiae Cox2p and Cox3p depends on targeting information in untranslated portions of their mRNAs. *Embo J* 17:5796-804.

48. St Johnston, D. (2005). Moving messages: the intracellular localization of mRNAs. *Nat Rev Mol Cell Biol* 6:363-75.

49. Stephens, S. B., Dodd, R. D., Lerner, R. S., Pyhtila, B. M. and Nicchitta, C. V. (2008). Analysis of mRNA partitioning between the cytosol and endoplasmic reticulum compartments of mammalian cells. *Methods Mol Biol* 419:197-214.

50. Inaba, T. and Schnell, D. J. (2008). Protein trafficking to plastids: one theme, many variations. *Biochem J* 413:15-28.

51. Chua, N. H. and Schmidt, G. W. (1979). Transport of proteins into mitochondria and chloroplasts. *J Cell Biol* 81:461-83.

52. Villarejo, A., Buren, S., Larsson, S., Dejardin, A., Monne, M., Rudhe, C., Karlsson, J., Jansson, S., Lerouge, P., Rolland, N., von Heijne, G., Grebe, M., Bako, L. and Samuelsson, G. (2005). Evidence for a protein transported through the secretory pathway en route to the higher plant chloroplast. *Nat Cell Biol* 7:1224-31.

53. Nanjo, Y., Oka, H., Ikarashi, N., Kaneko, K., Kitajima, A., Mitsui, T., Munoz, F. J., Rodriguez-Lopez, M., Baroja-Fernandez, E. and Pozueta-Romero, J. (2006). Rice plastidial N-glycosylated nucleotide pyrophosphatase/phosphodiesterase is transported from the ER-golgi to the chloroplast through the secretory pathway. *Plant Cell* 18:2582-92.

54. Radhamony, R. N. and Theg, S. M. (2006). Evidence for an ER to Golgi to chloroplast protein transport pathway. *Trends Cell Biol* 16:385-7.

55. Borkhsenious, O. N., Mason, C. B. and Moroney, J. V. (1998). The intracellular localization of ribulose-1,5-bisphosphate Carboxylase/Oxygenase in *chlamydomonas reinhardtii. Plant Physiol* 116:1585-91.

56. van Wijk, K. J., Knott, T. G. and Robinson, C. (1995). Evidence for SecA- and delta pH-independent insertion of D1 into thylakoids. *FEBS Lett* 368:263-6.

57. Eichacker, L. A. and Henry, R. (2001). Function of a chloroplast SRP in thylakoid protein export. *Biochim Biophys Acta* 1541:120-34.

58. Zhang, L. and Aro, E. M. (2002). Synthesis, membrane insertion and assembly of the chloroplast-encoded D1 protein into photosystem II. *FEBS Lett* 512:13-8.

59. Gutensohn, M., Fan, E., Frielingsdorf, S., Hanner, P., Hou, B., Hust, B. and Klosgen, R. B. (2006). *Toc, Tic, Tat et al.: structure and function of protein transport machineries in chloroplasts.* *J Plant Physiol* 163:333-47.

60. Amin, P., Sy, D. A., Pilgrim, M. L., Parry, D. H., Nussaume, L. and Hoffman, N. E. (1999). Arabidopsis mutants lacking the 43- and 54-kilodalton subunits of the chloroplast signal recognition particle have distinct phenotypes. *Plant Physiol* 121:61-70.

61. Zerges, W., Wang, S. and Rochaix, J. D. (2002). Light activates binding of membrane proteins to chloroplast RNAs in *Chlamydomonas reinhardtii. Plant Mol Biol* 50:573-85.

62. Nickelsen, J. (2003). Chloroplast RNA-binding proteins. *Curr Genet* 43:392-9.

63. Stoecklin, G. and Anderson, P. (2007). In a tight spot: ARE-mRNAs at processing bodies. *Genes Dev* 21:627-31.

64. Anderson, P. and Kedersha, N. (2006). RNA granules. *J Cell Biol* 172:803-8.

65. Kedersha, N. L., Gupta, M., Li, W., Miller, I. and Anderson, P. (1999). RNA-binding proteins TIA-1 and TIAR link the phosphorylation of eIF-2 alpha to the assembly of mammalian stress granules. *J Cell Biol* 147:1431-42.

66. Dunand-Sauthier, I., Walker, C., Wilkinson, C., Gordon, C., Crane, R., Norbury, C. and Humphrey, T. (2002). Sum1, a component of the fission yeast eIF3 translation initiation complex, is rapidly relocalized during environmental stress and interacts with components of the 26S proteasome. *Mol Biol Cell* 13:1626-40.

67. Nover, L., Scharf, K. D. and Neumann, D. (1989). Cytoplasmic heat shock granules are formed from precursor particles and are associated with a specific set of mRNAs. *Mol Cell Biol* 9:1298-308.

68. Cassola, A., De Gaudenzi, J. G. and Frasch, A. C. (2007). Recruitment of mRNAs to cytoplasmic ribonucleoprotein granules in trypanosomes. *Mol Microbiol* 65:655-70.

69. Kedersha, N. and Anderson, P. (2002). Stress granules: sites of mRNA triage that regulate mRNA stability and translatability. *Biochem Soc Trans* 30:963-9.

70. Kimball, S. R., Horetsky, R. L., Ron, D., Jefferson, L. S. and Harding, H. P. (2003). Mammalian stress granules represent sites of accumulation of stalled translation initiation complexes. *Am J Physiol Cell Physiol* 284:C273-84.

71. Tourriere, H., Chebli, K., Zekri, L., Courselaud, B., Blanchard, J. M., Bertrand, E. and Tazi, J. (2003). The RasGAP-associated endoribonuclease G3BP assembles stress granules. *J Cell Biol* 160:823-31.

72. Hua, Y. and Zhou, J. (2004). Rpp20 interacts with SMN and is re-distributed into SMN granules in response to stress. *Biochem Biophys Res Commun* 314:268-76.

73. Cougot, N., Babajko, S. and Seraphin, B. (2004). Cytoplasmic foci are sites of mRNA decay in human cells. *J Cell Biol* 165:31-40.

74. Teixeira, D. and Parker, R. (2007). Analysis of P-body assembly in Saccharomyces cerevisiae. *Mol Biol Cell* 18:2274-87.

75. Bashkirov, V. I., Scherthan, H., Solinger, J. A., Buerstedde, J. M. and Heyer, W. D. (1997). A mouse cytoplasmic exoribonuclease (mXRN1p) with preference for G4 tetraplex substrates. *J Cell Biol* 136:761-73.

76. Ingelfinger, D., Arndt-Jovin, D. J., Luhrmann, R. and Achsel, T. (2002). The human LSm1-7 proteins colocalize with the mRNA-degrading enzymes Dcp1/2 and Xrnl in distinct cytoplasmic foci. *Rna* 8:1489-501.

77. Andrei, M. A., Ingelfinger, D., Heintzmann, R., Achsel, T., Rivera-Pomar, R. and Luhrmann, R. (2005). A role for eIF4E and eIF4E-transporter in targeting mRNPs to mammalian processing bodies. *Rna* 11:717-27.

78. Eulalio, A., Behm-Ansmant, I. and Izaurralde, E. (2007). P bodies: at the crossroads of post-transcriptional pathways. *Nat Rev Mol Cell Biol* 8:9-22.

79. Kedersha, N., Stoecklin, G., Ayodele, M., Yacono, P., Lykke-Andersen, J., Fritzler, M. J., Scheuner, D., Kaufman, R. J., Golan, D. E. and Anderson, P. (2005). Stress granules and processing bodies are dynamically linked sites of mRNP remodeling. *J Cell Biol* 169:871-84.

80. Kwon, S., Zhang, Y. and Matthias, P. (2007). The deacetylase HDAC6 is a novel critical component of stress granules involved in the stress response. *Genes Dev* 21:3381-94.

81. McEwen, E., Kedersha, N., Song, B., Scheuner, D., Gilks, N., Han, A., Chen, J. J., Anderson, P. and Kaufman, R. J. (2005). Heme-regulated inhibitor kinase-mediated phosphorylation of eukaryotic translation initiation factor 2 inhibits

translation, induces stress granule formation, and mediates survival upon arsenite exposure. *J Biol Chem* 280:16925-33.

82. Gilks, N., Kedersha, N., Ayodele, M., Shen, L., Stoecklin, G., Dember, L. M. and Anderson, P. (2004). Stress granule assembly is mediated by prion-like aggregation of TIA-1. *Mol Biol Cell* 15:5383-98.

83. Moroney, J. V. and Ynalvez, R. A. (2007). Proposed carbon dioxide concentrating mechanism in *Chlamydomonas reinhardtii*. *Eukaryot Cell* 6:1251-9.

84. Spreitzer, R. J. and Salvucci, M. E. (2002). Rubisco: structure, regulatory interactions, and possibilities for a better enzyme. *Annu Rev Plant Biol* 53:449-75.

85. Ohad, I., Siekevitz, P. and Palade, G. E. (1967). Biogenesis of chloroplast membranes. II. Plastid differentiation during greening of a dark-grown algal mutant (*Chlamydomonas reinhardi*). *J Cell Biol* 35:553-84.

86. Lopez-Ruiz, A., Verbelen, J. P., Roldan, J. M. and Diez, J. (1985). Nitrate Reductase of Green Algae Is Located in the Pyrenoid. *Plant Physiol* 79:1006-1010.

87. Uniacke, J. and Zerges, W. (2007). Photosystem II assembly and repair are differentially localized in *Chlamydomonas*. *Plant Cell* 19:3640-54.

88. Uniacke, J. and Zerges, W. (2008). Stress induces the assembly of RNA granules in the chloroplast of *Chlamydomonas reinhardtii*. *J Cell Biol* 182:641-6.

89. Merchant, S. S., *et al.* (2007). The *Chlamydomonas* genome reveals the evolution of key animal and plant functions. *Science* 318:245-50.

90. Uniacke, J. and Zerges, W. (2009). Chloroplast protein targeting involves localized translation in *Chlamydomonas*. *Proc Natl Acad Sci U S A* 106:1439-44.

91. Hoober, J. K. (1989). The *Chlamydomonas* Sourcebook. A Comprehensive Guide to Biology and Laboratory Use. Elizabeth H. Harris. Academic Press, San Diego, CA, 1989. xiv, 780 pp., illus. $145. *Science* 246:1503-1504.

92. Gorman, D. S. and Levine, R. P. (1965). Cytochrome f and plastocyanin: their sequence in the photosynthetic electron transport chain of *Chlamydomonas reinhardi*. *Proc Natl Acad Sci U S A* 54:1665-9.

93. Malnoe, P., Mayfield, S. P. and Rochaix, J. D. (1988). Comparative analysis of the biogenesis of photosystem II in the wt and Y-1 mutant of *Chlamydomonas reinhardtii*. *J Cell Biol* 106:609-16.

94. Lee, J. and Herrin, D. L. (2002). Assessing the relative importance of light and the circadian clock in controlling chloroplast translation in *Chlamydomonas reinhardtii*. *Photosynth Res* 72:295-306.

95. Michaels, A. and Herrin, D. L. (1990). Translational regulation of chloroplast gene expression during the light-dark cell cycle of *Chlamydomonas*: evidence for control by ATP/energy supply. *Biochem Biophys Res Commun* 170:1082-8.

96. Dron, M., Rahire, M. and Rochaix, J. D. (1982). Sequence of the chloroplast DNA region of *Chlamydomonas reinhardii* containing the gene of the large subunit of ribulose bisphosphate carboxylase and parts of its flanking genes. *J Mol Biol* 162:775-93.

97. Erickson, J. M., Rahire, M. and Rochaix, J. D. (1984). *Chlamydomonas reinhardii* gene for the 32 000 mol. wt. protein of photosystem II contains four large introns and is located entirely within the chloroplast inverted repeat. *Embo J* 3:2753-2762.

98. Kuck, U., Choquet, Y., Schneider, M., Dron, M. and Bennoun, P. (1987). Structural and transcription analysis of two homologous genes for the P700 chlorophyll a-apoproteins in *Chlamydomonas reinhardii*: evidence for in vivo trans-splicing. *Embo J* 6:2185-2195.

99. Rochaix, J. D., Kuchka, M., Mayfield, S., Schirmer-Rahire, M., Girard-Bascou, J. and Bennoun, P. (1989). Nuclear and chloroplast mutations affect the synthesis or stability of the chloroplast psbC gene product in *Chlamydomonas reinhardtii*. *Embo J* 8:1013-21.

100. Erickson, J. M., Rahire, M., Malnoe, P., Girard-Bascou, J., Pierre, Y., Bennoun, P. and Rochaix, J. D. (1986). Lack of the D2 protein in a *Chlamydomonas reinhardtii psbD* mutant affects photosystem II stability and D1 expression. *Embo J* 5:1745-1754.

101. Redding, K., Cournac, L., Vassiliev, I. R., Golbeck, J. H., Peltier, G. and Rochaix, J. D. (1999). Photosystem I is indispensable for photoautotrophic growth, CO2 fixation, and H2 photoproduction in *Chlamydomonas reinhardtii*. *J Biol Chem* 274:10466-73.

102. Satagopan, S. and Spreitzer, R. J. (2004). Substitutions at the Asp-473 latch residue of *chlamydomonas* ribulosebisphosphate carboxylase/oxygenase cause

decreases in carboxylation efficiency and CO(2)/O(2) specificity. *J Biol Chem* 279:14240-4.

103. Fleming, G. H., Boynton, J. E. and Gillham, N. W. (1987). The cytoplasmic ribosomes of *Chlamydomonas reinhardtii*: characterization of antibiotic sensitivity and cycloheximide-resistant mutants. *Mol Gen Genet* 210:419-28.

104. Fleming, G. H., Boynton, J. E. and Gillham, N. W. (1987). Cytoplasmic ribosomal proteins from *Chlamydomonas reinhardtii*: characterization and immunological comparisons. *Mol Gen Genet* 206:226-37.

105. Schmidt, R. J., Richardson, C. B., Gillham, N. W. and Boynton, J. E. (1983). Sites of synthesis of chloroplast ribosomal proteins in *Chlamydomonas*. *J Cell Biol* 96:1451-63.

106. Schmidt, R. J., Myers, A. M., Gillham, N. W. and Boynton, J. E. (1984). Immunological similarities between specific chloroplast ribosomal proteins from *Chlamydomonas reinhardtii* and ribosomal proteins from Escherichia coli. *Mol Biol Evol* 1:317-34.

107. Randolph-Anderson, B. L., Gillham, N. W. and Boynton, J. E. (1989). Electrophoretic and immunological comparisons of chloroplast and prokaryotic ribosomal proteins reveal that certain families of large subunit proteins are evolutionarily conserved. *J Mol Evol* 29:68-88.

108. Yamaguchi, K., Prieto, S., Beligni, M. V., Haynes, P. A., McDonald, W. H., Yates, J. R., 3rd and Mayfield, S. P. (2002). Proteomic characterization of the small subunit of *Chlamydomonas reinhardtii* chloroplast ribosome: identification of a

novel S1 domain-containing protein and unusually large orthologs of bacterial S2, S3, and S5. *Plant Cell* 14:2957-74.

109. Lacoste-Royal, G. and Gibbs, S. P. (1987). Immunocytochemical Localization of Ribulose-1,5-Bisphosphate Carboxylase in the Pyrenoid and Thylakoid Region of the Chloroplast of *Chlamydomonas reinhardtii*. *Plant Physiol* 83:602-606.

110. Schroda, M., Kropat, J., Oster, U., Rudiger, W., Vallon, O., Wollman, F. A. and Beck, C. F. (2001). Possible role for molecular chaperones in assembly and repair of photosystem II. *Biochem Soc Trans* 29:413-8.

111. Schotz, F., Bathelt, H., Arnold, C. G. and Schimmer, O. (1972). [The architecture and organization of the *Chlamydomonas* cell. Results of serial-section electron microscopy and a three-dimensional reconstruction]. *Protoplasma* 75:229-54.

112. Gaffal, K. P., Arnold, C. G., Friedriches, G. J. and Gemple, W. (1995). Morphodynamical changes of the chloroplast of *Chlamydomonas reinhardtii* during the 1st round of division. *Arch. Protistenkd.* 145:10-23.

113. Jensen, K. H., Herrin, D. L., Plumley, F. G. and Schmidt, G. W. (1986). Biogenesis of photosystem II complexes: transcriptional, translational, and posttranslational regulation. *J Cell Biol* 103:1315-25.

114. van Wijk, K. J., Nilsson, L. O. and Styring, S. (1994). Synthesis of reaction center proteins and reactivation of redox components during repair of photosystem II after light-induced inactivation. *J Biol Chem* 269:28382-92.

115. Kettunen, R., Pursiheimo, S., Rintamaki, E., Van Wijk, K. J. and Aro, E. M. (1997). Transcriptional and translational adjustments of *psbA* gene expression in mature

chloroplasts during photoinhibition and subsequent repair of photosystem II. *Eur J Biochem* 247:441-8.

116. Shapira, M., Lers, A., Heifetz, P. B., Irihimovitz, V., Osmond, C. B., Gillham, N. W. and Boynton, J. E. (1997). Differential regulation of chloroplast gene expression in *Chlamydomonas reinhardtii* during photoacclimation: light stress transiently suppresses synthesis of the Rubisco LSU protein while enhancing synthesis of the PS II D1 protein. *Plant Mol Biol* 33:1001-11.

117. Eberhard, S., Drapier, D. and Wollman, F. A. (2002). Searching limiting steps in the expression of chloroplast-encoded proteins: relations between gene copy number, transcription, transcript abundance and translation rate in the chloroplast of *Chlamydomonas reinhardtii. Plant J* 31:149-60.

118. Lee, J. and Herrin, D. L. (2003). Mutagenesis of a light-regulated psbA intron reveals the importance of efficient splicing for photosynthetic growth. *Nucleic Acids Res* 31:4361-72.

119. Yohn, C. B., Cohen, A., Danon, A. and Mayfield, S. P. (1996). Altered mRNA binding activity and decreased translational initiation in a nuclear mutant lacking translation of the chloroplast psbA mRNA. *Mol Cell Biol* 16:3560-6.

120. Abramoff, M. D., Magelhaes, P. J. and Ram, S. J. (2004). Image processing with ImageJ. *Biophotonics International* 11:

121. Barnes, D., Cohen, A., Bruick, R. K., Kantardjieff, K., Fowler, S., Efuet, E. and Mayfield, S. P. (2004). Identification and characterization of a novel RNA binding

protein that associates with the 5'-untranslated region of the chloroplast psbA mRNA. *Biochemistry* 43:8541-50.

122. Schwarz, C., Elles, I., Kortmann, J., Piotrowski, M. and Nickelsen, J. (2007). Synthesis of the D2 protein of photosystem II in *Chlamydomonas* is controlled by a high molecular mass complex containing the RNA stabilization factor Nac2 and the translational activator RBP40. *Plant Cell* 19:3627-39.

123. Ohnishi, N. and Takahashi, Y. (2001). PsbT polypeptide is required for efficient repair of photodamaged photosystem II reaction center. *J Biol Chem* 276:33798-804.

124. Herrin, D. L., Michaels, A. S. and Paul, A. L. (1986). Regulation of genes encoding the large subunit of ribulose-1,5-bisphosphate carboxylase and the photosystem II polypeptides D-1 and D-2 during the cell cycle of *Chlamydomonas reinhardtii. J Cell Biol* 103:1837-45.

125. Zerges, W., Girard-Bascou, J. and Rochaix, J. D. (1997). Translation of the chloroplast *psbC* mRNA is controlled by interactions between its 5' leader and the nuclear loci TBC1 and TBC3 in *Chlamydomonas reinhardtii. Mol Cell Biol* 17:3440-8.

126. Trebitsh, T. and Danon, A. (2001). Translation of chloroplast *psbA* mRNA is regulated by signals initiated by both photosystems II and I. *Proc Natl Acad Sci U S A* 98:12289-94.

127. Bellafiore, S., Ferris, P., Naver, H., Gohre, V. and Rochaix, J. D. (2002). Loss of Albino3 leads to the specific depletion of the light-harvesting system. *Plant Cell* 14:2303-14.

128. Ossenbuhl, F., Gohre, V., Meurer, J., Krieger-Liszkay, A., Rochaix, J. D. and Eichacker, L. A. (2004). Efficient assembly of photosystem II in *Chlamydomonas reinhardtii* requires Alb3.1p, a homolog of Arabidopsis ALBINO3. *Plant Cell* 16:1790-800.

129. Barber, J., Nield, J., Morris, E. P. and Hankamer, B. (1999). Subunit positioning in photosystem II revisited. *Trends Biochem Sci* 24:43-5.

130. Vallon, O., Wollman, F. A. and Olive, J. (1985). Distribution of intrinsic and extrinsic subunits of the PS II protein complex between appressed and non-appressed regions of the thylakoid membrane: An immunocytochemical study. *FEBS Lett.* 183:245-250.

131. Swiatek, M., Kuras, R., Sokolenko, A., Higgs, D., Olive, J., Cinque, G., Muller, B., Eichacker, L. A., Stern, D. B., Bassi, R., Herrmann, R. G. and Wollman, F. A. (2001). The chloroplast gene *ycf9* encodes a photosystem II (PSII) core subunit, PsbZ, that participates in PSII supramolecular architecture. *Plant Cell* 13:1347-67.

132. Minai, L., Wostrikoff, K., Wollman, F. A. and Choquet, Y. (2006). Chloroplast biogenesis of photosystem II cores involves a series of assembly-controlled steps that regulate translation. *Plant Cell* 18:159-75.

133. Ris, H. and Plaut, W. (1962). Ultrastructure of DNA-containing areas in the chloroplast of *Chlamydomonas*. *J Cell Biol* 13:383-91.

134. Franklin, S., Ngo, B., Efuet, E. and Mayfield, S. P. (2002). Development of a GFP reporter gene for *Chlamydomonas reinhardtii* chloroplast. *Plant J* 30:733-44.

135. Mayfield, S. P. and Schultz, J. (2004). Development of a luciferase reporter gene, luxCt, for *Chlamydomonas reinhardtii* chloroplast. *Plant J* 37:449-58.

136. Mason, C. B., Bricker, T. M. and Moroney, J. V. (2006). A rapid method for chloroplast isolation from the green alga *Chlamydomonas reinhardtii*. *Nat Protoc* 1:2227-30.

137. Reski, R. (2002). Rings and networks: the amazing complexity of FtsZ in chloroplasts. *Trends Plant Sci* 7:103-5.

138. Ohad, I., Siekevitz, P. and Palade, G. E. (1967). Biogenesis of chloroplast membranes. I. Plastid dedifferentiation in a dark-grown algal mutant (*Chlamydomonas reinhardi*). *J Cell Biol* 35:521-52.

139. Ellgaard, L. and Helenius, A. (2003). Quality control in the endoplasmic reticulum. *Nat Rev Mol Cell Biol* 4:181-91.

140. Slavikova, S., Vacula, R., Fang, Z., Ehara, T., Osafune, T. and Schwartzbach, S. D. (2005). Homologous and heterologous reconstitution of Golgi to chloroplast transport and protein import into the complex chloroplasts of Euglena. *J Cell Sci* 118:1651-61.

141. Khrebtukova, I. and Spreitzer, R. J. (1996). Elimination of the *Chlamydomonas* gene family that encodes the small subunit of ribulose-1,5-bisphosphate carboxylase/oxygenase. *Proc Natl Acad Sci U S A* 93:13689-93.

142. Zhang, L., Paakkarinen, V., van Wijk, K. J. and Aro, E. M. (2000). Biogenesis of the chloroplast-encoded D1 protein: regulation of translation elongation, insertion, and assembly into photosystem II. *Plant Cell* 12:1769-82.

143. Edhofer, I., Muhlbauer, S. K. and Eichacker, L. A. (1998). Light regulates the rate of translation elongation of chloroplast reaction center protein D1. *Eur J Biochem* 257:78-84.

144. Durnford, D. G., Price, J. A., McKim, S. M. and Sarchfield, M. L. (2003). Light-harvesting complex gene expression is controlled by both transcriptional and post-transcriptional mechanisms during photoacclimation in *Chlamydomonas reinhardtii*. *Physiol Plant* 118:193-205.

145. Reinbothe, S., Reinbothe, C. and Parthier, B. (1993). Methyl jasmonate-regulated translation of nuclear-encoded chloroplast proteins in barley (Hordeum vulgare L. cv. salome). *J Biol Chem* 268:10606-11.

146. Emanuelsson, O., Nielsen, H., Brunak, S. and von Heijne, G. (2000). Predicting subcellular localization of proteins based on their N-terminal amino acid sequence. *J Mol Biol* 300:1005-16.

147. Carde, J. P., Joyard, J. and Douce, R. (1982). Electron microscopic studies of envelope membranes from spinach plastids. *Biol Cell* 44:315-324.

148. Gibbs, S. P. (1979). The route of entry of cytoplasmically synthesized proteins into chloroplasts of algae possessing chloroplast ER. *J Cell Sci* 35:253-66.

149. Pyhtila, B., Zheng, T., Lager, P. J., Keene, J. D., Reedy, M. C. and Nicchitta, C. V. (2008). Signal sequence- and translation-independent mRNA localization to the endoplasmic reticulum. *Rna* 14:445-53.

150. Green-Willms, N. S., Fox, T. D. and Costanzo, M. C. (1998). Functional interactions between yeast mitochondrial ribosomes and mRNA 5' untranslated leaders. *Mol Cell Biol* 18:1826-34.

151. Hippler, M., Redding, K. and Rochaix, J. D. (1998). *Chlamydomonas* genetics, a tool for the study of bioenergetic pathways. *Biochim Biophys Acta* 1367:1-62.

152. von Gromoff, E. D., Treier, U. and Beck, C. F. (1989). Three light-inducible heat shock genes of *Chlamydomonas reinhardtii*. *Mol Cell Biol* 9:3911-8.

153. Hoffmann, X. K. and Beck, C. F. (2005). Mating-induced shedding of cell walls, removal of walls from vegetative cells, and osmotic stress induce presumed cell wall genes in *Chlamydomonas*. *Plant Physiol* 139:999-1014.

154. Moseley, J. L., Chang, C. W. and Grossman, A. R. (2006). Genome-based approaches to understanding phosphorus deprivation responses and PSR1 control in *Chlamydomonas reinhardtii*. *Eukaryot Cell* 5:26-44.

155. Hideg, E., Kos, P. B. and Vass, I. (2007). Photosystem II damage induced by chemically generated singlet oxygen in tobacco leaves. *Physiol Plant* 131:33-40.

156. Murata, N., Takahashi, S., Nishiyama, Y. and Allakhverdiev, S. I. (2007). Photoinhibition of photosystem II under environmental stress. *Biochim Biophys Acta* 1767:414-21.

157. Fischer, B. B., Krieger-Liszkay, A. and Eggen, R. L. (2004). Photosensitizers neutral red (type I) and rose bengal (type II) cause light-dependent toxicity in *Chlamydomonas reinhardtii* and induce the Gpxh gene via increased singlet oxygen formation. *Environ Sci Technol* 38:6307-13.

158. Trebitsh, T., Levitan, A., Sofer, A. and Danon, A. (2000). Translation of chloroplast psbA mRNA is modulated in the light by counteracting oxidizing and reducing activities. *Mol Cell Biol* 20:1116-23.

159. Michael, R., McKay, L. and Gibbs, S. P. (1991). Composition and function of pyrenoids: cytochemical and immunocytochemical approaches. *Can. J. Bot.* 69:1040-1052.

160. Liu, C., Willmund, F., Whitelegge, J. P., Hawat, S., Knapp, B., Lodha, M. and Schroda, M. (2005). J-domain protein CDJ2 and HSP70B are a plastidic chaperone pair that interacts with vesicle-inducing protein in plastids 1. *Mol Biol Cell* 16:1165-77.

161. Anderson, P. and Kedersha, N. (2008). Stress granules: the Tao of RNA triage. *Trends Biochem Sci* 33:141-50.

162. Yosef, I., Irihimovitch, V., Knopf, J. A., Cohen, I., Orr-Dahan, I., Nahum, E., Keasar, C. and Shapira, M. (2004). RNA binding activity of the ribulose-1,5-bisphosphate carboxylase/oxygenase large subunit from *Chlamydomonas reinhardtii*. *J Biol Chem* 279:10148-56.

163. Knopf, J. A. and Shapira, M. (2005). Degradation of Rubisco SSU during oxidative stress triggers aggregation of Rubisco particles in *Chlamydomonas reinhardtii*. *Planta* 222:787-93.

164. Cohen, I., Sapir, Y. and Shapira, M. (2006). A conserved mechanism controls translation of Rubisco large subunit in different photosynthetic organisms. *Plant Physiol* 141:1089-97.

165. Stohr, N., Lederer, M., Reinke, C., Meyer, S., Hatzfeld, M., Singer, R. H. and Huttelmaier, S. (2006). ZBP1 regulates mRNA stability during cellular stress. *J Cell Biol* 175:527-34.

166. Kedersha, N., Cho, M. R., Li, W., Yacono, P. W., Chen, S., Gilks, N., Golan, D. E. and Anderson, P. (2000). Dynamic shuttling of TIA-1 accompanies the recruitment of mRNA to mammalian stress granules. *J Cell Biol* 151:1257-68.

167. Mazroui, R., Sukarieh, R., Bordeleau, M. E., Kaufman, R. J., Northcote, P., Tanaka, J., Gallouzi, I. and Pelletier, J. (2006). Inhibition of ribosome recruitment induces stress granule formation independently of eukaryotic initiation factor 2alpha phosphorylation. *Mol Biol Cell* 17:4212-9.

168. Nishiyama, Y., Allakhverdiev, S. I. and Murata, N. (2006). A new paradigm for the action of reactive oxygen species in the photoinhibition of photosystem II. *Biochim Biophys Acta* 1757:742-9.

169. Kuchitsu, K., Tsuzuki, M. and Miyachi, S. (1991). Polypeptide composition and enzyme activities of the pyrenoid and its regulation by CO, concentration in unicellular green algae. *Can. J. Bot.* 69:1062-69.

170. Mitra, M., Lato, S. M., Ynalvez, R. A., Xiao, Y. and Moroney, J. V. (2004). Identification of a new chloroplast carbonic anhydrase in *Chlamydomonas reinhardtii*. *Plant Physiol* 135:173-82.

171. Rawat, M., Henk, M., Lavigne, L. and Moroney, J. V. (1996). *Chlamydomonas reinhardtii* mutants without ribulose-l,5-bisphosphate carboxylase-oxygenase lack a detectable pyrenoid. *Planta* 198:263-270.

172. Takahashi, S. and Murata, N. (2005). Interruption of the Calvin cycle inhibits the repair of Photosystem II from photodamage. *Biochim Biophys Acta* 1708:352-61.

173. Takahashi, S. and Murata, N. (2006). Glycerate-3-phosphate, produced by CO2 fixation in the Calvin cycle, is critical for the synthesis of the D1 protein of photosystem II. *Biochim Biophys Acta* 1757:198-205.

174. Kuchitsu, K., Tsuzuki, M. and Miyachi, S. (1988). Characterization of the Pyrenoid Isolated from Unicellular Green Alga *Chlamydomonas reinhardtii*: Particulate Form of RuBisCO Protein. *Protoplasma* 144:17-24.

175. Schmidt, M., Gessner, G., Luff, M., Heiland, I., Wagner, V., Kaminski, M., Geimer, S., Eitzinger, N., Reissenweber, T., Voytsekh, O., Fiedler, M., Mittag, M. and Kreimer, G. (2006). Proteomic analysis of the eyespot of *Chlamydomonas reinhardtii* provides novel insights into its components and tactic movements. *Plant Cell* 18:1908-30.

176. Gold, N. D. and Martin, V. J. (2007). Global view of the Clostridium thermocellum cellulosome revealed by quantitative proteomic analysis. *J Bacteriol* 189:6787-95.

177. Schottkowski M, Gkalympoudis S, Tzekova N, Stelljes C, Schünemann D, Ankele E, Nickelsen J. (2009). Interaction of the periplasmic PratA factor and the PsbA (D1) protein during biogenesis of photosystem II in Synechocystis sp. PCC 6803. *J Biol Chem.* 284(3):1813-9.

178. Harris, E. (2009) The Chlamydomonas Sourcebook. London: Academic, 2009.